

Biophysical Properties of Experimental Compositions of a Synthetic Pulmonary Surfactant Synsurf® For Aerosolisation

By Chris-Maré Agenbag

Thesis presented for the degree of Master of Science (Medical Sciences in Pharmacology)

Division of Clinical Pharmacology

Faculty of Medicine and Health Sciences

Stellenbosch University



UNIVERSITEIT
iYUNIVESITHI
STELLENBOSCH
UNIVERSITY

Supervisor Prof Johann M van Zyl



(Associate Professor: Division of Clinical Pharmacology, Faculty of Medicine and Health Sciences,
Stellenbosch University)

Co-Supervisor Prof Johan Smith

(Department of Paediatrics & Child Health, Tygerberg Children's Hospital, Faculty of Medicine and
Health Sciences, Stellenbosch University)

March 2018

DECLARATION

By submitting this thesis electronically, I declare that the entirety of the work contained in this thesis is my own, original work and that I have not previously submitted it at another university for a degree in its entirety or in part.

Chris-Maré Agenbag

Date: 26 February 2018

Copyright © 2018 Stellenbosch University
All rights reserved

SUMMARY

Synthetic pulmonary surfactant consists of phospholipid mixtures, free fatty acids and/or sterols, as well as specific protein constructs that mimic the functions of surfactant associated proteins B and/or C. Treatment of neonatal respiratory distress syndrome with surfactant replacement therapy consists of an invasive technique of endotracheal intubation and administration into the airway. For this reason, a less invasive approach such as nebulisation in these frail patients would be beneficial.

Formulations of synthetic pulmonary surfactants intended for use, require that the *in vitro*-aerosolisation behaviour with regards to optimal particle size generation and conservation of surface tension, are ideal in order to maintain proper lung function. The objective of this study was to evaluate the suitability of different formulations of a new peptide-containing synthetic pulmonary surfactant Synsurf[®] during aerosolisation in comparison with the natural surfactants, Curosurf[®] (porcine) and Liposurf[®] (bovine).

Synsurf[®], was synthesised with and without alterations in key components that included cholesterol (1 % and 2 %), palmitic acid (11 %) and tripalmitin (7 %). An extrusion method through polycarbonate membranes with different pore sizes was also included during synthesis of the different formulations. Surfactants were aerosolised with the use of Aeroneb[®]Pro vibrating mesh nebuliser and particles generated were assessed with a Malvern Zetasizer[®] and visualised by scanning electron microscopy. Surface tension analyses was determined with a Drop Shape Analyser (DSA25).

The main findings of this study showed that nebulisation of non-extruded Synsurf[®] formulations as well as Curosurf[®] and Liposurf[®], produced a decrease of $\pm 80\%$ - 90% in particle size, that is below the desired distribution range of 1 - 3 μm for inhaled particles. However, extrusion included in the synthesis of Synsurf[®], generated larger particles post-nebulisation, within the desired range. Nebulisation also significantly influenced the density and viscosity of most Synsurf[®] preparations and natural surfactants. Additionally, an increase in cholesterol concentration showed a marked increase in viscosity of Synsurf[®].

With the exception of the original Synsurf[®] formulation, nebulisation diminished the surface tension lowering ability of all other surfactant preparations. Addition of palmitic acid/tripalmitin and 1 % cholesterol to the original Synsurf[®] formulation showed an overall pronounced reduction in surface tension in comparison to other formulations.

In conclusion, the data of this study indicate that the original formulation of Synsurf[®] with addition of palmitic acid/tripalmitin and low concentrations of cholesterol, aid in the conservation of the surface tension properties and ideal particle size generation of the surfactant during nebulisation with a vibrating mesh nebuliser.

OPSOMMING

Sintetiese pulmonêre surfaktant bestaan uit fosfolipiedmengsels, vry vetsure en/of sterole, sowel as spesifieke proteïenkonstrukte wat die funksies van surfaktant geassosieerde proteïene B en/of C naboots. Behandeling van neonatale respiratoriese-nood-sindroom behels surfaktantvervangingsterapie, 'n ingrypende tegniek van endotracheale intubasie en toediening in die lugpyp. 'n Minder ingrypende benadering soos nebulisering sal gevolglik voordeliger vir hierdie tingerige pasiënte wees.

Formulerings van sintetiese pulmonêre surfaktante wat vir gebruik bedoel is, vereis ideale *in vitro*-aërosoliseringswerking ten opsigte van die ontwikkeling van optimale partikelgrootte en die behoud van oppervlakspanning ten einde behoorlike longfunksie te handhaaf. Die doel van hierdie studie was om die geskiktheid tydens aërosolisering van verskillende formulerings van 'n nuwe peptiedbevattende sintetiese pulmonêre surfaktant, genaamd Synsurf[®], teenoor die natuurlike surfaktante Curosurf[®] (vark) en Liposurf[®] (bees) te evalueer.

Synsurf[®] is met en sonder veranderinge in sleutelkomponente soos cholesterol (1 % en 2 %), palmitiensuur (11 %) en tripalmitien (7 %) gesintetiseer. Ekstrusie by wyse van polikarbonaatmembrane met verskillende poriegroottes is tydens die sintese van die verskillende formulerings toegepas. Surfaktante is met behulp van 'n Aeroneb[®]Pro- vibrerende "mesh"-nebuliseerder geaërosoliseer, terwyl die partikels wat ontwikkel is aan die hand van 'n Malvern Zetasizer[®] geëvalueer en deur middel van 'n skandeer elektronmikroskoop gevisualiseer is. 'n Druppelvormontleider (Eng. *drop shape analyser*, die DSA25) is gebruik om oppervlakspanning te ontleed.

Die hoofbevindings van hierdie studie toon dat nebulisering van Synsurf[®]-formulerings, asook Curosurf[®] en Liposurf[®] die partikelgrootte met $\pm 80\%$ - 90% verminder het. Dit is benede die verlangde verdelingspektrum van 1 – 3 d. μ m vir geïnhaleerde partikels is. In die geval van Synsurf[®], egter, het die ekstrusie tydens sintetisering na nebulisering groter partikels opgelewer, maar steeds binne die verlangde spektrum. Nebulisering het ook die digtheid en viskositeit van die meeste Synsurf[®]-preparate

en natuurlike surfaktante aansienlik beïnvloed. Daarbenewens het 'n toename in cholesterolkonsentrasie 'n duidelike toename in die viskositeit van Synsurf[®] getoon.

Nebulisering het alle sufaktantpreparate buiten die oorspronklike Synsurf[®]-formulering se vermoë om oppervlakspanning te verlaag, verminder. Wanneer palmitiensuur/tripalmitien en 1 % cholesterol by die oorspronklike Synsurf[®]-formulering gevoeg is, was die totale vermindering in oppervlakspanning duidelik in vergelyking met ander formuleringe.

Ten slotte dui die studiedata aan dat die oorspronklike Synsurf[®]-formulering met die byvoeging van palmitiensuur/tripalmitien en lae konsentrasies cholesterol daartoe bydra dat die surfaktant se oppervlakspanningeenskappe en die ontwikkeling van ideale partikelgroottes behoue bly tydens nebulisering met 'n vibrerende “mesh”-nebuliseerder.

ACKNOWLEDGEMENTS

I would like to acknowledge the following organisations and individuals for their essential (financial/technical/moral) support during my studies. Deep appreciation and sincere thanks are due to:

Prof JM van Zyl, Division of Clinical Pharmacology, Faculty of Medicine and Health Sciences, Stellenbosch University

Prof J Smith, Department of Paediatrics & Child Health, Faculty of Medicine and Health Sciences, Stellenbosch University

Prof H Reuter, Division of Clinical Pharmacology, Faculty of Medicine and Health Sciences, Stellenbosch University

INNOVUS technology transfer (Pty) Ltd, Stellenbosch University, Stellenbosch, South Africa

Brink and De Kock Bursary, Faculty of Medicine and Health Sciences, Stellenbosch University

Mrs L Van Rensburg, Division of Clinical Pharmacology, Faculty of Medicine and Health Sciences, Stellenbosch University

Miss L Hanekom, Division of Clinical Pharmacology, Faculty of Medicine and Health Sciences, Stellenbosch University

Mrs H Small, Laboratory Technician, Chemical Engineering, Cape Peninsula University of Technology (CPUT)

Kansai Plascon (Pty) Ltd (Polymer Science) Stellenbosch, South Africa

Prof PGL Baker, Department of Chemistry, University of the Western Cape (UWC), Cape Town

Nutec Digital Ink (Pty) Ltd, Ottery, Cape Town

Mr JA Kloppers (известный как io мастер)

My Family (Father, Mother, Sister and Stella) & Milla Mariaan Moon

DISCLAIMER

Any opinion, findings, and conclusions or recommendations expressed in this material are those of the author(s) and therefore the Brink and De Kock Bursary does not accept any liability in regard thereto.

TABLE OF CONTENT

DECLARATION	i
SUMMARY	ii
OPSOMMING	iv
ACKNOWLEDGEMENTS	vi
DISCLAIMER	vii
List of Figures	1
List of Tables	6
List of Abbreviations	8
CHAPTER 1: Introduction	9
CHAPTER 2: Literature review.....	11
2.1 Structure of the lung.....	11
2.2 Foetal to neonatal lung adaptation	12
2.3 Infant respiratory distress syndrome	13
2.4 Surfactant replacement therapy.....	14
2.5 Composition of endogenous pulmonary surfactant.....	16
2.5.1 Composition of pulmonary surfactant lipids.....	16
2.5.2 Pulmonary surfactant-associated proteins.....	18
2.6 Role of lipids in pulmonary surfactant.....	19
2.6.1 Lipid monolayer structure	19
2.6.2 Interfacial film properties.....	21
2.7 Natural derived vs synthetic pulmonary surfactant.....	22
2.7.1 Animal derived “natural” surfactants.....	24

2.7.2	Synthetic surfactants	25
2.8	Challenges of non-invasive surfactant replacement therapy (NISRT) by aerosolisation .	27
2.8.1	Aerosol delivery	27
2.8.2	Patient factors.....	30
2.8.3	Choice of nebuliser	30
2.8.4	Aerosol deposition studies	31
2.8.5	Physiochemical conditioning of synthetic surfactant mixture	32
2.9	Study Rational.....	33
2.10	Aims	33
2.11	Research Objectives	34
CHAPTER 3: Experimental Materials and Methods		35
3.1	Materials	35
3.2	Research Design.....	36
3.2.1	Preparation of synthetic pulmonary surfactant Synsurf [®]	36
3.2.2	Liposome preparation and extrusion	37
3.2.3	Ageing and long-term storage of samples.....	37
3.2.4	Density experiments.....	38
3.2.5	Liquid surface tension experiments	38
3.2.6	Viscosity experiments	39
3.2.7	Surfactant preparation nebulisation experiments	40
3.2.8	Particle characterisation	40
3.3	Overview of research design.....	42
3.4	Data/statistical analysis	42

3.5	Ethics.....	43
CHAPTER 4: Results		44
4.1	Density	44
4.1.1	Density analysis of surfactants pre-nebulisation.....	44
4.1.2	Density analysis of surfactants post-nebulisation	44
4.1.3	Comparison of Synsurf [®] , Curosurf [®] and Liposurf [®] pre- and post-nebulisation	46
4.2	Viscosity	47
4.2.1	Viscosity of Synsurf [®] samples pre-nebulisation (with and without extrusion).....	47
4.2.2	Viscosity of Synsurf [®] samples post-nebulisation (with and without extrusion)	48
4.2.3	Viscosity analysis of natural surfactants, Curosurf [®] and Liposurf [®] pre- and post-nebulisation	49
4.3	Particle size determination	50
4.3.1	Comparison of Synsurf [®] preparations at day of synthesis (day 0).....	50
4.3.2	Comparison of Synsurf [®] preparations pre- and post-nebulisation	50
4.3.3	Changes in particle size with ageing of Synsurf [®] preparations.....	50
4.3.4	Changes in particle size of extruded Synsurf [®] preparations post-nebulisation.....	51
4.3.5	Particle size analyses of Curosurf [®] and Liposurf [®]	52
4.3.6	Scanning electron microscopy (SEM)	54
4.4	Interfacial surface tension reduction analyses.....	59
4.4.1	Interfacial surface tension reduction of surfactant samples pre-nebulisation	59
4.4.2	Interfacial surface tension reduction of surfactants pre- and post-nebulisation.....	61
4.4.3	Comparison of Synsurf [®] 1, Curosurf [®] and Liposurf [®] post-nebulisation	66
4.4.4	Interfacial surface tension reduction of Synsurf [®] samples with ageing	66

4.4.5	Interfacial surface tension reduction of Synsurf® samples extruded in synthesis	70
CHAPTER 5: Discussion.....		73
REFERENCES		78
APPENDICES/ADDENDUM A		89

List of Figures

CHAPTER 2:

Figure 2.1: Organs and structures of the human respiratory system. A) Normal lungs, showing the organs of the respiratory system, responsible for conducting air to the lungs. B) Shows the respiratory zone of the lung bronchioles leading to alveoli.¹⁵ 11

Figure 2.2: Illustration of airway trees marking the conduction and respiratory zones. Generation of descent is shown on the right-side of the sketch (annotated by Z) starting with the trachea = 0. Respiratory zone starts with respiratory bronchioles at generation = 16.¹⁸ 12

Figure 2.3: Represents a simplistic cycle of pulmonary surfactant (PS). Indicated at the bottom of the sketch, Type II pneumocyte secreting (via exocytosis) PS packed in lamellar bodies (LB) into the hypophase, after secretion, tubular myelin (TM) is formed supplying the surface-associated phase (SAP) with lipids and proteins.³³ ST = surface tension..... 17

Figure 2.4: Shows the typical composition of mammalian pulmonary surfactant, with percentages represented as a total of the surfactant mass analysed. Indicated in green, yellow and orange, the total lipid composition (PC = Phosphatidylcholine, PG = Phosphatidylglycerol, PL = Phospholipids, Chol = Cholesterol, NL = Neutral lipids). Surfactant protein composition is shown in red, indicating surfactant proteins (SP) (A, B, C, D).³² 18

Figure 2.5: Schematic presentation of pulmonary surfactant adsorption to the air-water interface. The movement (by diffusion) of surfactant bilayer (vesicles) structures through the surface-associated phase to the air-water interface. Hydrophobic surfactant proteins SP-B and SP-C (as shown), stabilise the fusion of the bilayer vesicle to the air water interface.³³ 20

CHAPTER 3:

Figure 3.1: Shows the KRÜSS DSA25 instrument, situated at Department of Chemistry and Polymer Science, Stellenbosch University. The enlarged image in the left-hand corner shows the drop as suspended from the pendent drop needle (sample = Synsurf[®] with no addition [PL] = 20 mg/mL). ... 39

Figure 3.2: Experimental set-up for collection of nebulised samples (Synsurf[®] preparations, Curosurf[®], and Liposurf[®]). The image shows the Aeroneb[®]Pro reservoir connected to the dilution container filled with thick nebulised mist generated with Synsurf[®]. 40

Figure 3.3: Flowchart of analytical methods used in the study. Starting with the synthesis and preparations of surfactants (shown at the top of the chart), followed by nebulisation and analyses.....42

CHAPTER 4:

Figure 4.1: Mean density (g/cm³) of Synsurf[®], Curosurf[®] and Liposurf[®], pre- and post-nebulisation at 25°C with PL [20 mg/mL]. * p = 0.0422. ** p = 0.0431 46

Figure 4.2: Average particle size (d.nm) of Synsurf[®] preparations 1 to 6, non-extruded and extruded with a 5 µm and 12 µm filter, post-nebulisation. Bars = SEM 51

Figure 4.3: A SEM image of Synsurf[®] 1 pre-nebulisation. Parameters of the recorded image are shown at the bottom. Arrows indicate the edges of a dehydrated liposome. Scale bar = 2 µm 55

Figure 4.4: A SEM image of Synsurf[®] 1 pre-nebulisation. Visible deflated liposome edges are indicated with black arrows and the inner diameter of another liposome is shown in the black dialog box (1.426 µm). Parameters of the recorded image are shown at the bottom. Scale bar = 2 µm..... 55

Figure 4.5: A SEM image of Synsurf[®] 3 pre-nebulisation. Semi-spherical liposome structures are shown on the surface of the image. Parameters of the recorded image are shown at the bottom. Scale bar = 2 µm..... 55

Figure 4.6: A SEM image of Synsurf[®] 4 pre-nebulisation. Black arrows indicate “beads on a string” like structures formed by liposomes. Parameters of the image are indicated at the bottom, including a bar scale = 10 µm..... 56

Figure 4.7: A SEM image of Synsurf[®] 5 pre-nebulisation showing dense compaction of similar shaped particles. Parameters of the recorded image are shown at the bottom. Scale bar = 2 µm..... 56

Figure 4.8: A SEM image of Synsurf[®] 6 pre-nebulisation. Parameters of the image are indicated at the bottom, including a bar scale = 2 µm..... 56

Figure 4.9: A SEM image of Curosurf[®] post-nebulisation. White measurement circle surrounding liposome = 598.5 d.nm. Parameters of the recorded image are shown at the bottom. Scale bar = 2 µm 57

Figure 4.10: A SEM image of Curosurf[®] post-nebulisation. Parameters of the recorded image are shown at the bottom. Scale bar = 1 µm 57

Figure 4.11: A SEM image of Liposurf[®] post-nebulisation. Parameters of the recorded image are shown at the bottom. Scale bar = 1 µm 57

Figure 4.12: A SEM image of Synsurf[®] 5 post-nebulisation. Parameters of the recorded image are shown at the bottom. Scale bar = 10 µm 58

Figure 4.13: A SEM image of Synsurf[®] 6 post-nebulisation. Parameters of the recorded image are shown at the bottom. Scale bar = 2 µm 58

Figure 4.14: Interfacial surface tension reduction (expressed in % and SEM bar indicated) of pre-nebulisation Synsurf[®] preparations over time. (*: p<0.05 vs Synsurf[®] 1-4)..... 60

Figure 4.15: Interfacial surface tension reduction (expressed in % and SEM bar indicated) of pre-nebulisation Synsurf[®] 1, Curosurf[®] and Liposurf[®] preparations over time. (*: p<0.05 vs Synsurf[®] 1 pre-nebulisation)..... 60

Figure 4.16: Interfacial surface tension reduction (expressed in % and SEM bar indicated) of pre- and post-nebulisation Synsurf[®] 1 preparation over time. The abbreviation Neb signifies the nebulisation status as post-nebulisation..... 61

Figure 4.17: Interfacial surface tension reduction (expressed in % and SEM bar indicated) of pre- and post-nebulisation Synsurf[®] 2 preparation over time. The abbreviation Neb signifies the nebulisation status as post-nebulisation. (*: p<0.05 vs Synsurf[®] 2 pre-nebulised). 62

Figure 4.18: Interfacial surface tension reduction (expressed in % and SEM bar indicated) of pre- and post-nebulisation Synsurf[®] 3 preparation over time. The abbreviation Neb signifies the nebulisation status as post-nebulisation. (*: p<0.05 vs Synsurf[®] 3 pre-nebulised). 62

Figure 4.19: Interfacial surface tension reduction (expressed in % and SEM bar indicated) of pre- and post-nebulisation Synsurf[®] 4 preparation over time. The abbreviation Neb signifies the nebulisation status as post-nebulisation. (*: p<0.05 vs Synsurf[®] 4 pre-nebulised) 63

Figure 4.20: Interfacial surface tension reduction (expressed in % and SEM bar indicated) of pre- and post-nebulisation Synsurf[®] 5 preparation over time. The abbreviation Neb signifies the nebulisation status as post-nebulisation. (*: p<0.05 vs Synsurf[®] 5 pre-nebulised). 63

Figure 4.21: Interfacial surface tension reduction (expressed in % and SEM bar indicated) of pre- and post-nebulisation Synsurf[®] 6 preparation over time. The abbreviation Neb signifies the nebulisation status as post-nebulisation..... 64

Figure 4.22: Interfacial surface tension reduction (expressed in % and SEM bar indicated) of pre- and post-nebulisation Curosurf[®] preparation over time. The abbreviation Neb signifies the nebulisation status as post-nebulisation. (*: p<0.05 vs Curosurf[®] pre-nebulised). 64

Figure 4.23: Interfacial surface tension reduction (expressed in % and SEM bar indicated) of pre- and post-nebulisation Liposurf[®] preparation over time. The abbreviation Neb signifies the nebulisation status as post-nebulisation. (*: p<0.05 vs Liposurf[®] pre-nebulised)..... 65

Figure 4.24: Interfacial surface tension reduction (expressed in % and SEM bar indicated) of post-nebulisation Synsurf® 1, Curosurf® and Liposurf® preparation over time. The abbreviation Neb signifies the nebulisation status as post-nebulisation. (*: $p < 0.05$ vs Synsurf® 1 post-nebulisation). 66

Figure 4.25: Interfacial surface tension reduction (expressed in % and SEM bar indicated) of pre- and post-nebulisation Synsurf® 1 preparation at day 0 and 105, over time. Neb = post- nebulisation. 67

Figure 4.26: Interfacial surface tension reduction (expressed in % and SEM bar indicated) of pre- and post-nebulisation Synsurf® 2 preparation at day 0 and 105, over time. Neb = post- nebulisation. 68

Figure 4.27: Interfacial surface tension reduction (expressed in % and SEM bar indicated) of pre- and post-nebulisation Synsurf® 3 preparation at day 0 and 105, over time. Comparison showed statistical differences between nebulised preparation at day 0 and 105 (shown in orange and yellow) between 600 – 900 seconds. Neb = post- nebulisation. (*: $p < 0.05$ vs Synsurf® 3 post-nebulised day 0)..... 68

Figure 4.28: Interfacial surface tension reduction (expressed in % and SEM bar indicated) of pre- and post-nebulisation Synsurf® 4 preparation at day 0 and 105, over time. Comparison showed statistical differences ($p < 0.05$) between nebulised preparation at day 0 and 105 (shown in orange and yellow). Neb = post- nebulisation. (*: $p < 0.05$ vs Synsurf® 4 post-nebulised day 0). 69

Figure 4.29: Interfacial surface tension reduction (expressed in % and SEM bar indicated) of pre- and post-nebulisation Synsurf® 5 preparation at day 0 and 105, over time. Neb = post- nebulisation. 69

Figure 4.30: Interfacial surface tension reduction (expressed in % and SEM bar indicated) of pre- and post-nebulisation Synsurf® 6 preparation at day 0 and 105, over time. Neb = post- nebulisation. 70

Figure 4.31: Interfacial surface tension reduction (expressed in % and SEM bar indicated) of pre-nebulisation Synsurf® 1 (extruded by 5 µm and 12 µm filter), over time. 71

Figure 4.32: Interfacial surface tension reduction (expressed in % and SEM bar indicated) of post-nebulisation Synsurf® 1, extruded by 5 µm and 12 µm filter, over time. Neb = post- nebulisation 72

List of Tables

CHAPTER 2:

Table 2.1: Incidence of IRDS, related to a decrease in gestational age. The first column indicates the gestational age (intervals 24 - 36 weeks) and classification of prematurity in conjunction with the incidence of each prematurity category (with relation to overall premature births) and incidence of IRDS presenting in neonates at birth or thereafter.¹⁹ 14

Table 2.2: Summary of established and experimental methods for the administration of surfactant replacement therapy. (Adapted from^{4,5}) 16

Table 2.3: Natural and synthetic surfactants. Information is displayed on the tradename, generic name, classification based on composition, source of material, concentration of PL's and manufacturing company (with location) of commercially available and preparations in development.^{30,32,39,46-48} (*Discontinued) (**Biophysical analysis at a PL = [25 mg/mL])⁴⁸ 23

Table 2.4: The three "stages" of particle deposition. Indicated in the central column are and the mean particle diameter sizes of particles (expressed = μm), that will deposit in the indicated anatomical structures of the respiratory tract (right-handed column).⁶⁹ 30

CHAPTER 3:

Table 3.1: Chemicals used in the synthesis and analyses of synthetic and natural surfactant preparations are indicated with the corresponding manufacturing company. 35

Table 3.2: The composition of 6 different Synsurf[®] preparations (# 1 is Synsurf[®] with no additions), 2-6 is Synsurf with the addition of PA, Chol and TriPA prepared for analyses. (*calculated on PL content = 20 mg/mL) 37

CHAPTER 4:

Table 4.1: The mean densities (g/cm^3) of Synsurf[®] preparations (1 to 6), Curosurf[®] and Liposurf[®] pre-nebulisation are expressed in bold, with temperature maintained at 25°C. Additionally, standard deviation (\pm SD) and interquartile range (IQR), which includes p25, median and p75, are indicated. (*:p>0.05 vs Synsurf[®] 5; **:p>0.001 vs Synsurf[®] 5; +:p>0.05 vs Synsurf[®] 2) 45

Table 4.2: The mean densities (g/cm^3) of Synsurf[®] preparations (1 to 6), Curosurf[®] and Liposurf[®] post-nebulisation are expressed in bold, with temperature maintained at 25°C. Additionally, standard deviation (\pm SD) and interquartile range (IQR), which includes p25, median and p75, are indicated. Significant changes (*: p<0.05 vs pre-nebulisation) in density post-nebulisation are marked in blue = decreased and yellow = increased..... 45

Table 4.3: Viscosity (cP) \pm SD of Synsurf[®] preparations with additional extrusion steps (5 μm or 12 μm filter), pre-nebulisation. (*:p<0.05 vs Synsurf[®] 1) 48

Table 4.4: Viscosity (cP) of nebulised preparations, collected from the dilution container. Viscosity is shown for non-extruded and extruded samples post-nebulisation \pm SD. (*:p<0.05 vs pre-nebulisation) 49

Table 4.5: Viscosity cP \pm SD of Curosurf[®] and Liposurf[®] pre- and post-nebulisation. Both surfactants were diluted to a phospholipid concentration of [20 mg/mL]..... 49

Table 4.6: Z-Average particle sizes of preparations pre- and post-nebulisation. The average particle size (\pm SD) is expressed in diameter in nanometres (d.nm) for Synsurf[®] preparations (ageing 105 days and extrusion with a 5 μm or 12 μm filter). Curosurf[®] and Liposurf[®] shown pre- and post-nebulisation. . 53

List of Abbreviations

CHOL	Cholesterol
CI	Confidence Interval
COPD	Chronic Obstructive Pulmonary Disease
CPAP	Continuous Positive Airway Pressure
DLS	Dynamic Light Scattering
DPPC	1,2-Dipalmitoyl-sn-glycero-3-phosphocholine
ET	Endotracheal Tube
HMD	Hyaline-Membrane Disease
IRDS	Infant Respiratory Distress Syndrome
LB	Lamellar Bodies
MV	Mechanical Ventilation
NEB	Nebulised
NISRT	Non-Invasive Surfactant Replacement Therapy
NLs	Neutral Lipids
PA	Palmitic Acid
PC	Phosphatidylcholine
PG	Phosphatidylglycerol
PLs	Phospholipids
POPC	1-palmitoyl-2-oleoyl-sn-glycero-3-phosphocholine
POPG	1-palmitoyl-2-oleoylglycero-3-phosphoglycerol
PS	Pulmonary Surfactant
RDS	Respiratory Distress Syndrome
SAP	Surface-Associated Phase
SD	Standard Deviation
SEM	Scanning Electron Microscopy
SEM	Standard Error of the Mean
SP	Surfactant Proteins
SRT	Surfactant Replacement Therapy
ST	Surface Tension
TEM	Transmission Electron Microscopy
TM	Tubular Myelin
triPA	Tripalmitin

CHAPTER 1: Introduction

Surfactant replacement therapy (SRT) has been established as an effective and safe therapy for premature-related pulmonary surfactant deficiency since the late 1980s.¹ Since then, direct intratracheal instillation of surfactant has been shown to reduce mortality and morbidity in infants with respiratory distress syndrome (RDS) and is the standard mode of administration.^{1,2} However, there have been associated complications that arise from intratracheal instillation which can be divided into two clusters: (1) procedural and (2) physiological complications. Procedural complications include the plugging of endotracheal tubes, hypoxia-induced bradycardia, hemoglobin desaturation and suboptimal deposition (pharyngeal or single lung deposition and suboptimal dosing). Physiological complications include the possible occurrence of pulmonary hemorrhages, mucus plug formation, barotrauma, and hyper- or hypoventilation causing changes in cerebral blood flow.³ Thus, alternative administration techniques have been investigated to reduce the invasive endotracheal intubation or duration thereof. These include laryngeal mask delivery, the INSURE method (short intubation followed by continuous positive airway pressure), nasopharyngeal instillation, aerosolised preparations and intratracheal catheters. However, rapid endotracheal instillation is still the mode of choice to date.^{4,5}

Non-invasive surfactant replacement therapy (NISRT) by means of nebulisation with the use of jet aerosol and ultrasonic nebuliser generators have received ample attention in the past, but showed to be inferior/non-beneficial in comparison to endotracheal administration. NISRT demonstrated technical and clinical challenges due to its sub-optimal intra-pulmonary delivery and variations in clinical effectiveness.^{6,7} The development of an effective SRT by nebulisation would require the surfactant to remain unaltered post-nebulisation and maintain bio-activity with optimal distribution in the distal areas of the lung thus highlighting the importance of surfactant composition and particle size generated by aerosolisation.⁸ Recent advances in nebulisation technologies have paved the way for the possibility of therapy by aerosolisation. Most recently, vibrating mesh nebulisers have emerged, producing highly uniform particles with reduced shear stress on nebulised surfactant which decreases the denaturation of

proteins.¹ Animal studies indicated a >14% increase of pulmonary deposition when using mesh nebulisers compared to the standard jet aerosol generators.^{4,9}

Particle size generated by aerosolisation is an important factor in pulmonary distribution and many deposition studies using glucocorticoids and bronchodilators have indicated that particles should be smaller than 5 μm to be able to surpass the upper airway.⁴ The ideal particle size for optimal distribution in the peripheral regions of the lungs is not clearly defined, but the recommended range has been established between 1000 nm to 3000 nm.^{10,11} However, submicron particles may result in less than desirable deposition resulting in minimal interaction with the lung surface due to reduced gravitational forces and are most likely to be exhaled. Aerosol delivery can be influenced by various factors including aerosol characteristics, particle density, patient interface, device selection and ventilation parameters.¹² For the purpose of this study, emphasis is placed on the biophysical properties of a synthetic surfactant aerosol generated by a vibrating mesh nebuliser. The feasibility of effective nebulisation administration of a novel synthetic surfactant, Synsurf[®], with alterations in composition to assist in bio-activity preservation after aerosol administration is also investigated.

CHAPTER 2: Literature review

2.1 Structure of the lung

The uptake of oxygen and removal of carbon dioxide by the respiratory system is essential to maintain cellular metabolism and acid-base balance. The respiratory system is illustrated in Figure 2.1, and consists of the following organs: nose, pharynx, larynx, trachea, bronchial trees and lungs (containing alveolar sacs (alveoli)).^{13,14} Alveoli, described as small sacs, are shown in the cross section of the lung (Figure 2.1 - **B**).

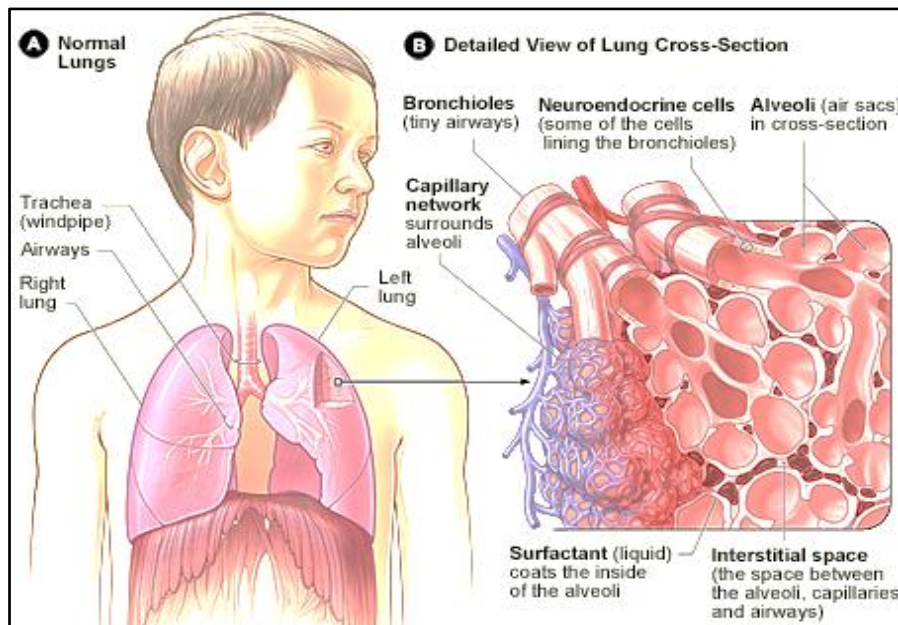


Figure 2.1: Organs and structures of the human respiratory system. A) Normal lungs, showing the organs of the respiratory system, responsible for conducting air to the lungs. B) Shows the respiratory zone of the lung bronchioles leading to alveoli.¹⁵

Inhaled air passes through the nose/mouth, into the pharynx, past the larynx and into the trachea, to the conduction zone which includes (bronchi, bronchioles and terminal bronchioles), this zone is responsible for the movement of air, leading to the respiratory zone (respiratory bronchioles, alveolar ducts and alveolar sacs) as shown in Figure 2.1 (**B**). The respiratory zone is where gas exchange occurs.¹⁶ Figure 2.2 shows 23 generations of branching within the lung, with each descent into the lungs, narrowing, shortening and increase in quantity of structures, allowing for a large surface area

(~ 60 to 100 m²) required for effective gas exchange. The exponential decrease in diameter of each section and zone, limits the deposition of inhaled materials. Only particles with a diameter less than 2 µm are expected to deposit (settle) in the terminal respiratory zone.¹⁷

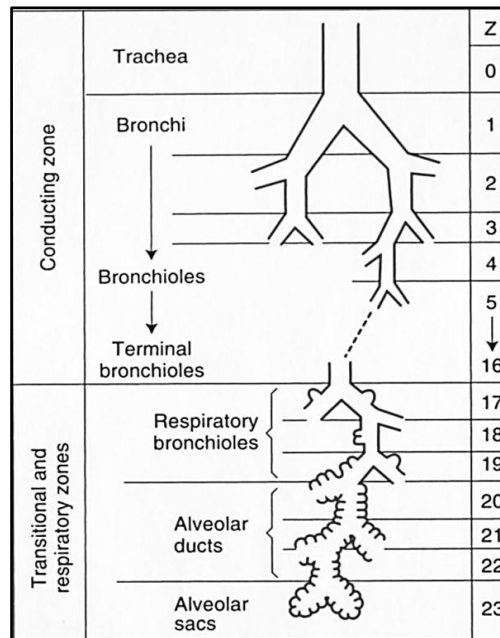


Figure 2.2: Illustration of airway trees marking the conduction and respiratory zones. Generation of descent is shown on the right-side of the sketch (annotated by Z) starting with the trachea = 0. Respiratory zone starts with respiratory bronchioles at generation = 16.¹⁸

2.2 Foetal to neonatal lung adaptation

Intrauterine to neonatal transition is a complex physiological adaptation essential for survival. Effective management and treatment of neonatal pulmonary abnormalities are crucial but remains challenging. However, to understand and treat term and pre-term infant lung abnormalities, it is necessary to comprehend normal pulmonary development and foetal-neonatal transition.¹⁹ Neonatal transition entails three key components that include: (1) the clearance of foetal lung fluid, (2) secretion of pulmonary surfactant and (3) the onset of consistent breathing.²⁰ Although many factors influence the transition from foetal to the neonatal phase, one of the most clinically relevant is the production and secretion of surfactant. Pulmonary surfactant (PS) is essential for surface tension reduction, a process required for stabilising and inflation of alveoli, thus allowing gas exchanges and contributing to stable breathing.^{13,19,20}

2.3 Infant respiratory distress syndrome

Infant respiratory distress syndrome (IRDS) previously known as hyaline-membrane disease (HMD) is the most common respiratory/pulmonary disorder in pre-term infants.¹⁹ IRDS is characterised by a lack of sufficient PS in preterm infants or malfunction in PS in older infants, of different aetiologies (which can include a mutation in associated surfactant proteins).¹⁹

In a review article published in the Bulletin of the World Health Organisation, it was estimated that the global prevalence of pre-term births in 2005 was 12.9 million (which related to 9.6 % of all births worldwide), of which the bulk (85 %) was concentrated in Africa and Asia (collectively 10.9 million). Southern Africa showed a high rate of pre-term births of 17.5% (95% confidence interval (CI) = ranges from 14.6 % to 20.36 %).²¹

Many factors are linked to the risk for developing IRDS, however, with decreased gestation age an increased risk and severity of IRDS is observed as shown in Table 2.1.¹⁹ IRDS is described as progressive and the stages can be clearly distinguished when analysing the radiographic, histopathological and clinical manifestations.²² Infant prematurity results in (1) inadequate PS and a (2) structurally immature lung, resulting in a “mismatch” of ventilation and perfusion that is reflected in the recordings of hypoxia, hypercapnia, acidosis, cell injury and ultimately results in lung injury and respiratory failure.^{22,23} Clinical treatment/management guidelines have received ample attention; however, some controversies exist and have not been resolved.²³ SRT has been deemed essential in the treatment and possible prevention (by prophylactic administration) of IRDS.^{19,21,23}

Table 2.1: Incidence of IRDS, related to a decrease in gestational age. The first column indicates the gestational age (intervals 24 - 36 weeks) and classification of prematurity in conjunction with the incidence of each prematurity category (with relation to overall premature births) and incidence of IRDS presenting in neonates at birth or thereafter.¹⁹

Gestational age	Classification of prematurity	Incidence in pre-mature births (%)	Incidence of IRDS (%)
24 - 25 weeks	Extreme	5%	92%
26 - 27 weeks			88%
28 - 29 weeks	Severe	15%	76%
30 - 31 weeks	Moderate	20%	57%
32 - 36 weeks	Near-Term	60-70%	20-25%

2.4 Surfactant replacement therapy

The first model illustrating the administration of exogenous PS for the treatment of respiratory distress syndrome (RDS) arising from prematurity in the rabbit model was shown in 1972 by Enhörning and Robertson.²⁴ Since then many prevention and treatment strategies have been developed for treatment of infant respiratory distress syndrome (IRDS), this includes SRT, in combination with assisted ventilation and supportive care and can include the administration of antepartum glucocorticoids. The possibility of administering corticosteroids to stimulate the foetal adrenal cortex and accelerating lung maturity has been studied and a decrease in mortality rate is observed.²⁵ However, the long term risks have not been evaluated.²³ Delivery room stabilisation is essential in all pre-term and term deliveries however, some additional stabilisation techniques that include oxygen therapy and positive pressure lung inflation is not evidence based and additional studies need to be conducted.^{19,23}

SRT, is considered the golden standard in the treatment of infants presenting with IRDS. An European consensus guideline published in 2013 stated that the optimal time, dose and best preparation of exogenous surfactant is unclear, at different gestational ages.²³ However, proceeding guidelines (2016) concluded that natural surfactants at a higher initial dose in combination with early rescue therapy should be instated as standard therapy.²⁶ Recommendations for prophylactic administration of SRT is

problematic to construct due to controversies in administration based on gestational age⁵, use of stabilising non-invasive respiratory support²³ and possible downstream financial consideration.

Animal and human studies have indicated that early SRT can reduce ventilatory induced lung injury as the distribution of exogenous surfactant in the lung is optimised.^{27,28} However, due to the necessity for the use of an endotracheal tube (ET) to administer SRT and mechanical ventilation (MV), ethical considerations (due to pain management) and side-effects, an improvement in SRT administration techniques are required.⁵ Currently, rapid instillation, most commonly using endotracheal intubation of exogenous surfactant is the only approved mode of administration in IRDS and is routinely followed by MV. Complications arising from this intervention can include; acute airway obstruction, bradycardia, hypoxia and reduced cerebral blood flow. Prolonged MV can increase the risk of ventilator-associated lung injury, chronic lung disease, and pneumonia. With a notable risk of co-morbidities associated with the use of intubation and MV, the necessity of alternative less-invasive administration techniques has increased.²³ Minimal and non-invasive surfactant therapy which include nasopharyngeal instillation, intratracheal catheters, laryngeal masks and aerosolisation by nebulisation have been suggested as an alternative to the standard endotracheal tube instillation. However, lack of clinical data and technical challenges arising from these techniques have hampered the routine use of alternative modes of administration. Delivery of SRT is under review and many studies have investigated the possibility of alternative administration routes; however, to date no true minimal invasive SRT is being utilised.^{5,23} Table 2.2 explores the advantages/disadvantages of alternative administration routes being investigated and also includes the traditional administration by endotracheal tube instillation.

Table 2.2: Summary of established and experimental methods for the administration of surfactant replacement therapy. (Adapted from^{4,5})

Categories:	Method of administration	Advantages	Disadvantages
Traditional method of administration	Endotracheal tube instillation	Widely used, most studies conducted applied this method	Painful, physiological effects of MV and endotracheal tube.
Minimal invasive surfactant replacement therapy (MISRT)	Nasopharyngeal instillation, laryngeal mask, feeding and intratracheal catheters	Less-painful than traditional methods, supraglottic device, easy to use	Loss of surfactant, and lack of trained personal
Non-invasive surfactant replacement therapy (NISRT)	Aerosolisation	Pain-less, external interface, easy to use and can be applied immediately	Technical challenges

2.5 Composition of endogenous pulmonary surfactant

Healthy lungs contain millions of alveoli (as shown in Figure 2.1), of which the inner walls are coated with an aqueous fluid, described as the hypophase, preventing the desiccation (“drying”) of respiratory epithelium. As the hypophase is aqueous based, high surface tension is generated, which increases the work of breathing and decreases surface area. PS is a membrane based lipid-protein complex, that forms a monolayer on top of the hypophase, decreasing surface tension and maintaining alveolar stability at expiration thus decreasing ventilation difficulty.¹⁴ The composition of human PS (obtained by bronchiolar lavage) is well defined however, in the last decade many studies have been carried out to clarify the purpose of key compounds within PS.^{14,29,30}

2.5.1 Composition of pulmonary surfactant lipids

Type II pneumocytes are responsible for the production and secretion of PS, into the hypophase as tubular myelin (TM) as shown in Figure 2.3. After secretion a monolayer is formed, consisting mainly

of phospholipids (PL's), neutral lipids (NL's) and surfactant-associated proteins (as shown in Figure 2.4).³¹ It is notable to consider that the exact composition of the monolayer formed at the air-water interface is dependent on the phase of the respiratory cycle.

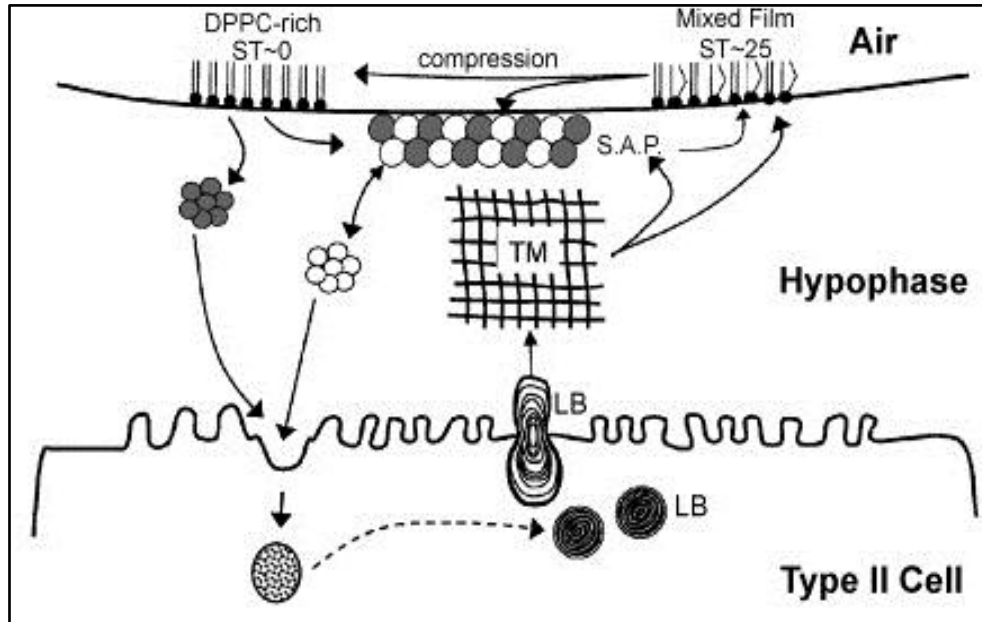


Figure 2.3: Represents a simplistic cycle of pulmonary surfactant (PS). Indicated at the bottom of the sketch, Type II pneumocyte secreting (via exocytosis) PS packed in lamellar bodies (LB) into the hypophase, after secretion, tubular myelin (TM) is formed supplying the surface-associated phase (SAP) with lipids and proteins.³³ ST = surface tension

Lipids are the main constituent in mammalian PS, contributing ~ 90% - 95% of total composition, of which phospholipids (PLs) are predominant.³⁰ Phosphatidylcholine (PC) is the most abundant PL and specific PC compounds include dipalmitoylphosphatidylcholine (DPPC), a saturated PC, containing two saturated acyl chain.^{30,32} Analytical studies comparing the composition of mouse, rat, rabbit, porcine and human PS shows remarkable similarities and differences. However, in all of the species studied, PC was found to contribute at least 80% of the total mass of which approximately half consisted of DPPC.³⁰ Phosphatidylglycerol (PG) and neutral lipids (NLs) (of which cholesterol is the most prevalent) are present in relatively large quantities, contributing significantly to surfactant lipid composition (as shown in Figure 2.4).³⁴ Many other species of PC (phosphatidylserine, phosphatidylinositol) and neutral lipids (cholesterol esters, diglycerides, triglycerides) are present in lower quantities.^{32,34}

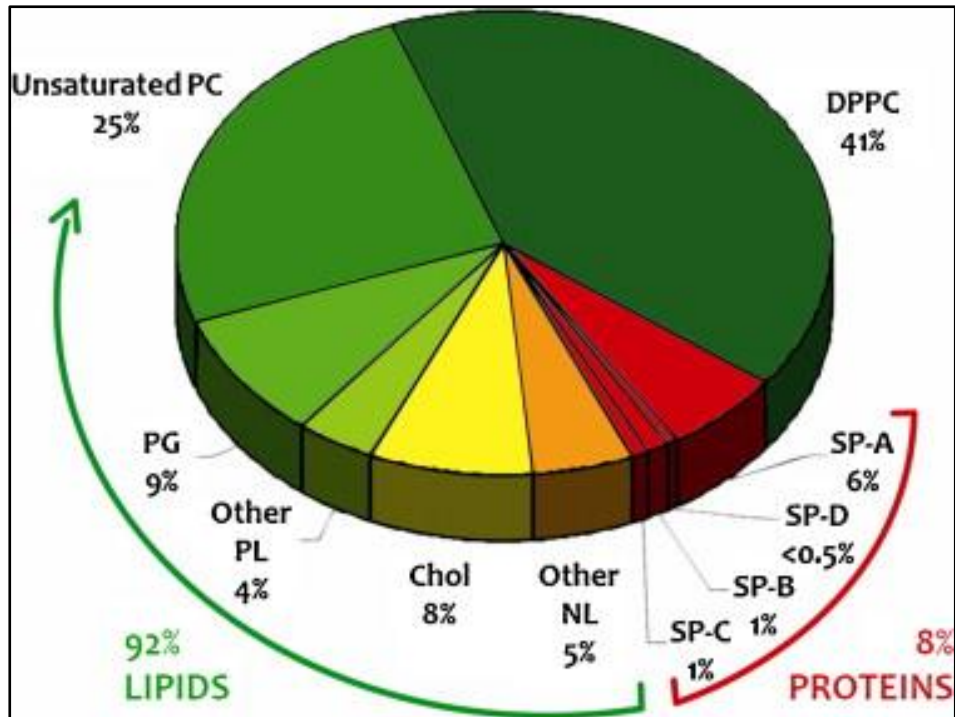


Figure 2.4: Shows the typical composition of mammalian pulmonary surfactant, with percentages represented as a total of the surfactant mass analysed. Indicated in **green**, **yellow** and **orange**, the total lipid composition (PC = Phosphatidylcholine, PG = Phosphatidylglycerol, PL = Phospholipids, Chol = Cholesterol, NL = Neutral lipids). Surfactant protein composition is shown in **red**, indicating surfactant proteins (SP) (A, B, C, D).³²

2.5.2 Pulmonary surfactant-associated proteins

Surfactant proteins (SP) account for approximately ~ 5 % to 10 % of the total weight of PS in humans.³⁰ Four surfactant proteins (SP), have been identified, this includes SP-A, SP-B, SP-C and SP-D (as shown in Figure 2.4). SP-B and SP-C are hydrophobic proteins, expressed by type II cells in the mature lungs and accelerate the adsorption and stabilisation of the monolayer (surface active film), responsible for reducing of surface tension.^{1,35} SP-D and SP-A are collagen based calcium dependent lectins, also known as collectins, involved in pulmonary immunity. By weight SP-A is the most abundant surfactant protein, and is capable of binding lipids, type II pneumocytes and foreign surfaces (e.g. microorganisms).³⁶ Surfactant proteins play prominent roles in surfactant surface behaviour as well as in immune defence and particle clearance however, SP-B and SP-C is clinically the most relevant with regards to the facilitation of surface tension reduction.^{32,36,37}

2.6 Role of lipids in pulmonary surfactant

Differences in attractive forces between molecules at the air-water interface, leads to high surface tension, which resist the expansion of surface area. PS forms a surface active monolayer of approximately 0.8 – 5 nm that actively decreases the surface tension from ~70 m/Nm to near zero values at physiological temperatures.^{1,19,38}

2.6.1 Lipid monolayer structure

The biophysical functionality of the monolayer formed by PS is dependent on its composition. Lipids are responsible for the formation of the surface active film at the air-water interface and additionally provide a matrix for surfactant structure assembly^{31,32} (As shown in Figure 2.5). The monolayer formed at the air-water interface is additionally dependent on the concentration of PL's, as higher concentrations lead to less water molecules exposed to the air, thus lower surface tension. Hydrophilic head groups are orientated towards the “water phase” and hydrophobic acyl groups (on DPPC molecules) are orientated towards the “air phase”.^{30,31}

Lowering in surface tension decreases the energy needed to enlarge the area during inspiration. Lipid and protein components of surfactant can contribute to the biophysical function by either, reducing surface tension like DPPC or assisting in spreading/adsorption of PS's. Lipids show different levels of molecular ordering and mobility, dependent on temperature. This is important when considering the transition of a membrane from a gel phase (ordered state) to a liquid phase (fluid state), when thermal temperature increases or decreases.³⁹ The temperature at which an equilibrium exists between gel and fluid phase is deemed the melting temperature (T_m). For the saturated phospholipid DPPC, the melting point is high ($T_m = \sim 41^\circ\text{C}$) and for unsaturated PC species i.e. 1-palmitoyl-2-oleoyl-sn-glycero-3-phosphocholine (POPC) the melting temperature is low ($T_m = \sim -3^\circ\text{C}$).³⁹⁻⁴¹

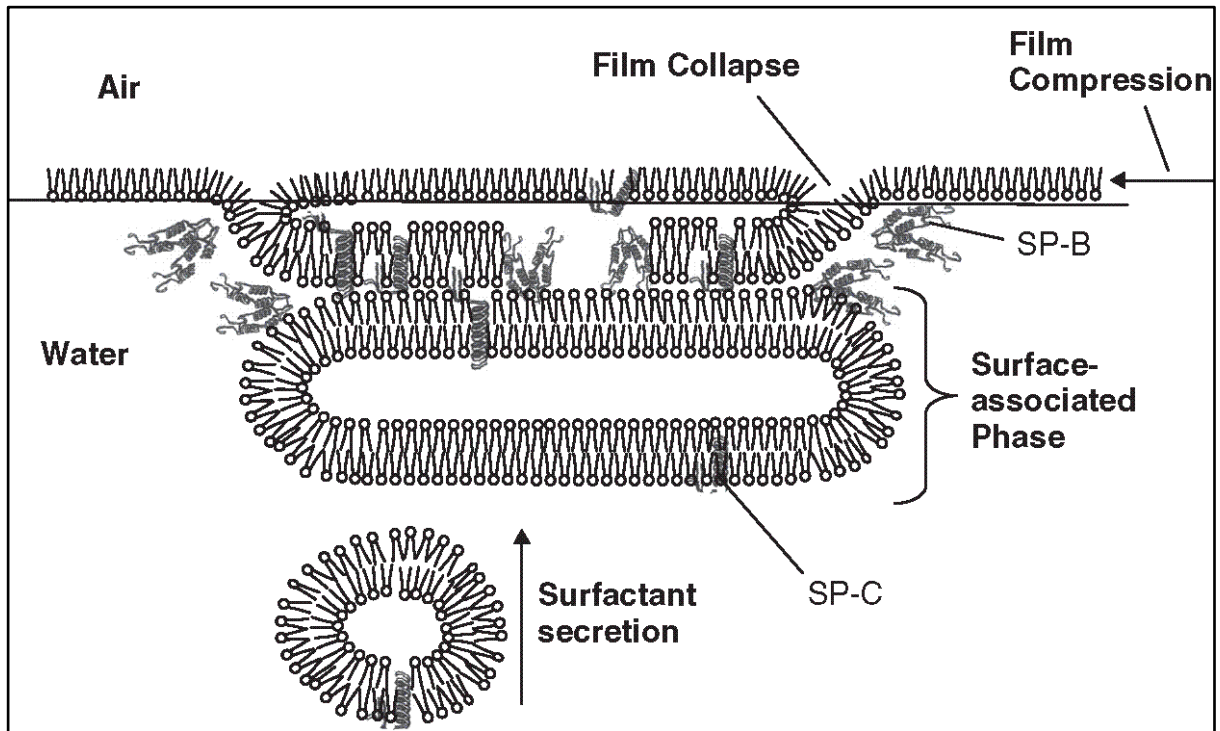


Figure 2.5: Schematic presentation of pulmonary surfactant adsorption to the air-water interface. The movement (by diffusion) of surfactant bilayer (vesicles) structures through the surface-associated phase to the air-water interface. Hydrophobic surfactant proteins SP-B and SP-C (as shown), stabilise the fusion of the bilayer vesicle to the air water interface.³³

As shown in Figure 2.4, PS is a mixture of complex lipids, with a range of melting temperatures, co-existing in liquid and gel phases and presents as a monolayer (at the air water interface) or a bilayer structure within the surface associated phase as shown Figure 2.5. The monolayer formed at the air-water interface, serves as a barrier between the environment and lung epithelium. The fusion of the double layer structure to the surface (to produce a surface monolayer) is facilitated by interactions between PL's and surfactant proteins (SP-B and SP-C). Additionally, SP-B and SP-C, modulate PL permeability, increasing PL flow.⁴² Although the main PL compound in endogenous PS is DPPC, a significant proportion of PL's are unsaturated PC (~ 20 %) and neutral lipids, mainly cholesterol (~ 8%), with melting temperatures below 41°C. This complex mixture of lipids allows native surfactant with a high concentration of DPPC (~ 45 %) to have a transitional (ordered/gel \rightleftharpoons fluid/liquid) temperature close to 37°C.^{30,31,34,43}

The presence of cholesterol might change the packing properties of lipid membranes in PS as the addition of cholesterol has a profound effect on the ordered and fluid state of the membrane. Cholesterol disrupts the highly ordered phase membrane, leading to a more fluid state and orientates the fluid phase membrane, thus decreasing fluidity.³¹ Moreover, cholesterol has a profound effect (even at low concentrations) on the order and adherence properties of monolayer formation, actively lowering the transition temperature of the phospholipid mixture.^{30,31} Other effects have been described which include increased lipid vesicle adsorption at the air-water interface and enhancement of re-spreading and stabilisation of the interfacial monolayer.³⁹ In addition, studies also show that the lateral phase separation can be achieved independent of the presence of SP, and dependent on key lipid components including cholesterol.³¹ However, an increase in cholesterol concentration is linked to the inhibition of bilayer rearrangement and prevents obtainment of low surface tension values.⁴⁴ Other minor lipid components, found in mammalian PS, might contribute to maintain a low surface viscosity thus enabling effective spreading. This is an important consideration when developing an exogenous surfactant as preparations with lower surface viscosity are preferred for ET administration.³⁹

2.6.2 Interfacial film properties

Interfacial film formation includes the adsorption of the lipids and proteins mixture to the air-water interface. The compression a DPPC-enriched monolayer that is formed, is often referred to as “squeezing-out” of non-DPPC components.⁴⁰ DPPC is the surface-active component, and is active in reduction of surface tension (from ~ 70 mN/m) to near-zero values at end-expiration.³⁰ The ability of DPPC in formation of a tight and orderly packed monolayer is due to the lack of double bonds (saturated), which leads to high resistance against collapse.^{29,30} Studies conducted with a captive bubble tensiometer, illustrated that DPPC films could reduce surface tension to less than ~ 2 mN/m and the surface area could be maintained for extended periods of time before returning to equilibrium.⁴⁵ However, due to the high melting temperature of DPPC, formation of a monolayer is slow and therefore, isolated use of DPPC as surfactant replacement is not feasible and the presence of other lipid components that include unsaturated PC and cholesterol is essential.³⁰ On the other hand unsaturated PC is not as effective in the formation of a monolayer as the chains are bent (due to double bonds),

leading to less dense packing conformation.⁴³ PG accelerate the adsorption thus aiding in rapid reduction of surface tension to low (near 0) values. However, film generated with only unsaturated PC (thus lacking DPPC) show an inability to reduce surface tension to low near 0 values (~15 – 20 mN/m) and return the equilibrium as soon as dynamic compression is stopped.³⁹ From this it can be concluded that the combination of DPPC and PG is required for optimal functionality (interfacial film formation). However, it has been stated that in the absence of hydrophobic lipoproteins (like SP-B and SP-C) or an adsorbance-assistance factor, adsorption will be insufficient and/or at a notable decreased rate.⁴³

2.7 Natural derived vs synthetic pulmonary surfactant

Exogenous surfactant is roughly divided into 2 main groups, which includes (1) animal “natural” derived surfactants and (2) synthetic surfactants (contains proteins or peptides). All natural and synthetic surfactants commercially available are DPPC based.^{46,47} A few examples of each group are shown in Table 2.3. It is important to note that not all exogenous surfactants listed are commercially available (some have been discontinued as shown by * moreover, numerous comparative studies have been conducted with the majority of the surfactants shown in Table 2.3 (below).

Table 2.3: Natural and synthetic surfactants. Information is displayed on the tradename, generic name, classification based on composition, source of material, concentration of PL's and manufacturing company (with location) of commercially available and preparations in development.^{30,32,39,46-48}

(*Discontinued) (**Biophysical analysis at a PL = [25 mg/mL])⁴⁸

Brand /Generic Name	Preparation	Animal Source	Concentration PL mg/mL	Manufacturing company
Animal derived surfactants (Porcine and Bovine)				
Alveofact® (Bovactant)	Derived from lung lavage	Bovine	40 mg/mL	Boehringer Ingelheim Co., Ingelheim, Germany
Curosurf® (Poractant)	Derived from animal lung tissue	Porcine	80 mg/mL	Chiesi Farmaceutici SpA (Parma, Italy)
Infrasurf® (Calfactant)	Derived from lung lavage	Bovine	35 mg/mL	Forest Laboratories, Inc., Missouri, USA
Liposurf®	Derived from lung lavage	Bovine	27 mg/mL	BLES Biochemicals Inc., Canada
Survanta® (Beractant)	Derived from animal lung tissue and supplemented	Bovine	25 mg/mL	Abbott laboratories, IL, USA
Protein- free synthetic surfactant				
*Exosurf® (Colfosceril palmitate)	Protein-free (only lipids)	-	13.5 mg/mL	GlaxoSmithKline, Uxbridge, Middlesex, UK
*ALEC® (Pumactant)	Protein-free (only lipids)	-	25 mg/mL	Britannia Pharmaceutical, Redhill, Surrey, UK
Synthetic surfactants containing peptides and recombinant proteins				
CHF5633 (SP-B and SP-C analogue)	SP-B and SP-C enriched synthetic surfactant	-	**80 mg/mL	Chiesi Farmaceutici SpA (Parma, Italy)
*Surfaxin® (Lucinactant)	Peptide-containing (novel KL4 peptide)	-	30 mg/mL	Discovery Laboratories, Warrington, Pennsylvania, USA
Synsurf®	Poly-L-lysine and poly-L-glutamic acid construct	-	60 mg/mL	Innovus, RSA
Venticute® (rSP-C surfactant)	Recombinant SP-C protein	-	50 mg/mL	Nycomed GmbH, Konstanz, Germany

2.7.1 Animal derived “natural” surfactants

Natural derived surfactants differ significantly from each other however, all showcase similar morphology to human surfactant and can be classified by: (1) Origin, most natural surfactants are extracted from bovine or porcine sources, (2) extraction, by means of bronchiolar lavage or minced tissue, and (3) addition of compounds to natural PS (supplementation) that can include PL's and neutral lipids (NL's).⁴⁷

Natural surfactants can be produced by bronchiolar lavage or minced tissue extraction; however, a decreased risk of deactivation of surface-active properties (of extracted surfactant) by plasmatic and/or tissue compounds is observed when isolated by bronchiolar lavage.^{32,47} Curosurf[®] is a porcine lipid extracted surfactant from minced lung tissue, with a final phospholipid concentration of 80 mg/ml (Table 2.3). It consists of 99 % PL's which represents the highest concentration of PL's for an animal derived surfactant and 1 % apoproteins (SP-A and SP-B).^{46,49} During the manufacture of Curosurf[®] an additional purification step (gel-liquid chromatography) is added to remove NL's from the mixture, thus allowing for a higher concentration of polar lipids.⁴⁹ Survanta[®] (Beractant) is an example of a bovine minced lung extract with supplemented with DPPC, free fatty acids (~ 5.6 % to 14 %) and triglycerides (~ 2 % to 7 %).^{38,47} It stands to reason that even with careful preparation of natural surfactants, differences in biochemical composition can occur (possibly due to differences in source of materials), thus some natural preparations are supplemented, mostly with DPPC and palmitic acid.³⁹

Many clinical studies with mortality as the main comparative outcome, have been conducted comparing natural surfactants with each other. However, due to poor enrolment (inadequate sample size) an increased risk of type-2 errors (false negative) is observed.⁵⁰ As shown in Table 2.3 natural surfactants differ significantly from each other with regards to composition, reflecting differences in the therapeutic effects of each preparation. In a recent randomized clinical trial in Iran, Curosurf[®] and Survanta[®] were compared and although no differences could be identified with regards to complications arising from treatment, Curosurf[®] decreased the need for endotracheal tube (ET) and continuous positive airway pressure (CPAP).⁵¹

It is known that Curosurf[®] [PL's = 80 mg/mL] compared to Survanta[®] [PL's = 25 mg/mL] shows a significant decrease in need for re-dosing when administered at an initial dose of 200mg/kg.^{47,52} Although many studies have compared natural surfactants indicating differences in primary outcomes (e.g. need for re-dosing), no differences in the secondary outcomes, which include; occurrence of chronic lung disease, period on MV and mortality, were observed.³⁹

2.7.2 Synthetic surfactants

Synthetic surfactants can be subdivided into (1) protein-free synthetic surfactants, (2) protein analogue containing synthetic surfactants and (3) synthetic peptide-containing surfactants. Composition of synthetic surfactants are carefully planned and surfactant mixtures with a decreased DPPC content prove useful in maintaining surface activity even at concentrations below that of natural surfactant.³⁹ The addition of specific anionic PL (this includes PG), are essential for promoting optimal surface-activity, and most surfactants (natural and synthetic) are DPPC:PG based.^{30,32,39} Another additive/supplement commonly observed in natural and synthetic preparations is palmitic acid (PA). Initial adsorption and re-spreading of surfactant is accelerated by PA, but it is cleared from the air-space rapidly, and does not contribute to the long-term stability of the film. However, the action of PA could potentially assist in rapid action of nebulised preparations, as slow onset has been a concern in previous studies.⁵³ Protein-free synthetic surfactants also known as “old synthetic surfactants” include Pumactant (ALEC[®]) which consists predominantly of dipalmitoylphosphatidylcholine (DPPC) and phosphatidylglycerol (PG) and Colfosceril palmitate (Exosurf[®]), which is no-longer commercially available (as shown in Table 2.3).

Protein and peptide containing synthetic surfactants also named “new generation synthetic surfactants” include (but is not limited to), CHF5633, Lucinactant (trade name: Surfaxin[®]), rSP-C surfactant (Venticute[®]) and Synsurf[®]. The addition of peptides and proteins to PL's is in order to mimic the function of SP-C and/or SP-B.

CHF5633 is a synthetic surfactant containing a phospholipid mixture of DPPC:POPG 1:1 (w/w) with both an SP-B and an SP-C analogue. CHF5366 showed great tolerability and efficacy in animal and

human (Phase 1) studies⁵⁴ with additional resistance to deactivation by albumin in comparison to Curosurf[®].⁴⁸ A related aspect to consider is that the PL concentration of CHF5633 and Curosurf[®] are the same (80 mg/mL), but most studies evaluating the biophysical properties of these surfactants, diluted the preparations to lower concentrations.^{48,55} Recently developed Surfaxin[®] contains a KL4 peptide, believed to mimic the function of SP-B and can be produced in large quantities.⁵⁶ It must be noted that most synthetic surfactants can be used at room temperature; however, Surfaxin[®], is a gel at room and body temperature and requires heating in a water bath for 15 min at 44°C, which might have led to its discontinuation. Moreover, nebulisation attempts with a commercially available vibrating mesh nebuliser (available for purchase at pharmacies or online) showed clogging indicating that the Surfaxin[®] preparation was suboptimal for the equipment, due to high viscosity of the preparation.⁵⁷ Presently a KL4 containing preparation intended for aerosolisation (Aerosurf[®]) in combination with a new aerosolisation technology (capillary aerosol generator), is being developed by Discovery Laboratories (Warrington, Pennsylvania, USA). Initial animal studies with Aerosurf[®], administered by endotracheal tube or aerosol administration (via only capillary aerosol generator) have indicated similar results with regards to improvement of acute lung injury.⁵⁸

Venticute[®] contains synthetic lipids (DPPC, PG and PA) with the addition of recombinant SP-C, produced by SP-C expressed bacteria.³⁹ Synsurf[®] on the other hand is a novel synthetic peptide containing surfactant, that consists of DPPC and PG, complexed with a poly-L-lysine and poly-L-glutamic acid construct that displays cationic and hydrophobic characteristics. The rationale behind this is that poly-L-lysine interacts with the PL bi-layer and provides some structural and/or functional properties, similar to SP-B in native (human) surfactant. Moreover, the overall positive characteristics of poly-L-lysine could possibly also mimic SP-C in a similar fashion. In a rabbit model of surfactant depletion the ability of Synsurf[®] to increase oxygenation by effectively reducing pulmonary shunt was established.^{59,60}

Both natural and synthetic surfactants are effective as prophylactic and rescue therapy in the treatment of IRDS. However, natural surfactants shows superiority with regards to decrease in mortality and ventilatory requirements⁶¹, but a comparison of mortality (due to IRDS), between “new – generation

surfactants” i.e. Lucinactant[®], Survanta[®] and Curosurf[®] are nevertheless similar.^{61,62} Moreover, complications observed in neonates treated with natural surfactants were found to be similar to those treated with synthetic surfactants. However, the therapeutic effects differed amongst preparations used.⁶² To clarify these findings a large-scale, randomized clinical trial will provide the long sought after answers concerning safety and efficacy, although it may be a difficult and even near impossible task.⁶¹

The efficacy of protein-free synthetic surfactants and commercially available natural surfactants have been investigated in many randomized controlled trials, showcasing the ability to reduce mortality and morbidity arising from IRDS. In the clinical setting however, animal derived surfactants are being utilised more often due to superiority over protein-free synthetic surfactants.^{4,47,61,62} This has been attributed to the presence of surfactant-proteins aiding in adsorption, with a fast onset of action. However, studies including recombinant-protein and peptide-containing surfactants vs natural surfactant have indicated no significant difference in primary outcomes which included mortality and chronic lung disease at 36 weeks.⁶³

2.8 Challenges of non-invasive surfactant replacement therapy (NISRT) by aerosolisation

Effective delivery of NISRT is dependent on an amalgamation of factors that include; ventilatory parameters, airway physiology, preparation (drug) composition and aerosolisation device. These factors contribute to the optimal and uniform distribution of surfactant in the lungs.

2.8.1 Aerosol delivery

Aerosols are defined as any suspension, which include liquids and solids, dispensed in a carrier gas.⁶⁴ Two main technologies are currently utilised for the aerosolisation of liquid suspensions, (1) pressurised meter dose inhalers (pMDI's) and (2) nebulisers. Nebulisers can use compressed air or atomised energy to produce a dense mist and will be discussed later in this section.

The administration of dry powdered (solid) surfactant formulations are being investigated and thus far animal studies have generated promising results in the treatment of acute RDS with severe PS dysfunction.⁶⁵ Some natural derived (bovine) surfactants have been freeze-dried to prolong shelf life; however, all suspensions available for the treatment of IRDS are re-suspended in saline and not administered as a powder. For the purpose of this study only liquid formulations were investigated.

The efficacy of an surfactant administered by aerosol is dependent on the dose deposition at the site of action (alveoli), and distribution within the lungs.¹¹ Aerosol deposition is divided into “stages”, referring to the anatomical location and mechanism of deposition within the airway, this includes (1) inertial impaction, (2) gravitational sedimentation and (3) diffusion. Additionally, deposition is dependent on the particle settling velocity (described by aerodynamic diameter (μm) of particles in an aerosol).

Aerodynamic diameter for a particle suspended in air is a hypothetical diameter of a sphere that entails the same density and settling velocity as the particle being investigated. If the particle under investigation has a smooth spherical shape the aerodynamic diameter, is close or equal to the actual diameter. Aerodynamic diameter is used to directly compare the settling behaviours amongst aerosols that might contain particles of non-spherical shape.⁹ However, analysis techniques using high-airflow conditions, are less applicable for imitation of neonatal breathing conditions⁶⁶, thus analysis of the actual particle diameter of by means of laser diffraction is frequently used.

Table 2.4 shows the “stages” or mechanism of deposition with the indicated particle sizes, expected to deposit in the various areas of the airway. Larger particles ($5\ \mu\text{m} - 10\ \mu\text{m}$ in diameter), are expected to deposit in the upper respiratory tract (trachea and bronchi) by means of impaction, due to the turbulent and high air velocity associated with aerosolisation. Impaction is an optimal site for drug deposition in the treatment of asthma and chronic obstructive pulmonary disease (COPD). Sedimentation (shown as the secondary “stage”) is due to a decrease in velocity of air in the secondary bronchus and bronchioles, with particles typically ranging from $1\ \mu\text{m} - 5\ \mu\text{m}$ in diameter. At alveolar level diffusion is believed to be the predominant mechanism of deposition (due to minimal air velocity) of aerosolised preparations, for particles larger than $0.5\ \mu\text{m}$ in diameter.¹¹ Particles smaller than $0.5\ \mu\text{m}$ are expected

to be expelled upon exhalation however, this is based on healthy airway geometry.⁶⁷ Neonates show low tidal volumes and high respiratory rates, in combination with smaller airways, shortening the particle's residence time, thus deposition by sedimentation (requiring sufficient time to settle due to gravitational force) and/or diffusion need to be investigated via deposition studies^{11,66,67} however, due to the inability to use radiolabels in the neonate population, data is limited. Although the aerodynamic diameter of particles are essential for distribution studies, other factors which include particle geometry, morphology and surface properties (surface activity), should be considered in the development of preparations for NISRT.^{4,7,68} For the development of NISRT focus is placed on diffusion (third stage of deposition) and particles with a diameter of less than 2 μm . Brownian motion (diffusion) plays a crucial part in distal lung deposition and is more applicable for particles $<1 \mu\text{m}$.^{65,69} Modelling of turbulent flow in the human lung have shown uniform particle deposition with larger quantities of 1 μm in comparison to particles of 5 μm and 10 μm in diameter.⁷⁰ The involvement of each "stage" is dependent on many factors that include: patient factors and ventilation, biophysical properties of the aerosol and airway anatomy.⁷¹ Consideration of aerosol deposition mechanics are essential, since the objective of NISRT is to deposit sufficient amounts of exogenous surfactant in the distal areas of the lung. However, precision physiochemical planning with regards to the size of particles are required as the respiratory zone is protected from deposition by extensive branching as shown in Figure 2.2. With a decrease in diameter of conduction and respiratory zones, an increased risk of premature deposition in upper respiratory tract is expected.^{9,68,71}

Table 2.4: The three “stages” of particle deposition. Indicated in the central column are and the mean particle diameter sizes of particles (expressed = μm), that will deposit in the indicated anatomical structures of the respiratory tract (right-handed column).⁶⁹

Mechanism	Particle size (diameter in μm)	Anatomical structures
Impaction	5 - 10	Trachea and primary bronchus
Sedimentation	1 - 5	Secondary bronchus and bronchioles
Diffusion (Brownian motion)	1 – 0.5	Alveolar sacs

2.8.2 Patient factors

The application of NISRT in pre-term infants can be challenging due to small tidal volume combined with low inspiratory flow and possible irregular respiratory rates and high risk of obstruction due to narrow upper and lower airways.⁶⁸ The application of MV in combination with aerosol SRT is favoured as the inspiratory time can be significant increased with a reduction in respiratory rate.^{4,68} However, MV is invasive and in addition not always considered for spontaneously breathing infants. Additionally, standard ventilatory care includes the delivery of heated and humidified air. With the application of humidified and heated air an increase in particle size (leading to impaction) and \pm 40% decrease in aerosol lung deposition was observed.⁶⁶ Additional challenges i.e. patient optimal positioning due to low birth weight and physical conformation of equipment with patient interface which is challenging and can lead to additional upper airway and gastric deposition of aerosolised surfactant. Most studies conducted using pre-term infants treated with MISRT and NISRT only included patients from 28 weeks.⁴

2.8.3 Choice of nebuliser

Particle size is influenced by the device used for aerosolisation, this can be demonstrated by the mean diameter of particles generally produced by different nebulisers. Thus the choice of nebuliser is key,

and currently four major types of nebulisers are being considered for NISRT. Ultrasonic nebulisers produce larger particles ranging from (0.5 μm to 3.0 μm) in diameter, depending of the frequency acoustic wave generated by the piezoelectric crystal. However, due to the risk of denaturing proteins within surfactant preparations, ultrasonic nebulisers are not generally considered for NISRT.⁴ On the other hand jet nebulisers break liquid into droplets with the use of high velocity air and particles exposed to the interface/mouth piece can be regulated by a baffle, which will return larger particles to the preparation pool. These nebulisers are cost effective when only considering the device; however, as a large portion of the surfactant sample applied is lost due to residence within equipment, efficacy of jet nebulisers are low when administering surfactant. Moreover, the diameter of droplets generated by jet nebulisers is dependent on characteristic of the liquid (viscosity and surface tension) and the interface of the nebuliser itself which includes airflow and diameter of the attached nozzle. A study conducted using a jet nebuliser illustrated that only $\pm 1\%$ of drug dose reached the distal regions of the lung.⁷

The recently developed vibrating mesh (membrane) nebulisers, produce particles through a mesh by a vibrating action of the piezoelectric plate.¹² Advantages of this technology include, smaller interface, silent operation, reduction in aerosol dilution and the generation of uniform particles. The reduction of shear stress on the preparation allows for nebulisation of proteins and other fragile molecules.^{9,72} However, vibrating mesh nebulisers are not compatible with viscous liquids as clogging is of concern.⁷³⁻
⁷⁵ In another development, Discovery Laboratories introduced capillary aerosol generating technology (CAG), intended for the use in conjunction with Aerosurf[®].⁴ Although this method of aerosol generation is known, the technology was not available for analysis at the time of this review.

2.8.4 Aerosol deposition studies

The first trial reporting the use of a synthetic surfactant using nebulisation was published in 1964. DPPC was nebulised with a jet generator and introduced into the incubator however, no clinical relevant beneficial effects were observed but it could be concluded that for aerosolisation the preparation would need to be monodisperse (uniform in mass and morphology in the dispersed phase) and particles no larger than 1 μm in diameter.⁷⁶ Although many studies have been conducted with the use of an array of

nebulisers and commercial/experimental exogenous surfactants, to date no nebulised surfactant is being utilised in the treatment of IRDS.⁵

Animal studies comparing direct tracheal instillation to nebulisation have reported mixed outcomes.⁵ However, a study indicated that Survanta[®] showed an equal and superior efficacy when nebulised compared to tracheal instillation of animal bronchiolar lavage derived surfactants.⁷⁷ This is a clear indication that composition and delivery are closely interlinked and modulate the interaction of surfactant with the pulmonary environment independent of the surface active component and concentration in the preparation. Although limited studies are available comparing nebulised surfactant in the treatment of IRDS, the findings and outcomes of these studies have provided essential information for the development of more effective preparations.⁴ Studies evaluating the effect of Curosurf[®] administered by nebulisation with the addition of CPAP showed no changes in the period on MV or duration of CPAP compared to infants only receiving CPAP. This could be indicative for the need of aerosol preparation refinement.⁵³ An open-label pilot study conducted with Aerosurf[®] nebulised with a vibrating mesh nebuliser showed good tolerability and feasibility of administration. Although the study did not include a control group, the primary outcome was to assess the viability of the method of administration. The particles generated maintained bio-activity (i.e. ability to reduce surface tension), post-nebulisation.⁵⁶

2.8.5 Physiochemical conditioning of synthetic surfactant mixture

The development of a synthetic surfactant intended for nebulisation, could provide a safe, non-invasive alternative to conventional SRT. However, physiochemical conditioning with regards to the surfactant composition (formulation) needs to be investigated as this, in combination with patient factors and device selection will influence the deposition and activity of NISRT.¹² Modification and design of an aerosol for optimal functionality (termed aerosol conditioning⁷⁴), includes aspects such as the (1) composition, (2) particle size generated, (3) preservation of bio-activity and (4) lower preparation viscosity⁷⁴ (liquid consistency), to avoid clogging⁷⁴ of nebulisation equipment. Thus for successful application of NISRT, DPPC (surface-active compound) and assisting compounds (e.g. cholesterol,

palmitic acid and peptides) particles ideally should range from 0.5 μm to 2 μm ⁶⁵ and must rapidly deposit to form a DPPC-rich monolayer.³²

2.9 Study Rational

The main purpose of this study was to evaluate the suitability of a synthetic pulmonary surfactant, Synsurf[®] for aerosolisation with additions in composition, to aid in the bioactivity of particles generated by nebulisation. Additionally, Synsurf[®] (a synthetic surfactant), was compared to natural (animal derived surfactants), based on key considerations for the development of aerosol delivery of SRT. Due to a lack of information regarding development of a synthetic lung surfactant intended for nebulisation, biophysical properties need to be defined that include: viscosity of samples (relating to compatibility with nebulisation equipment), surface activity and particle size after nebulisation, thus leading to the aims of this study.

2.10 Aims

As part of an on-going development program of a novel synthetic peptide-containing surfactant, Synsurf[®] (Stellenbosch University Patent No. 2012/06987), we want to develop and optimise the composition of this product for non-invasive administration of SRT i.e.

1. Development of an ideal formulation of synthetic surfactant with regards to different concentrations of phosphatidylglycerol (PG), the disaturated phospholipid dipalmitoylphosphatidylcholine (DPPC), cholesterol, tripalmitin and palmitic acid for nebulisation.
2. Establish nebulised liposome stability with age, size, surface tension properties and viscosity of these preparations.

Results obtained can contribute to development of an aerosolised synthetic surfactant for use in the treatment of IRDS.

2.11 Research Objectives

- i. To prepare synthetic surfactant, Synsurf[®] with the addition of varying concentrations of cholesterol (Chol), tripalmitin (triPA) and palmitic acid (PA).
- ii. To examine changes in particle characteristics with the use of laser diffraction and determine the stability of particles within different preparations post-nebulisation, by the use of a vibrating mesh (membrane) nebuliser.
- iii. To determine changes in density, viscosity and surface tension of surfactant preparations under (i), and compare findings to commercially available natural surfactant, Curosurf[®] and Liposurf[®] at a similar PL concentration (20 mg/mL).
- iv. To extrapolate the results obtained and contribute to future deposition studies for the development of an optimal formulation and preparation (by possible extrusion) of Synsurf[®] surfactant, administered by nebulisation.

CHAPTER 3: Experimental Materials and Methods

3.1 Materials

Chemicals used and company/source are shown in Table 3.1. All chemicals used were of the highest analytical grade. Curosurf[®] (poractant alfa, porcine PS, classified as a natural surfactant) and Liposurf[®] (bovine lipid extract surfactant, classified as a natural surfactant) were analysed in the same way as Synsurf[®] preparations, with regards to density, viscosity, particle characteristic pre- and post-nebulisation and surface tension lowering ability. Curosurf[®] (containing 80 mg/mL phospholipid) and Liposurf[®] (containing 27 mg/mL phospholipid) were diluted with (0.1M NaCl) to an overall phospholipid concentration of 20 mg/mL, thus all surfactants used in the study had a final PL concentration of 20 mg/mL.

Table 3.1: Chemicals used in the synthesis and analyses of synthetic and natural surfactant preparations are indicated with the corresponding manufacturing company.

#	Chemical/Material	Company/Source
1	1,2 Dipalmitoyl-L- α -phosphatidylcholine (DPPC)	Avanti Polar Lipids (Alabaster, Alabama, USA)
2	1,2-Dipalmitoyl-L- α -phosphatidylglycerol (PG)	Sigma-Aldrich (St Louis, Missouri, USA)
3	1-Hexadecanol (Cetyl alcohol)	Sigma-Aldrich (St Louis, Missouri, USA)
4	Tyloxapol - BioXtra	Sigma-Aldrich (St Louis, Missouri, USA)
6	Poly-L-lysine (Molecular weight 16 kDa)	Sigma-Aldrich (St Louis, Missouri, USA)
7	Poly-L-glutamic acid (Molecular weight 12 kDa)	Sigma-Aldrich (St Louis, Missouri, USA)
8	Cholesterol (Chol)	Sigma-Aldrich (St Louis, Missouri, USA)
9	Glyceryl Tripalmitate (Tripalmitin) (triPA)	Sigma-Aldrich (St Louis, Missouri, USA)
10	Palmitic Acid (Hexadecanoic Acid) (PA)	Sigma-Aldrich (St Louis, Missouri, USA)
11	Sterile filtered water	Sigma-Aldrich (St Louis, Missouri, USA)
12	NaCl (0.1 M solution)	Sigma-Aldrich (St Louis, Missouri, USA)
13	Chloroform (CHROMASOLV [®] -plus for HPLC)	Sigma-Aldrich (St Louis, Missouri, USA)

3.2 Research Design

3.2.1 Preparation of synthetic pulmonary surfactant Synsurf[®]

Synsurf[®] was synthesised as described previously by, van Zyl JM, Smith J & Hawtrey A.⁶⁰ Table 3.2 show the different preparations of Synsurf[®] used in this study.

Synsurf[®] was prepared by gently mixing DPPC, 1-Hexadecanol and PG (with the addition of Chol, TriPA and/or PA – see Table 3.2) in chloroform until all constituents were dissolved. The DPPC: Hexadecanol: PG: Additive (Chol, triPa, PA) mixture was transferred to a round-bottomed (250 mL) flask and kept at room temperature (23°C) for 90 min. Thereafter organic solvent (chloroform) was removed via rotary evaporation for 15 min at 37°C. The remainder of organic solvent was removed by continuous flow of N₂ gas and the dried lipid mixture was stored overnight (sealed under N₂). The dried lipid mixtures were hydrated with NaCl-solution which included a poly-L-lysine and poly-L-glutamic acid construct (4.35 %). After the addition of the construct and NaCl-solution, the mixture was stored for an additional 12 hours, under N₂, for optimal hydrating of lipids. Larger multimellar vesicles were disrupted via ultrasonification to produce smaller unimellar vesicles. Ultrasonification was done with a Qsonica Q500 (Newton, Connecticut, USA) with a tip diameter of 25 mm. The amplitude was 30 µm and a total energy of ~ 7550 J was applied. After ultrasonification, preparations were rested overnight under N₂ atmosphere (at 4°C). Tyloxapol was added and the mixture stirred thoroughly, followed by an additional resting period of 12 hours under a N₂ environment at 4°C. After the final resting period preparations were stored in sterile vials under N₂, at 4°C, ready for analysis. The final PL concentration was 20 mg/mL.

Table 3.2: The composition of 6 different Synsurf[®] preparations (# 1 is Synsurf[®] with no additions), 2-6 is Synsurf with the addition of PA, Chol and TriPA prepared for analyses. (*calculated on PL content =20 mg/mL))

Code	Synsurf [®] samples with additions	Composition
1	Synsurf [®] with no additions	20 mg/mL PL
2	Synsurf [®] + Palmitic acid	20 mg/mL PL + *11 % PA
3	Synsurf [®] + 2 % Cholesterol	20 mg/mL PL + *2 % Chol
4	Synsurf [®] + 2 % Cholesterol + Palmitic acid	20 mg/mL PL + *2 % Chol + *11 % PA
5	Synsurf [®] + 1 % Cholesterol	20 mg/mL PL + *1 % Chol
6	Synsurf [®] + Palmitic acid + Tripalmitin	20 mg/mL PL + *11% PA + *7 % triPA

3.2.2 Liposome preparation and extrusion

Extrusion is used to reduce the size and lamellarity of vesicles within lipid mixtures, thus refining target size of liposomes that increases stability.⁷⁸ Thus including the process of extrusion during the synthesis of Synsurf[®] preparation, assists in the attainment of liposomes within the recommended size range.

To investigate the effect of extrusion on particle characteristics and bio-activity (surface tension lowering ability), 10 mL of Synsurf[®] samples (as shown in Table 3.2) were extruded with a LiposoFast[®] LF-50 instrument at 600 psi/ 40 bar. The temperature was maintained with a water bath regulated sleeve at 45°C. Extruded samples were stored in sterile vials and used for analysis within one week of extrusion.

3.2.3 Ageing and long-term storage of samples

Synsurf[®] preparations sealed in sterile vials (under N₂) were aged at 4°C, for 105 days (15 weeks), after which the samples were analysed for changes in bio-activity and particle characteristics. These analyses were included to establish a preliminary “shelf-life” of Synsurf[®] with additions.

3.2.4 Density experiments

For the analysis of surface tension, with the DSA25, the difference in density of the surrounding phase (air for non-submerged pendant drop) and liquid used for drop, is required. The densities of all samples were determined by the use of an AccuPyc™ 1330 Pycnometer at Cape Peninsula University of Technology (CPUT), Chemical Engineering Laboratories. Pure water (Sigma-Aldrich®) was tested before each run with temperature maintained at $25.0^{\circ}\text{C} \pm 0.2^{\circ}\text{C}$ and displayed a density of $0.996 \pm 0.03 \text{ g/cm}^3$. This is in accordance with the biophysical properties of pure water by Sigma-Aldrich® of 0.9970 g/cm^3 at 25°C . Analyses were conducted at 25°C to determine density for each Synsurf®, Curosurf® and Liposurf® surfactant preparation, pre- and post-nebulisation (n=5).

3.2.5 Liquid surface tension experiments

A drop shape analysis system by KRÜSS (DSA25, KRÜSS Inc., Germany) was used to determine the semi-dynamic surface tension changes over time of prepared surfactant samples. KRÜSS DSA25 instruments (Figure 3.1) located at the Department of Chemistry and Polymer Science laboratories at Stellenbosch University, Nutec Digital Ink (Pty) Ltd, Ottery and University of Western Cape, Chemistry Department were used (depending on the availability). The instruments (DSA25) were calibrated with distilled water with a surface tension value of 72 mN/m (as recommended by operational/software manual). After the addition of density values (as determined in 3.3.4) to the software data base, samples were suspended from a steel needle as shown in Figure 3.1 in the upper left corner.⁷⁹ Surface tension changes were recorded over 900 seconds (15 min). All analyses were completed in triplicate. Decrease in surface tension was calculated by means of a normalization ratio, determined by the initial reading at time point 0 (for each sample), divided by the decreasing values recorded at 15 second intervals.

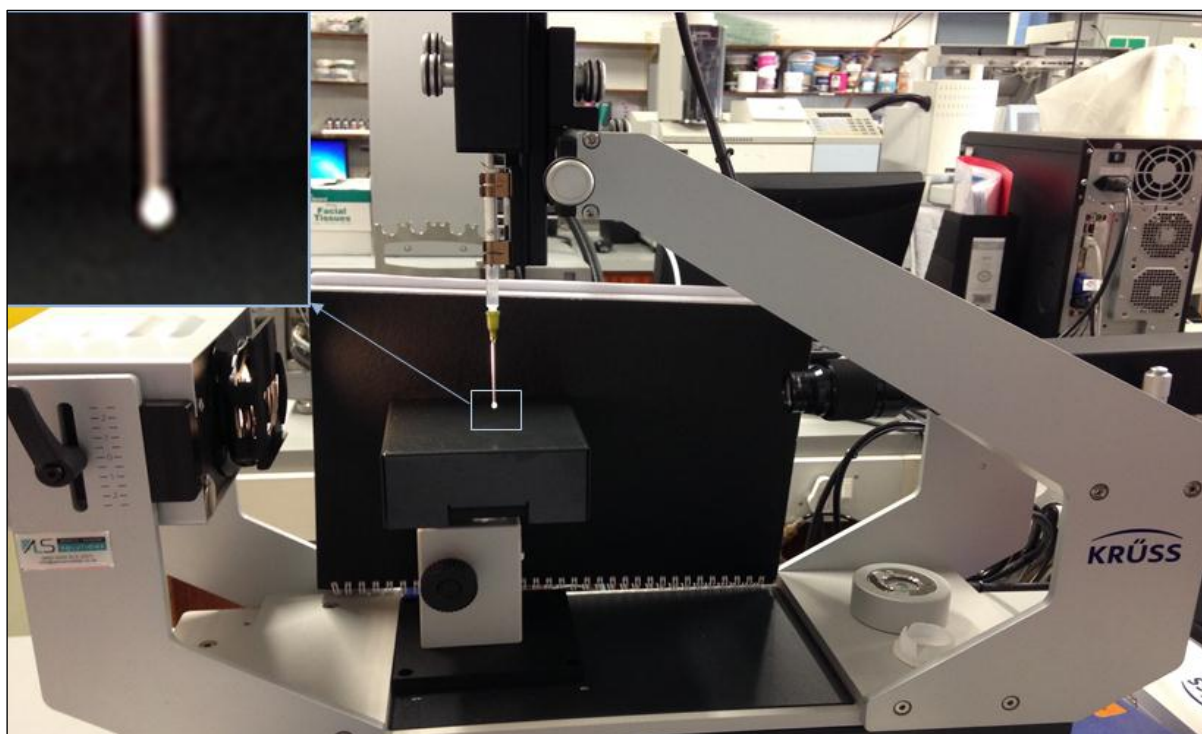


Figure 3.1: Shows the KRÜSS DSA25 instrument, situated at Department of Chemistry and Polymer Science, Stellenbosch University. The enlarged image in the left-hand corner shows the drop as suspended from the pendent drop needle (sample = Synsurf[®] with no addition [PL] = 20 mg/mL).

3.2.6 Viscosity experiments

The viscosity of samples could be semi-quantified with the use of Leja[®] 4-Chamber slides with defined dimensions (depth 20 μm , length 21 mm, width 6 mm). The viscosity of a specific fluid indicates the resistance against natural flow. Thus the theoretical assumption is made that a linear relationship exists between filling time of the slide and the viscosity of the specific liquid.⁸⁰ Leja[®] 4-Chamber precision slides were purchased from Delfran (Pty) Ltd. Slides were placed on a level surface and filling times were recorded with a stopwatch. Filling times were logged between applications of the sample at the inlet of the slide until the tapered outlet of the slide was reached. Pure water was used as a control, with the temperature maintained close to 25°C (0.912 ± 0.02 cP). All analyses were completed in triplicate. Conversion tables as provided by the Leja[®] official website were used to convert the filling times to centipoise (cP).⁸¹

3.2.7 Surfactant preparation nebulisation experiments

Synsurf[®] preparations (aged and extruded samples included), Curosurf[®] and Liposurf[®] were nebulised with the use of the Aeronet[®]Pro vibrating mesh nebuliser. An experimental set-up for aerosol delivery and capturing of generated surfactant particles was constructed, which consisted of the Aeronet[®]Pro nebuliser, connected to a glass dilution container and a medical oxygen line that propelled the aerosol into the dilution container (Figure 3.2). A flow regulator was fitted to the medical oxygen line to maintain the oxygen flow rates at 2.0 L/min. All samples were nebulised for 10 min and liquid collection from the dilution container was sealed in glass vials, and used for analyses thereafter.



Figure 3.2: Experimental set-up for collection of nebulised samples (Synsurf[®] preparations, Curosurf[®], and Liposurf[®]). The image shows the Aeronet[®]Pro reservoir connected to the dilution container filled with thick nebulised mist generated with Synsurf[®].

3.2.8 Particle characterisation

Z-Average particle size:

Particles within samples which included Synsurf[®], Curosurf[®] and Liposurf[®] preparations were analysed with the use of a Malvern Zetasizer[®] Nano-S ZEN 1600 stationed at the Chemistry and Polymer Science

laboratories at Stellenbosch University. The z-average particle size, is a hydrodynamic parameter, and can only be analysed for molecules in a suspension with dynamic light scattering (DLS). Z-average size is typically larger than “dry-particle” analyses (this can include SEM and TEM), and particles size is dependent on the concentration of the solution (this includes particle structure) and the ion contents.⁸² NaCl-solution (0.1 M) was prepared with sterile water and filtered with a 0.22 µm nylon filter attached to a standard sterile 10 ml syringe. Nebulised samples collected from the dilution container generated during nebulisation as well as non-nebulised samples were diluted 1:2 with filtered NaCl-solution and placed in a standard polystyrene cuvette (10 x 10 x 45 mm). The cuvette was filled to 1/3 of its total capacity. Z-average particle size (expressed as diameter in nanometres (d.nm)) was recorded as calculated by the software. Results included (13 x 3) particle analyses per run done in triplicate at 25°C. The poly dispersion index (Pdi) (ranging from 0 to 1) is a size distribution parameter and values closer to 0 indicate monomodal (near spherical shape) and/or monodisperse (narrow width of distribution) particles. A Pdi ranging from 0.7 to 1 will be rejected as the sample is not suitable for DLS analyses. For the optimal operation of the software (calculations), the Pdi range from 0.08 to 0.7.⁸³

Visualisation of particles by scanning electron microscopy (SEM):

Particles within nebulised and non-nebulised samples of Synsurf[®], Curosurf[®] and Liposurf[®] were visualised with the use of ZEISS EVO MA15VP, scanning electron microscope (SEM) located at the Central Analytical Facility of Stellenbosch University. Microparticles were prepared by placing a droplet (of the liquid surfactant) on a “stub” (sample holder) covered with a 1 cm x 1 cm piece of double sided carbon tape. After drying in an enclosed glass dome, (for a period of 24 hours in atmospheric air at room temperature), samples were coated with a thin layer of gold to ensure conductivity required for accurate measurements and images generated were saved on the instrument software.

3.3 Overview of research design

The flowchart below provides an overview of the research design and includes: synthesis, preparation and analyses of synthetic and natural surfactants.

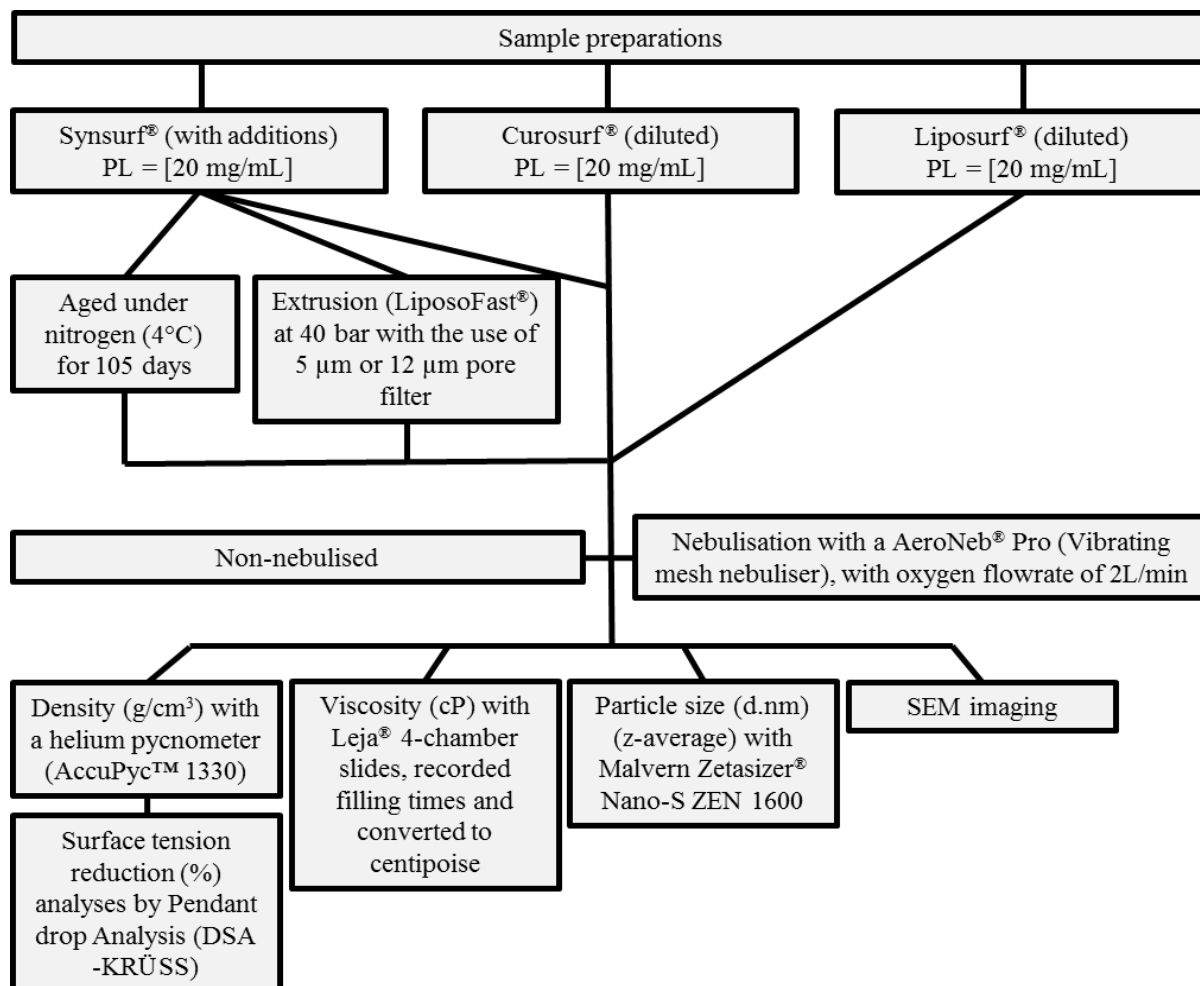


Figure 3.3: Flowchart of analytical methods used in the study. Starting with the synthesis and preparations of surfactants (shown at the top of the chart), followed by nebulisation and analyses.

3.4 Data/statistical analysis

Data analyses were conducted by the Centre of Evidence-Based Health Care, Stellenbosch University. A non-parametric, Kruskal–Wallis test was used and data are expressed as mean \pm standard deviation, p25, median (p50) and p75. Additionally, all particle size data (nm in diameter) falling within the size requirements are investigated based on mean \pm CI (95%). The confidence interval (CI) of 95% was

calculated based on the mean and significant difference was accepted at p-values of < 0.05 . Surface tension decrease (DSA25 experiments) was re-calculated to give a normalisation ratio (initialising at 100% at time point 15 seconds – based on the initial reading), and preparation's ability to decrease surface tension, was compared by utilising a rank correlation test (Spearman's rank correlation). This method is used frequently⁸⁴ as no assumptions are made about the underlying density parameters. Analyses included all data collected over 15 min at 15 second intervals ($n = 3$). However, for simplicity only time points (15, 150, 300, 450, 600, 750, 900 seconds) are indicated on graphs (See Results 4.4). Spearman's rank correlation coefficient (ρ), with a value of less than 0.4 indicate a non-linear decrease in surface tension and two variables were considered to show significant correlation at p-values < 0.05 .

3.5 Ethics

Ethics approval by the Health Research Ethics Committee 2 (HREC 2) of Tygerberg Campus, Stellenbosch University for this project was granted from 01 June 2015 to 01 June 2016 under the reference code: S15/04/088. Re-application with the submission of a progress report in 2016 was successful, and extension was granted from 09 March 2016 to 08 March 2017 under the reference code stated above.

CHAPTER 4: Results

4.1 Density

Density (ρ) of liquid preparations, which included Synsurf[®] (Syn), Curosurf[®] and Liposurf[®] were evaluated pre- and post-nebulisation, Table 4.1 and Table 4.2.

4.1.1 Density analysis of surfactants pre-nebulisation

Synsurf[®] preparations exhibited an array of densities ranging from 1.106 g/cm³ to 1.235 g/cm³ (Table 4.1). Statistical comparison indicated that the density of Synsurf[®] 5 (Chol [1 %]) is significantly higher than that of Synsurf[®] 1 (*p < 0.05), Syn 2 (**p < 0.001) and lower than, Syn 6 (*p < 0.05). In addition, the density of Synsurf[®] 2 in comparison to Syn 3 is significantly lower (p < 0.05). Synsurf[®] 4 (PA and Chol [2 %]) indicated no considerable differences in density in comparison to the other preparations analysed. This also includes the densities of the natural surfactants, Curosurf[®] and Liposurf[®].

4.1.2 Density analysis of surfactants post-nebulisation

A comparison of surfactant samples pre- and post-nebulisation showed a significant decrease in density in most preparations post-nebulisation. This included Synsurf[®] 4, 6 and Liposurf[®] as indicated in blue in Table 4.2. However, Synsurf[®] 3, 5 and Curosurf[®] showed an increase in density post-nebulisation as marked in yellow in Table 4.2. Statistical analysis (Wilcoxon signed rank test) indicated that only Synsurf[®] 1 and 2 displayed no differences when nebulised, while the densities of all other surfactant preparations were significantly different post-nebulisation (*p < 0.05), with either an increase or decrease.

Table 4.1: The mean densities (g/cm^3) of Synsurf[®] preparations (1 to 6), Curosurf[®] and Liposurf[®] pre-nebulisation are expressed in bold, with temperature maintained at 25°C. Additionally, standard deviation (\pm SD) and interquartile range (IQR), which includes p25, median and p75, are indicated. (*: $p > 0.05$ vs Synsurf[®] 5; **: $p > 0.001$ vs Synsurf[®] 5; +: $p > 0.05$ vs Synsurf[®] 2)

#	Sample Name:	PRE-NEBULISATION				
		Mean density (g/cm^3)	\pm SD	IQR		
				p25	Median	p75
1	Synsurf [®]	1.128*	± 0.002	1.126	1.126	1.129
2	Synsurf [®] with palmitic acid (PA) [11 %]	1.106**	± 0.003	1.106	1.107	1.108
3	Synsurf [®] with cholesterol (Chol) [2 %]	1.123⁺	± 0.004	1.121	1.125	1.126
4	Synsurf [®] with palmitic acid (PA) [11 %] + cholesterol (Chol) [2 %]	1.148	± 0.002	1.145	1.149	1.149
5	Synsurf [®] with cholesterol (Chol) [1 %]	1.187	± 0.012	1.184	1.187	1.193
6	Synsurf [®] with palmitic acid (PA) [11 %] + tripalmitin (triPA) [7 %]	1.235*	± 0.011	1.230	1.239	1.244
OTHER SURFACTANTS: PRE-NEBULISATION						
C	Curosurf [®] (Diluted = PL [20 mg/mL])	1.151	± 0.008	1.143	1.151	1.157
L	Liposurf [®] (Diluted = PL [20 mg/mL])	1.161	± 0.006	1.164	1.164	1.165

Table 4.2: The mean densities (g/cm^3) of Synsurf[®] preparations (1 to 6), Curosurf[®] and Liposurf[®] post-nebulisation are expressed in bold, with temperature maintained at 25°C. Additionally, standard deviation (\pm SD) and interquartile range (IQR), which includes p25, median and p75, are indicated. Significant changes (*: $p < 0.05$ vs pre-nebulisation) in density post-nebulisation are marked in blue = decreased and yellow = increased.

#	Sample Name:	POST-NEBULISATION				
		Mean density (g/cm^3)	\pm SD	IQR		
				p25	Median	p75
1	Synsurf [®]	1.124	± 0.004	1.123	1.123	1.124
2	Synsurf [®] with palmitic acid (PA) [11 %]	1.110	± 0.004	1.109	1.110	1.112
3	Synsurf [®] with cholesterol (Chol) [2 %]	1.151*	± 0.003	1.150	1.151	1.151
4	Synsurf [®] with palmitic acid (PA) [11 %] + cholesterol (Chol) [2 %]	1.108*	± 0.004	1.106	1.110	1.111
5	Synsurf [®] with cholesterol (Chol) [1 %]	1.234*	± 0.001	1.227	1.238	1.243
6	Synsurf [®] with palmitic acid (PA) [11 %] + tripalmitin (triPA) [7 %]	1.082*	± 0.012	1.082	1.238	1.087
OTHER SURFACTANTS: POST-NEBULISATION						
C	Curosurf [®] (Diluted = PL [20 mg/mL])	1.198*	± 0.001	1.188	1.196	1.207
L	Liposurf [®] (Diluted = PL [20 mg/mL])	1.153*	± 0.008	1.151	1.152	1.154

4.1.3 Comparison of Synsurf[®], Curosurf[®] and Liposurf[®] pre- and post-nebulisation

Synsurf[®] 1 (original formulation) showed no change in density after nebulisation (Figure 4.1). On the other hand, Curosurf[®] displayed an increase in density ($\pm 3.9\%$) post- nebulisation, while Liposurf[®] showed a decrease ($\pm 0.7\%$). Both changes were found to be significant as indicated in the Figure 4.1

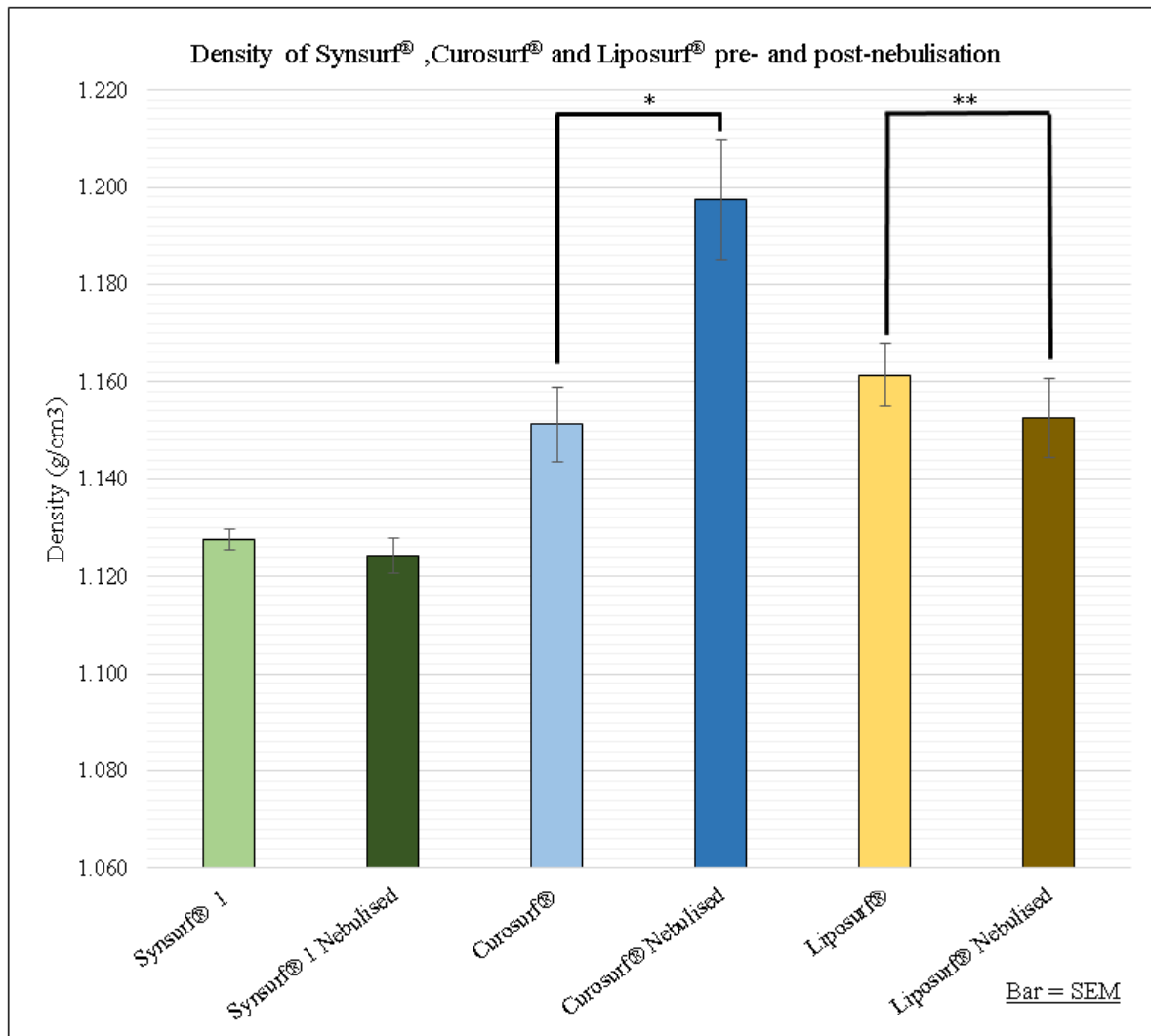


Figure 4.1: Mean density (g/cm³) of Synsurf[®], Curosurf[®] and Liposurf[®], pre- and post-nebulisation at 25°C with PL [20 mg/mL]. * p = 0.0422. ** p = 0.0431

4.2 Viscosity

Results of viscosity determination of Synsurf[®] preparations pre- and post-nebulisation (with and without extrusion through a 5 µm and 12 µm filter), Curosurf[®] and Liposurf[®] are shown in Table 4.3, 4.4 and 4.5.

4.2.1 Viscosity of Synsurf[®] samples pre-nebulisation (with and without extrusion)

Synsurf[®] preparations showed varying viscosities ranging from 6.772 ± 0.006 cP to 26.080 ± 0.003 cP (Table 4.3). All Synsurf[®] formulations showed significant differences with additions, with Synsurf[®] 2-5 showing higher viscosity values and Synsurf[®] 6 with palmitic acid and tripalmitin had a lower viscosity. However, statistical comparison of non-extruded in comparison to extruded samples (with either a 5 µm or 12 µm filters) showed no significant inter-formulation differences. Synsurf[®] 4 (PA and chol [2 %]) had the highest viscosity, followed by Synsurf[®] 3 (chol [2 %]). In contrast to this, Synsurf[®] 5 (1 % chol) had a lower viscosity of 9.008 ± 0.003 cP, more similar to that of Synsurf[®] 1. The lowest viscosity was found for Synsurf[®] 6. However, this formulation was unable to extrude with a 5 µm pore filter due to clogging and thus no data is available, as indicated in the Tables.

Table 4.3: Viscosity (cP) \pm SD of Synsurf[®] preparations with additional extrusion steps (5 μ m or 12 μ m filter), pre-nebulisation. (*:p<0.05 vs Synsurf[®] 1)

PRE-NEBULISATION				
#	Sample Name:	Non-Extruded	Extruded 5 μ m	Extruded 12 μ m
		Viscosity (cP) mean \pm SD		
1	Synsurf [®]	7.789 \pm 0.092	7.595 \pm 0.103	7.620 \pm 0.109
2	Synsurf [®] with palmitic acid (PA) [11 %]	10.608 \pm 0.085*	10.426 \pm 0.076	10.553 \pm 0.111
3	Synsurf [®] with cholesterol (Chol) [2 %]	21.081 \pm 0.169*	20.752 \pm 0.158	21.080 \pm 0.002
4	Synsurf [®] with palmitic acid (PA) [11 %] and cholesterol (Chol) [2 %]	26.080 \pm 0.207*	25.62 \pm 0.157	25.736 \pm 0.058
5	Synsurf [®] with cholesterol (Chol) [1 %]	9.008 \pm 0.052*	8.966 \pm 0.086	8.890 \pm 0.358
6	Synsurf [®] with palmitic acid (PA) [11 %] and tripalmitin (triPA)[7 %]	6.772 \pm 0.204*	*unable extrude	6.399 \pm 0.020

4.2.2 Viscosity of Synsurf[®] samples post-nebulisation (with and without extrusion)

Nebulised Synsurf[®] preparations (2-6) showed a statistical significant inter-formulation decrease in viscosity (Table 4.4) post-nebulisation ranging from 4.733 \pm 0.005 cP to 9.351 \pm 0.007 cP (*p < 0.05). Similar to results in Table 4.3, inclusion of an extrusion step in the synthesis, did not result in a statistical significant difference in viscosity post-nebulisation. Synsurf[®] 6 (addition of PA and triPA) was again unable to extrude through a 5 μ m pore filter due to clogging. However, with a 12 μ m pore filter extrusion was possible with no change in viscosity post-nebulisation. Compared to non-nebulised preparations, Synsurf[®] formulations showed a significant decrease in viscosity post-nebulisation however, Synsurf[®] 1 showed no changes in viscosity after nebulisation.

Table 4.4: Viscosity (cP) of nebulised preparations, collected from the dilution container. Viscosity is shown for non-extruded and extruded samples post-nebulisation \pm SD. (*:p<0.05 vs pre-nebulisation)

POST-NEBULISATION				
#	Sample Name:	Non-Extruded	Extruded 5 μ m	Extruded 12 μ m
		Viscosity (cP) mean \pm SD		
1	Synsurf [®]	7.514 \pm 0.011	7.375 \pm 0.010	7.26 \pm 0.094
2	Synsurf [®] with of palmitic acid (PA) [11%]	8.868 \pm 0.178*	8.604 \pm 0.010	8.468 \pm 0.028
3	Synsurf [®] with cholesterol (Chol) [2%]	7.507 \pm 0.165*	7.487 \pm 0.200	7.149 \pm 0.187
4	Synsurf [®] with palmitic acid (PA) [11%] and cholesterol (Chol) [2%]	9.351 \pm 0.182*	9.280 \pm 0.193	9.998 \pm 0.204
5	Synsurf [®] with cholesterol (Chol) [1%]	5.378 \pm 0.114*	5.289 \pm 0.054	4.973 \pm 0.067
6	Synsurf [®] with palmitic acid (PA) [11%] and tripalmitin (triPA) [7%]	4.733 \pm 0.184*	*unable extrude	4.525 \pm 0.091

4.2.3 Viscosity analysis of natural surfactants, Curosurf[®] and Liposurf[®] pre- and post-nebulisation

Analyses of commercially available natural surfactants displayed lower viscosities at the same PL concentration as Synsurf[®] preparations. No statistical significant differences were found between Curosurf[®] and Liposurf[®], pre- and post-nebulisation, respectively.

Table 4.5: Viscosity cP \pm SD of Curosurf[®] and Liposurf[®] pre- and post-nebulisation. Both surfactants were diluted to a phospholipid concentration of [20 mg/mL].

CUROSURF [®] AND LIPOSURF [®]			
#	Sample Name:	PRE-NEBULISATION	POST-NEBULISATION
		Viscosity (cP) mean \pm SD	
C	Curosurf [®]	3.012 \pm 0.013	2.834 \pm 0.007
L	Liposurf [®]	4.064 \pm 0.020	3.084 \pm 0.018

4.3 Particle size determination

The z-average particle size \pm SD of samples tested pre- and post-nebulisation, are shown in Table 4.6. Particle dimensions are expressed as diameter in nanometres (d.nm). As mentioned previously, the optimal particle size post-nebulisation should ideally range from 1000 nm to 3000 nm in diameter.

4.3.1 Comparison of Synsurf[®] preparations at day of synthesis (day 0)

Particle size analyses of Synsurf[®] preparations, immediately after synthesis indicated an array of particle sizes amongst the different formulations. Synsurf[®] 2 (PA) and 4 (PA plus Chol [2 %]) showed large particles approximately 6339 d.nm and 7908 d.nm in diameter. However, Synsurf[®] 6 (PA and triPA) contained smaller particles (3150 d.nm). Synsurf[®] 1 and 5 had smaller particles, in comparison to other formulations, pre-nebulisation (2336 d. nm and 2911 d.nm) and comparison of Synsurf[®] 3 and 5 (with cholesterol [2 %] and [1 %]) respectively showed similar particle diameter.

4.3.2 Comparison of Synsurf[®] preparations pre- and post-nebulisation

Nebulisation of Synsurf[®] preparations showed a considerable decrease in the diameter of particles collected after aerosolisation. Post-nebulisation, particles ranged from \pm 351 d.nm to \pm 779 d.nm (Table 4.6). In comparison to other Synsurf[®] formulations that showed a decrease \sim 80% – 90%, Synsurf[®] 6 had a lower decrease in particles diameter of \sim 44%. Statistical analysis indicated a 95% CI that the particles generated by nebulisation of Synsurf[®] 6 fell within the desired size range. (indicated in green in Table 4.6)

4.3.3 Changes in particle size with ageing of Synsurf[®] preparations

Although not significant, Synsurf[®] preparations showed slight changes in particles diameter pre- and post-nebulisation on day 105 in comparison to day 0.

4.3.4 Changes in particle size of extruded Synsurf[®] preparations post-nebulisation

The addition of extrusion as synthesis step changed the average particles diameter observed in almost all Synsurf[®] preparations. An overall increase in post-nebulisation particle diameters is observed for extruded preparations, in comparison to non-extruded formulations as shown in Figure 4.2.

Synsurf[®] 1 - 5 (extruded with 5 μm or 12 μm filter) showed an increase in post-nebulisation particles in comparison to non-extruded nebulised preparations. However, Synsurf[®] 6 was unable to be extruded with a 5 μm filter (0 in Figure 4.2) and showed a large decrease in particle size when extruded with a 12 μm filter and nebulised.

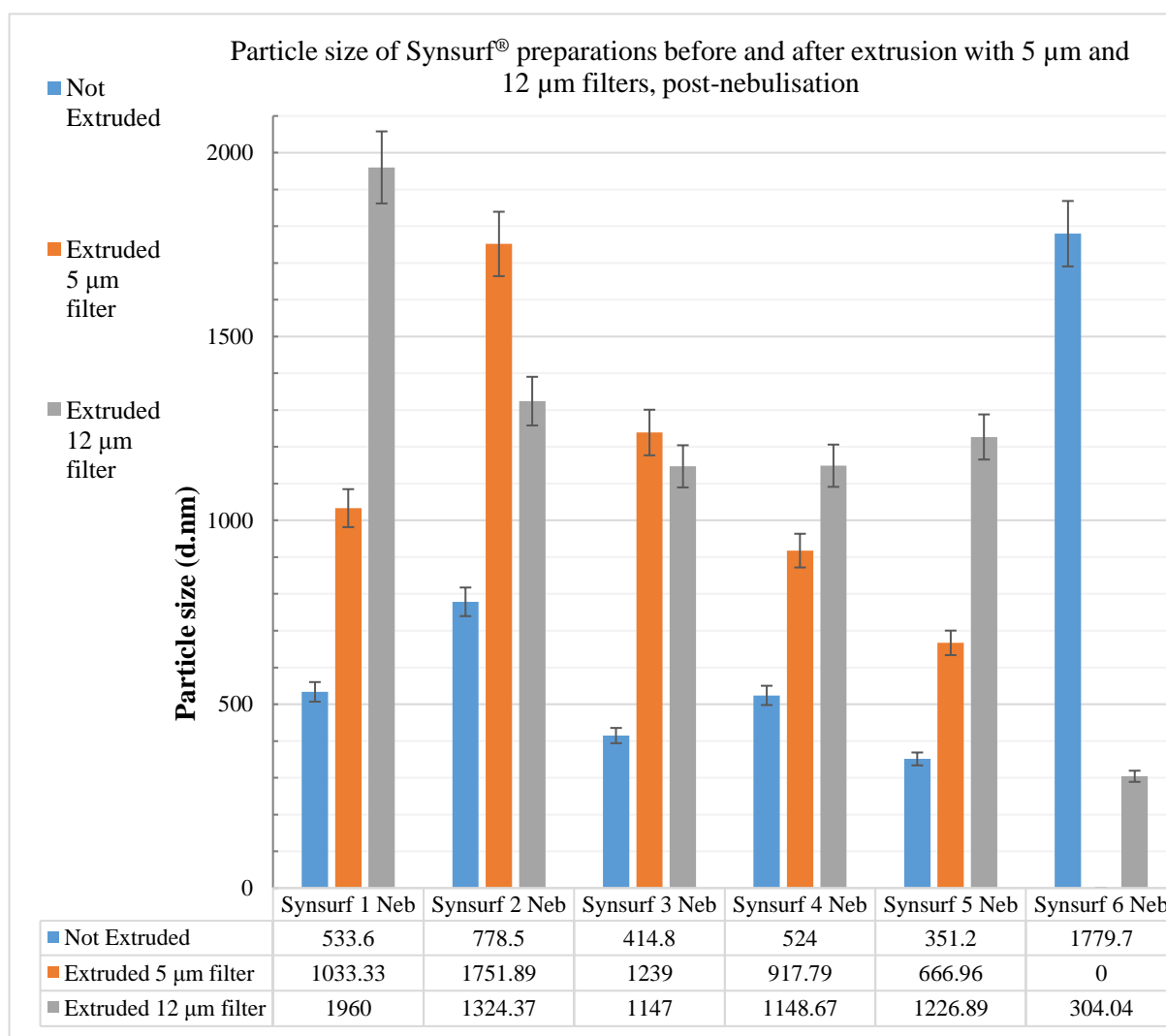


Figure 4.2: Average particle size (d.nm) of Synsurf[®] preparations 1 to 6, non-extruded and extruded with a 5 μm and 12 μm filter, post-nebulisation. Bars = SEM

4.3.5 Particle size analyses of Curosurf[®] and Liposurf[®]

Curosurf[®] and Liposurf[®] showed average particles diameters comparable (but statistically different) to Synsurf[®] 1, 3 and 5 (see Table 4.6) post-nebulisation. Curosurf[®] and Liposurf[®] generated particles smaller than the suggested (optimal) range for nebulised aerosols.

Table 4.6: Z-Average particle sizes of preparations pre- and post-nebulisation. The average particle size (\pm SD) is expressed in diameter in nanometres (d.nm) for Synsurf[®] preparations (ageing 105 days and extrusion with a 5 μ m or 12 μ m filter). Curosurf[®] and Liposurf[®] shown pre- and post-nebulisation.

Batch	Sample Name	# 1 Synsurf [®]		# 2 Synsurf [®] (PA)		# 3 Synsurf [®] (Chol 2 %)		# 4 Synsurf [®] (PA and Chol 2 %)		# 5 Synsurf [®] (Chol 1 %)		# 6 Synsurf [®] (PA and triPA)	
	Nebulisation Status:	Pre-Neb	Post-Neb	Pre-Neb	Post-Neb	Pre-Neb	Post-Neb	Pre-Neb	Post-Neb	Pre-Neb	Post-Neb	Pre-Neb	Post-Neb
Day 0	Z-average particle size (diameter in nm) \pm SD	2336 (\pm 69)	534 (\pm 7)	6339 (\pm 42)	779 (\pm 26)	3420 (\pm 49)	415 (\pm 30)	7908 (\pm 63)	524 (\pm 12)	2911 (\pm 24)	351 (\pm 23)	3150 (\pm 64)	1780 (\pm 53)
Day 105		2758 (\pm 52)	479 (\pm 36)	6005 (\pm 69)	789 (\pm 43)	3801 (\pm 61)	423 (\pm 46)	7911 (\pm 55)	500 (\pm 8)	2898 (\pm 22)	394 (\pm 9)	2911 (\pm 53)	1789 (\pm 50)
Extruded with a 5 μ m filter		3247 (\pm 43)	1033 (\pm 54)	4887 (\pm 46)	1752 (\pm 29)	4878 (\pm 49)	1239 (\pm 30)	4345 (\pm 28)	918 (\pm 12)	1941 (\pm 22)	667 (\pm 15)	no reading	no reading
Extruded with a 12 μ m filter		4296 (\pm 69)	1960 (\pm 10)	8047 (\pm 20)	1324 (\pm 26)	6554 (\pm 26)	1147 (\pm 20)	8554 (\pm 25)	1149 (\pm 11)	3823 (\pm 36)	1227 (\pm 23)	2176 (\pm 83)	304 (\pm 5)
Curosurf [®] and Liposurf [®]		Curosurf [®]		Liposurf [®]									
		2083 (\pm 55)	427 (\pm 17)	3260 (\pm 121)	403 (\pm 7)								

4.3.6 Scanning electron microscopy (SEM)

SEM visualisation was performed for all Synsurf[®] preparations, Curosurf[®] and Liposurf[®] pre – and post nebulisation. However, due to the topographical nature of SEM, not all images generated were of excellent quality and/or provided structural information about particles/liposomes, thus only images that complied are included. In all the Figures (4.3 to 4.13) dehydration and collapse of liposomes can be seen. A single dehydrated liposome (Synsurf[®] 1) is shown in Figure 4.3. The elevation surrounding the liposome, giving a “doughnut-like” appearance is likely due to rapid dehydration deployed in the fixing process. Particle diameter (z-average) determined by DLS for Synsurf[®] 1 is ± 2336 d.nm (2.3 d. μ m), as shown in Table 4.6 and Figure 4.3 show the liposome is similar in size as determined by the SEM. Although SEM provided topographical imaging of surfactant preparations, some edges of the deflated liposomes (Synsurf[®] 1), indicated in Figure 4.4 by black arrows could be observed, whilst others were tucked under the surface, thus not showing the complete structure. Dense patches of collapsed liposomes are illustrated in Figure 4.5 and 4.8 (Synsurf[®] 3 and 6 pre-nebulisation), similar to the average particle size (± 3.4 d. μ m and ± 3.6 d. μ m) as determined by DLS analyses. However, some liposomes are embedded and the full structure is not visible. Arrangement of liposomes in Synsurf[®] 4 pre-nebulisation is shown in Figure 4.6. Liposomes presented in a “beads on a string” like structure, indicated with arrows. SEM imaging of Synsurf[®] 5 (Chol [1 %]) pre-nebulisation showed very dense packed spherical liposomes, with a topographic covering (Figure 4.7). Although the liposome structures are covered, an estimate particle size of $\pm 2 - 3$ d. μ m is seen. Nebulisation generated particles much smaller than those found in solutions pre-nebulisation (Table 4.6). Figure 4.9 and 4.10 show Curosurf[®] post- nebulisation. The measured liposome is indicated in a dialog box in Figure 4.9, and show a rough diameter of ± 600 d.nm. Liposurf[®] post-nebulisation shows a dense, almost cluster-like, packing of liposomes (Figure 4.11). Synsurf[®] 5 (Chol [1%]), that had the smallest particles post-nebulisation (Table 4.6), Figure 4.12 illustrates a rough surface with numerous liposomes, presents as white specs spread evenly throughout the image. Synsurf[®] 6 maintained particle size within the desired range post-nebulisation (Table 4.6), and is presented in Figure 4.13.



Figure 4.3: A SEM image of Synsurf[®] 1 pre-nebulisation. Parameters of the recorded image are shown at the bottom. Arrows indicate the edges of a dehydrated liposome. Scale bar = 2 μ m

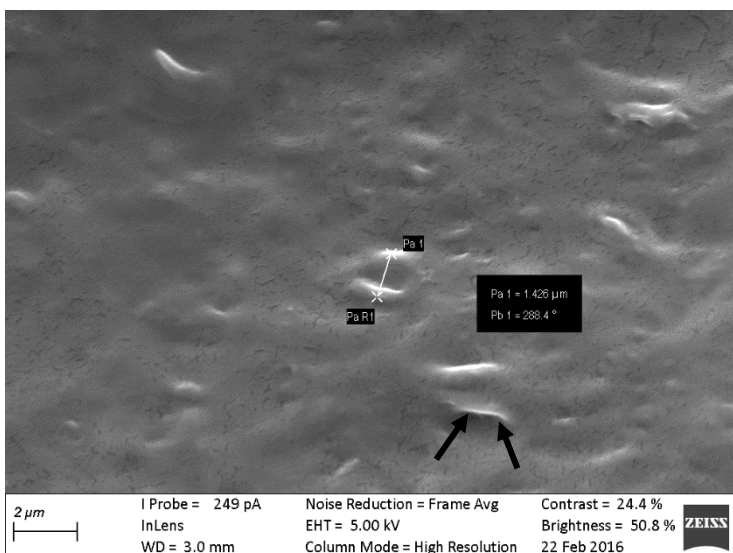


Figure 4.4: A SEM image of Synsurf[®] 1 pre-nebulisation. Visible deflated liposome edges are indicated with black arrows and the inner diameter of another liposome is shown in the black dialog box (1.426 μ m). Parameters of the recorded image are shown at the bottom. Scale bar = 2 μ m

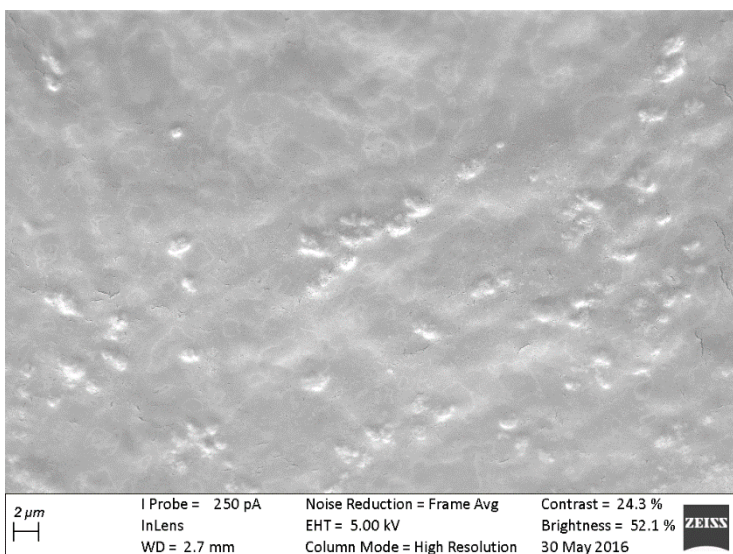


Figure 4.5: A SEM image of Synsurf[®] 3 pre-nebulisation. Semi-spherical liposome structures are shown on the surface of the image. Parameters of the recorded image are shown at the bottom. Scale bar = 2 μ m

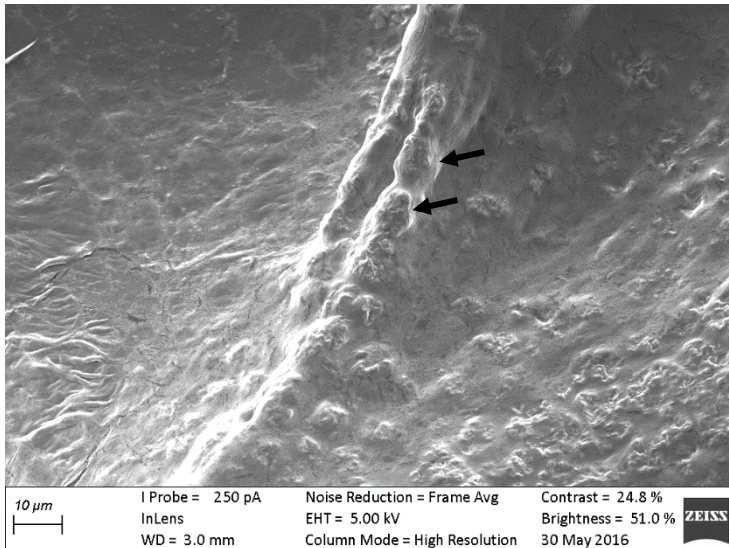


Figure 4.6: A SEM image of Synsurf® 4 pre-nebulisation. Black arrows indicate “beads on a string” like structures formed by liposomes. Parameters of the image are indicated at the bottom, including a bar scale = 10 μm.

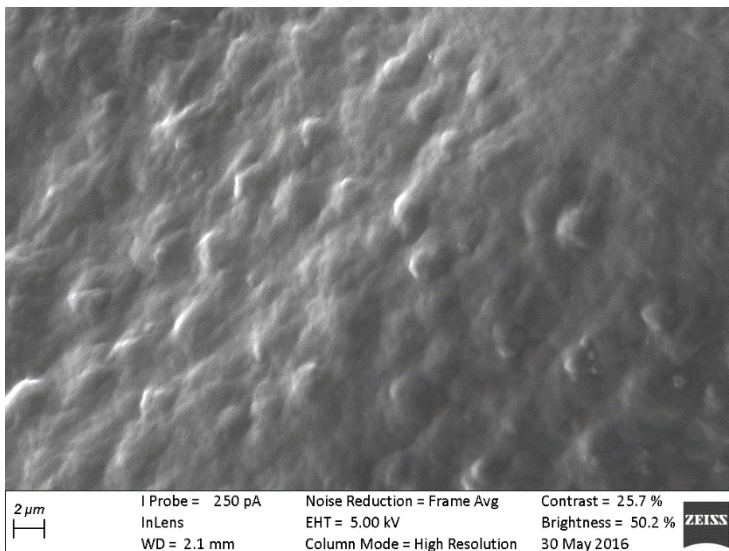


Figure 4.7: A SEM image of Synsurf® 5 pre-nebulisation showing dense compaction of similar shaped particles. Parameters of the recorded image are shown at the bottom. Scale bar = 2 μm

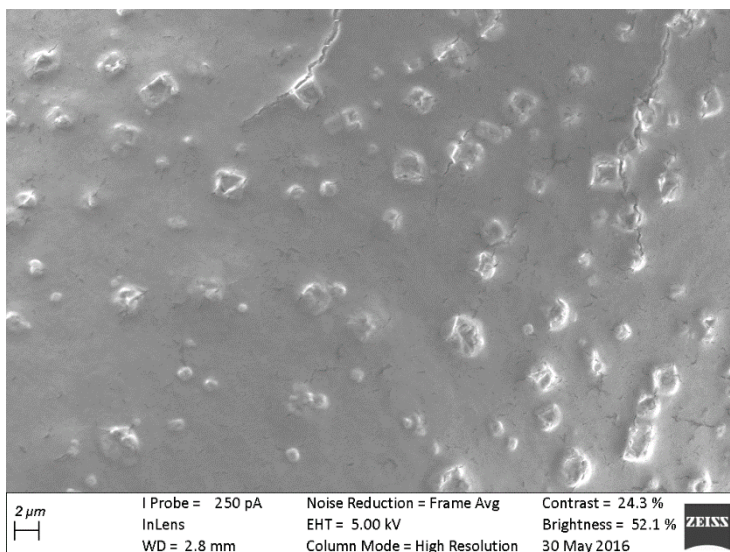


Figure 4.8: A SEM image of Synsurf® 6 pre-nebulisation. Parameters of the image are indicated at the bottom, including a bar scale = 2 μm.

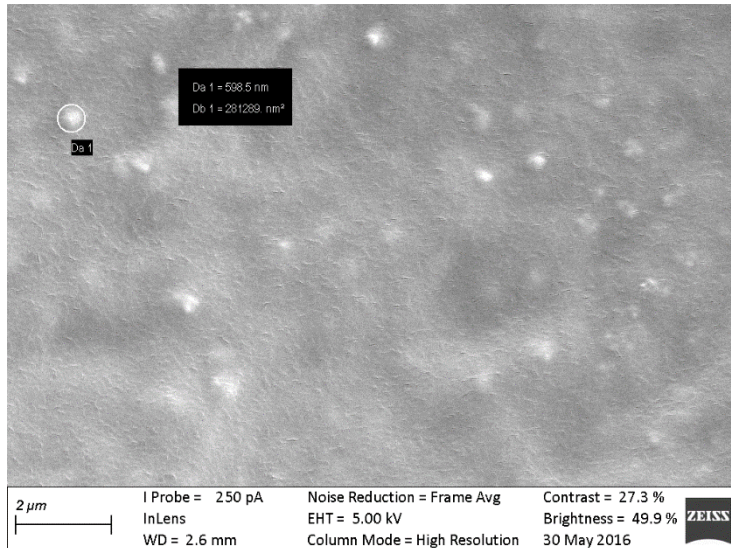


Figure 4.9: A SEM image of Curosurf[®] post-nebulisation. White measurement circle surrounding liposome = 598.5 d.nm. Parameters of the recorded image are shown at the bottom. Scale bar = 2 μ m

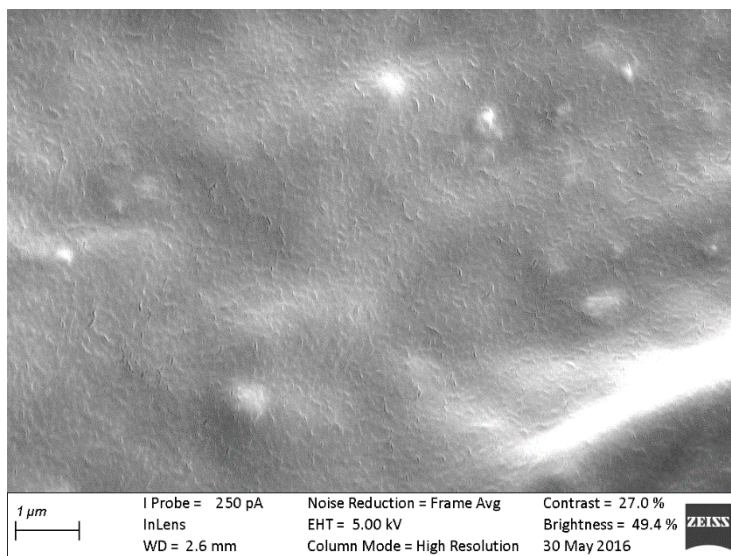


Figure 4.10: A SEM image of Curosurf[®] post-nebulisation. Parameters of the recorded image are shown at the bottom. Scale bar = 1 μ m

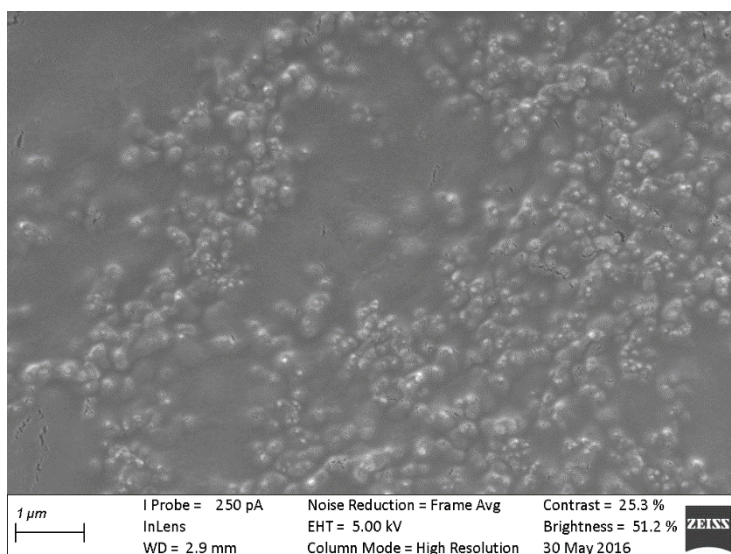


Figure 4.11: A SEM image of Liposurf[®] post-nebulisation. Parameters of the recorded image are shown at the bottom. Scale bar = 1 μ m

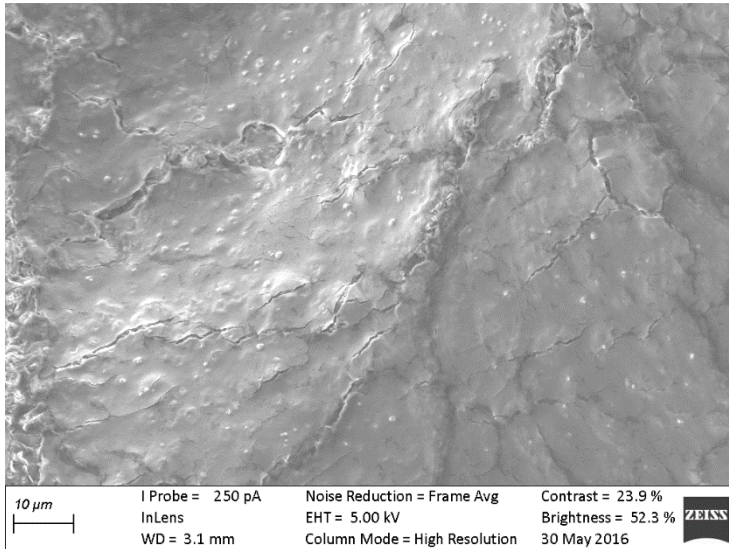


Figure 4.12: A SEM image of Synsurf® 5 post-nebulisation. Parameters of the recorded image are shown at the bottom. Scale bar = 10 μm

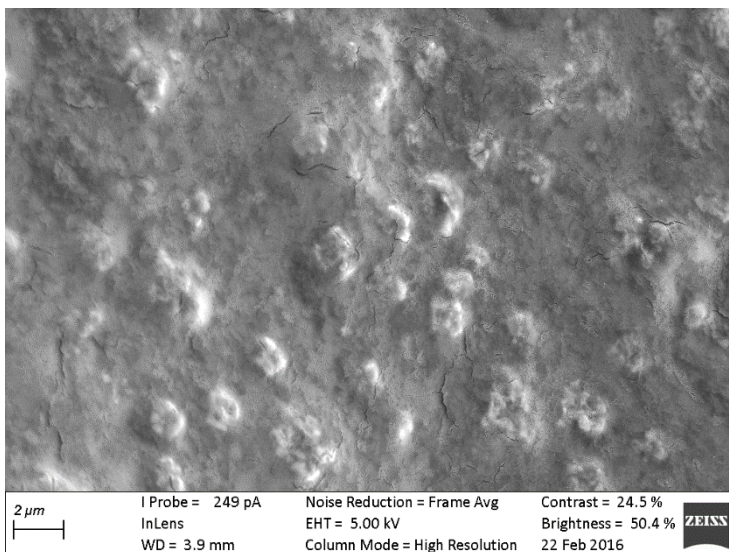


Figure 4.13: A SEM image of Synsurf® 6 post-nebulisation. Parameters of the recorded image are shown at the bottom. Scale bar = 2 μm

4.4 Interfacial surface tension reduction analyses

The following sections show the results of interfacial surface tension analyses of all surfactants pre- and post-nebulisation. Surface tension changes were analysed by pendant drop method for 900 seconds (as described in Materials and Methods 3.2.5). To compare changes in nebulisation status pre- and post-nebulisation, aging and addition of extrusion in synthesis of Synsurf[®] samples, results recorded in m/Nm, were converted to a normalisation ratio (%) to depict the reduction of surface tension of preparations.

4.4.1 Interfacial surface tension reduction of surfactant samples pre-nebulisation

The reduction in surface tension (%) over 900 seconds of Synsurf[®] 1 - 6 is shown in Figure 4.14. A decrease in surface tension is observed for all Synsurf[®] preparations. However, Synsurf[®] 5 and 6 showed an overall more rapid decrease in surface tension over the total observation period ($\pm 26\%$ and $\pm 23\%$, respectively). Comparative analysis showed that the decrease in surface tension of Synsurf[®] 1 - 4 was significantly different to that of Synsurf[®] 5 and 6. Moreover, no statistical difference was found between Synsurf[®] 5 and 6, pre-nebulisation.

Surface tension reduction of Synsurf[®] 1, Curosurf[®] and Liposurf[®] showed vast differences, although a decrease in surface tension was presented by all surfactants, Curosurf[®] and Liposurf[®] showed an overall greater decrease in surface tension within the first 150 seconds, that was significantly different to Synsurf[®] preparation 1. After a plateau of about 150 seconds Liposurf[®] decreased surface tension further in comparison to both Curosurf[®] and Synsurf[®] 1 (Figure 4.15).

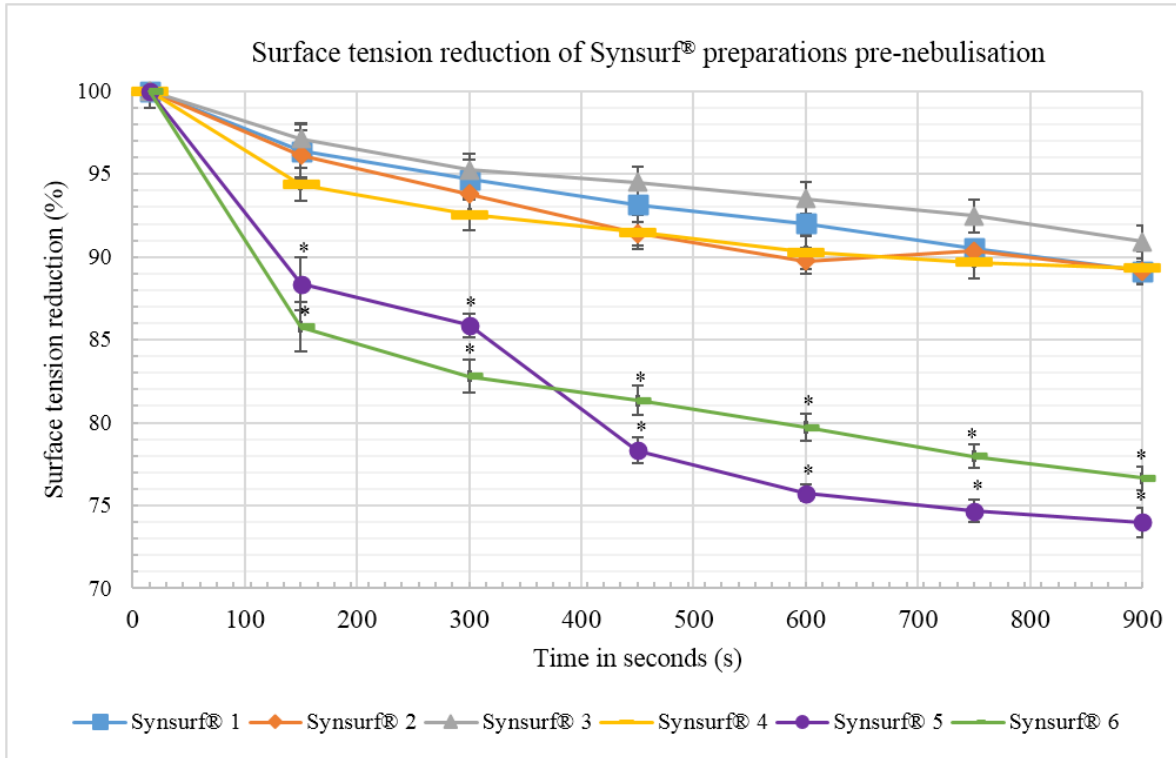


Figure 4.14: Interfacial surface tension reduction (expressed in % and SEM bar indicated) of pre-nebulisation Synsurf® preparations over time. (*: $p < 0.05$ vs Synsurf® 1-4).

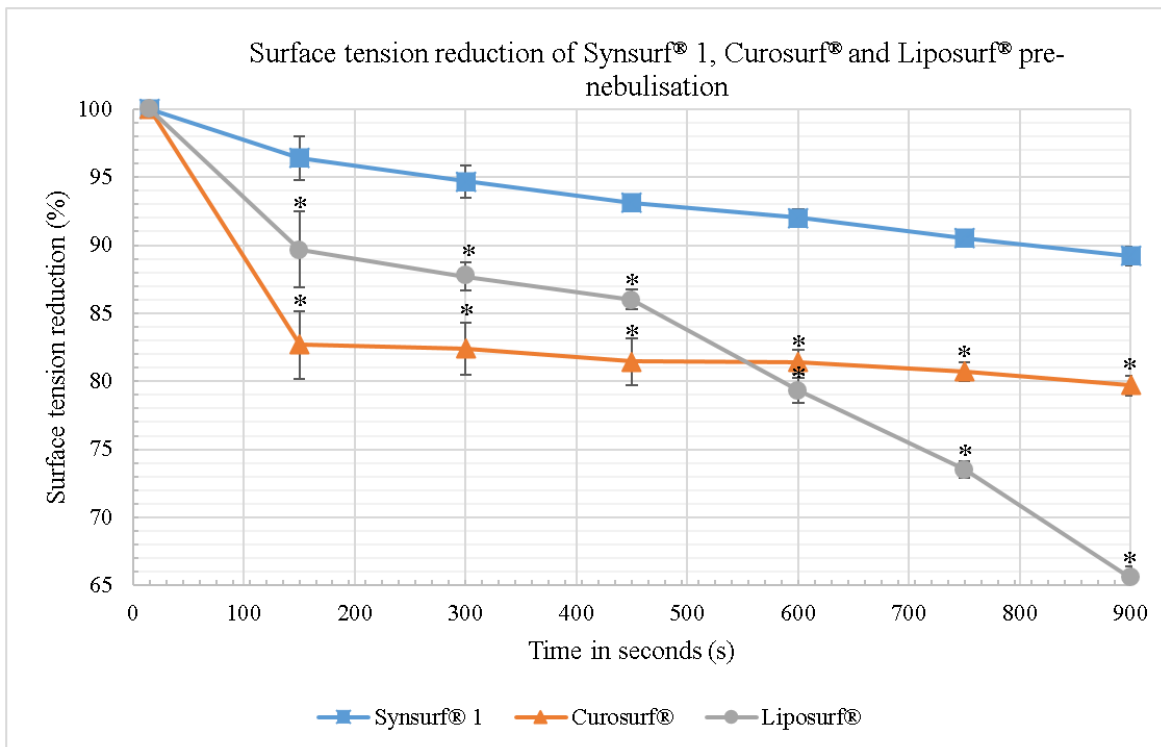


Figure 4.15: Interfacial surface tension reduction (expressed in % and SEM bar indicated) of pre-nebulisation Synsurf® 1, Curosurf® and Liposurf® preparations over time. (*: $p < 0.05$ vs Synsurf® 1 pre-nebulisation)

4.4.2 Interfacial surface tension reduction of surfactants pre- and post-nebulisation

Changes in interfacial surface tension reduction pre- and post-nebulisation of Synsurf[®], Curosurf[®] and Liposurf[®] preparations are shown in Figures 4.16 to 4.24. Synsurf[®] 2, 3, 4 and 5 showed statistical significant differences with regards to reduction of surface tension, with post-nebulisation samples over 900 seconds (see Figures 4.17 to 4.20). However, Synsurf[®] 1 and 6 showed no significant changes in interfacial surface tension reduction pre- and post-nebulisation over the 900 second period (Figures 4.16 and 4.21). Similar, to Synsurf[®] preparations 2 - 5, Curosurf[®] and Liposurf[®] showed statistical significant change in interfacial surface tension reduction post-nebulisation, over the observation period. (see Figures 4.22 and 4.23). Although Synsurf[®] preparations 2, 3, 4 and 5 showed a significant decline in surface tension post-nebulisation, the changes observed were less profound in comparison to Curosurf[®] and Liposurf[®].

Synsurf[®] preparation 1:

Synsurf[®] 1 showed no statistical significant changes in surface tension reduction ability post-nebulisation over the observation period.

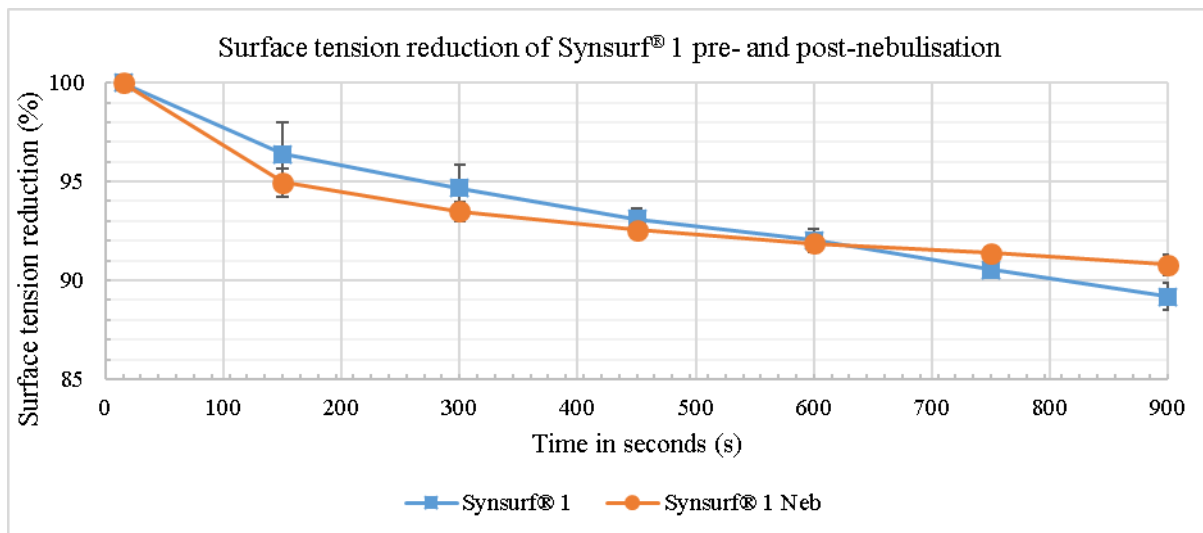


Figure 4.16: Interfacial surface tension reduction (expressed in % and SEM bar indicated) of pre- and post-nebulisation Synsurf[®] 1 preparation over time. The abbreviation Neb signifies the nebulisation status as post-nebulisation.

Synsurf[®] preparation 2:

Synsurf[®] 2 showed statistical significant differences in reduction of surface tension over the observation period.

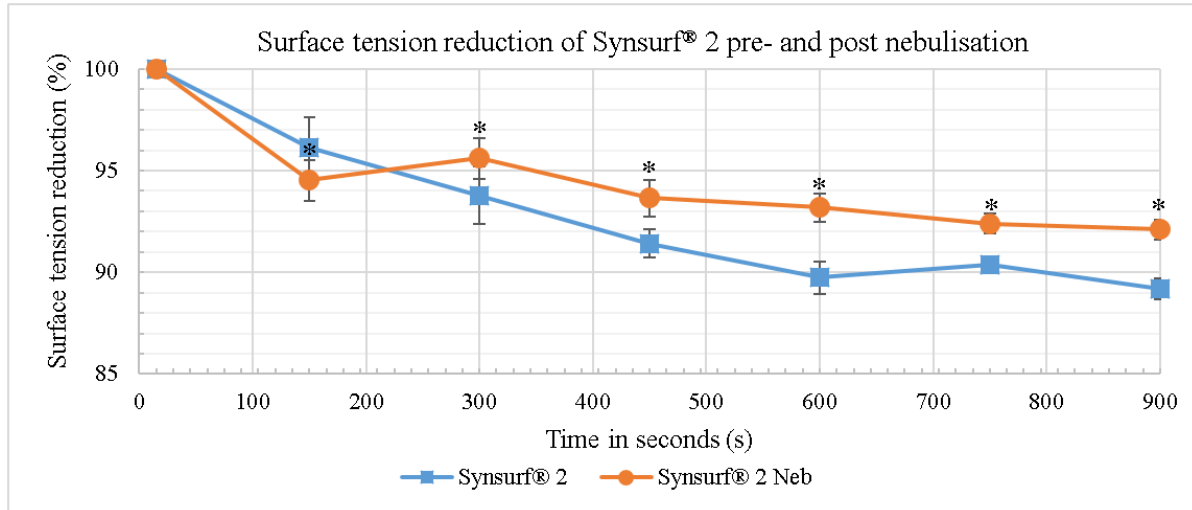


Figure 4.17: Interfacial surface tension reduction (expressed in % and SEM bar indicated) of pre- and post-nebulisation Synsurf[®] 2 preparation over time. The abbreviation Neb signifies the nebulisation status as post-nebulisation. (*: $p < 0.05$ vs Synsurf[®] 2 pre-nebulised)

Synsurf[®] preparation 3:

Synsurf[®] 3 showed statistical significant differences in reduction of surface tension over the observation period.

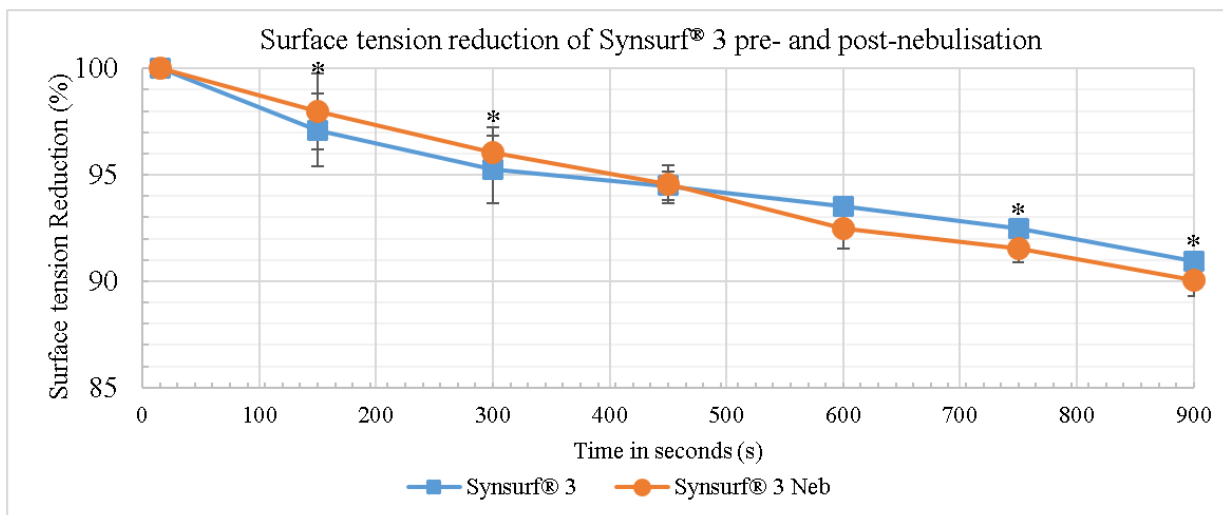


Figure 4.18: Interfacial surface tension reduction (expressed in % and SEM bar indicated) of pre- and post-nebulisation Synsurf[®] 3 preparation over time. The abbreviation Neb signifies the nebulisation status as post-nebulisation. (*: $p < 0.05$ vs Synsurf[®] 3 pre-nebulised)

Synsurf® preparation 4:

Synsurf® 4 showed statistical significant differences in reduction of surface tension over the observation period.

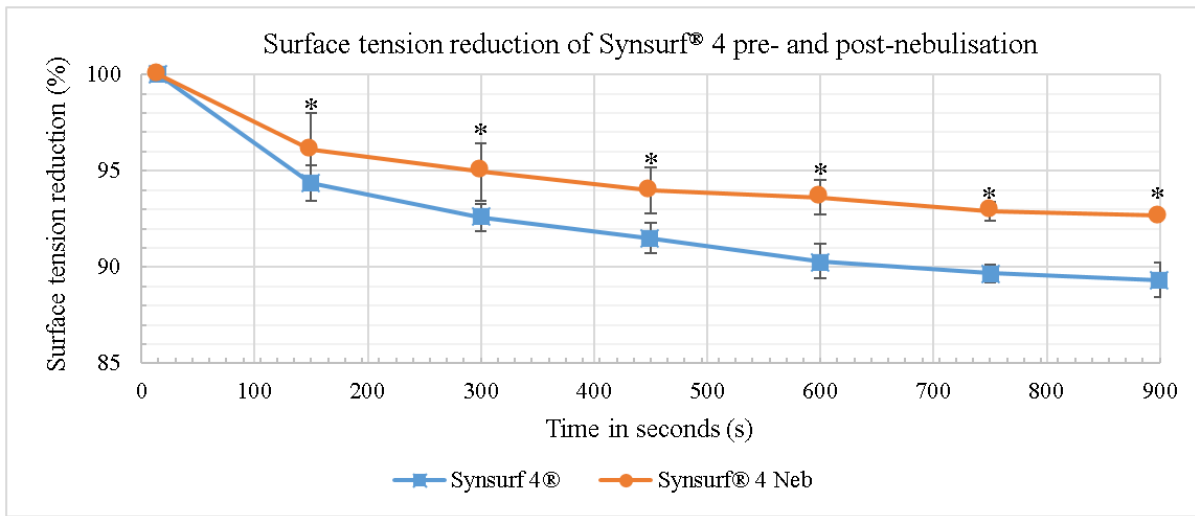


Figure 4.19: Interfacial surface tension reduction (expressed in % and SEM bar indicated) of pre- and post-nebulisation Synsurf® 4 preparation over time. The abbreviation Neb signifies the nebulisation status as post-nebulisation. (*: $p < 0.05$ vs Synsurf® 4 pre-nebulised)

Synsurf® preparation 5:

Synsurf 5 showed statistical significant differences in reduction of surface tension over the observation period.

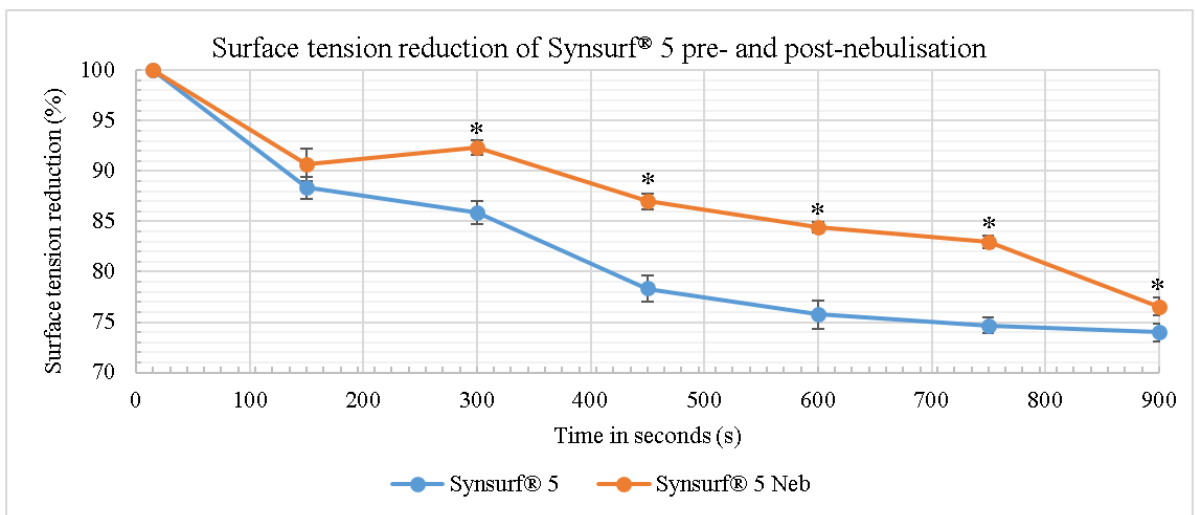


Figure 4.20: Interfacial surface tension reduction (expressed in % and SEM bar indicated) of pre- and post-nebulisation Synsurf® 5 preparation over time. The abbreviation Neb signifies the nebulisation status as post-nebulisation. (*: $p < 0.05$ vs Synsurf® 5 pre-nebulised)

Synsurf[®] preparation 6:

Synsurf[®] 6 showed no statistical significant changes in surface tension reduction ability post-nebulisation over the observation period.

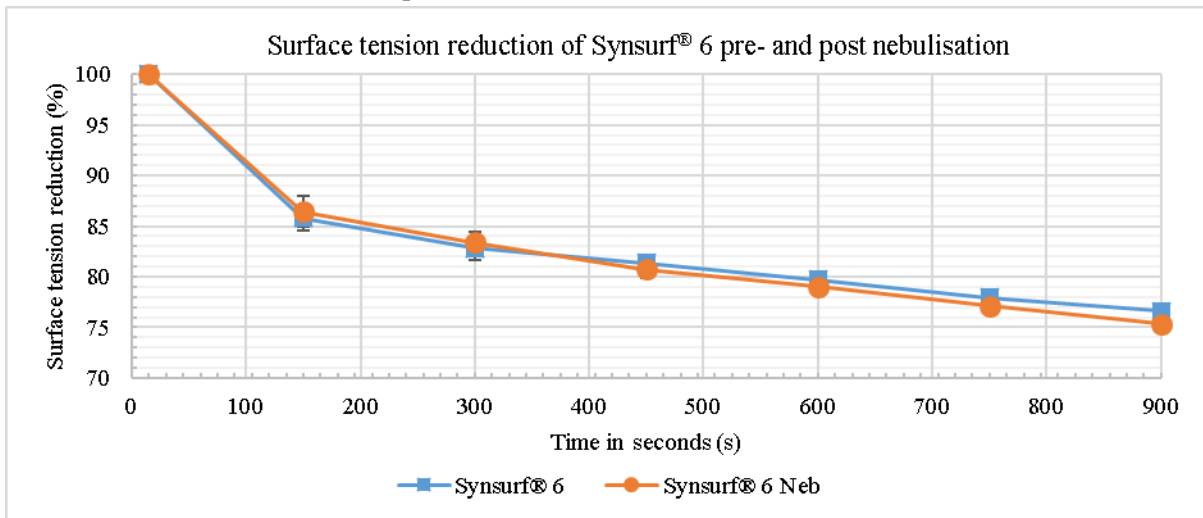


Figure 4.21: Interfacial surface tension reduction (expressed in % and SEM bar indicated) of pre- and post-nebulisation Synsurf[®] 6 preparation over time. The abbreviation Neb signifies the nebulisation status as post-nebulisation.

Curosurf[®]:

Curosurf[®] showed statistical significant differences in reduction of surface tension over the observation period.

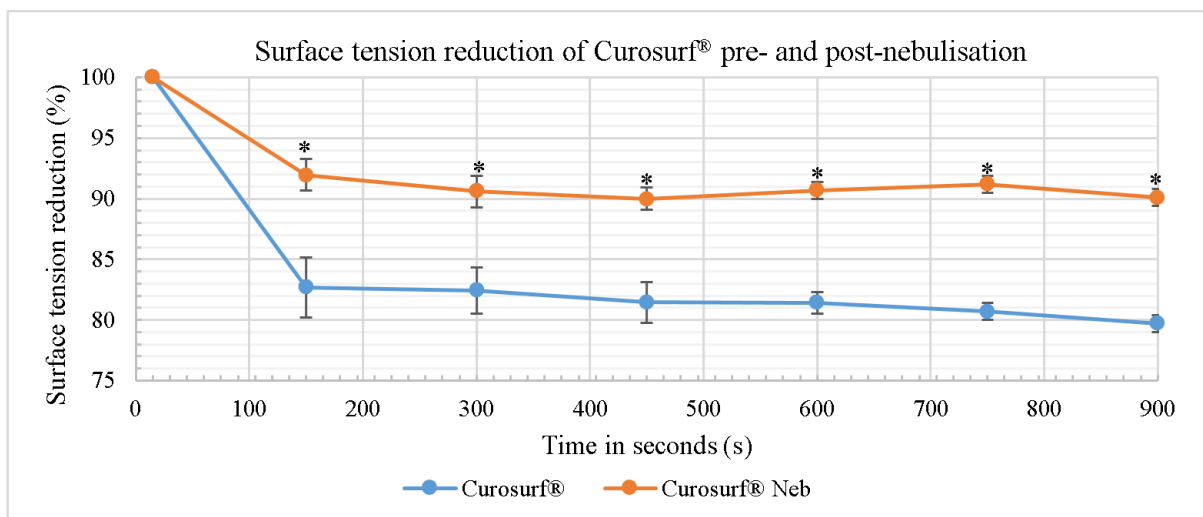


Figure 4.22: Interfacial surface tension reduction (expressed in % and SEM bar indicated) of pre- and post-nebulisation Curosurf[®] preparation over time. The abbreviation Neb signifies the nebulisation status as post-nebulisation. (*: $p < 0.05$ vs Curosurf[®] pre-nebulised)

Liposurf[®]:

Liposurf[®] showed statistical significant differences in reduction of surface tension over the observation period.

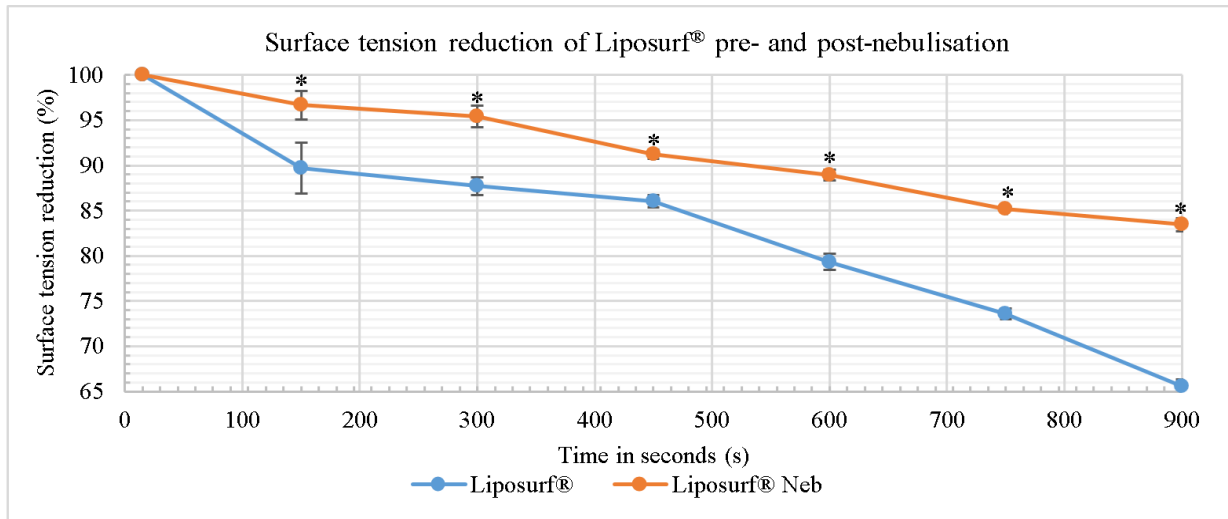


Figure 4.23: Interfacial surface tension reduction (expressed in % and SEM bar indicated) of pre- and post-nebulisation Liposurf[®] preparation over time. The abbreviation Neb signifies the nebulisation status as post-nebulisation. (*: $p < 0.05$ vs Liposurf[®] pre-nebulised)

4.4.3 Comparison of Synsurf[®] 1, Curosurf[®] and Liposurf[®] post-nebulisation

Figure 4.24 shows that nebulised samples of Synsurf[®] 1, Curosurf[®] and Liposurf[®] had an overall similar trend in the reduction of surface tension. Synsurf[®] 1 Neb is signified in blue, Curosurf[®] Neb in orange and Liposurf[®] in grey. However, Liposurf[®] showed a significant further reduction in surface tension between 600 – 900 seconds.

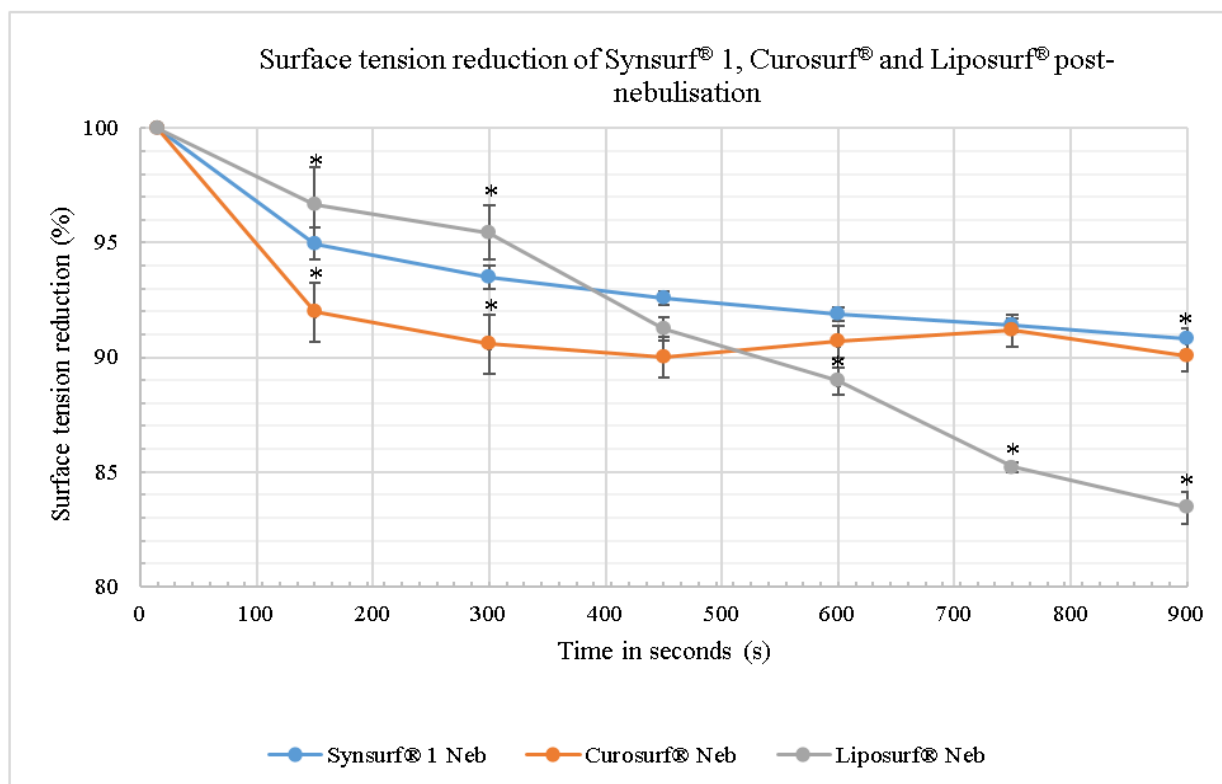


Figure 4.24: Interfacial surface tension reduction (expressed in % and SEM bar indicated) of post-nebulisation Synsurf[®] 1, Curosurf[®] and Liposurf[®] preparation over time. The abbreviation Neb signifies the nebulisation status as post-nebulisation. (*: $p < 0.05$ vs Synsurf[®] 1 post-nebulisation)

4.4.4 Interfacial surface tension reduction of Synsurf[®] samples with ageing

Changes in interfacial surface tension reduction (%) was determined for Synsurf[®] preparations on the day of synthesis (marked as day 0) and after ageing (at 105 days). The results are shown in Figure 4.25 to 4.30. Synsurf[®] preparations 1, 2, 5 and 6 showed no significant changes in surface tension reduction over the 105 days with samples pre- and post-nebulisation. However, Synsurf[®] preparation 3 showed a decrease in surface tension lowering ability after 105 days when nebulised (in comparison to un-aged

sample). Indicated in **yellow** in Figure 4.27, a slight diminishing in surface tension reduction was observed between 600 to 900 seconds. Synsurf® 4 showed a slight increase in interfacial surface tension reduction post-nebulisation with aging as shown in Figure 4.28.

Synsurf® preparation 1:

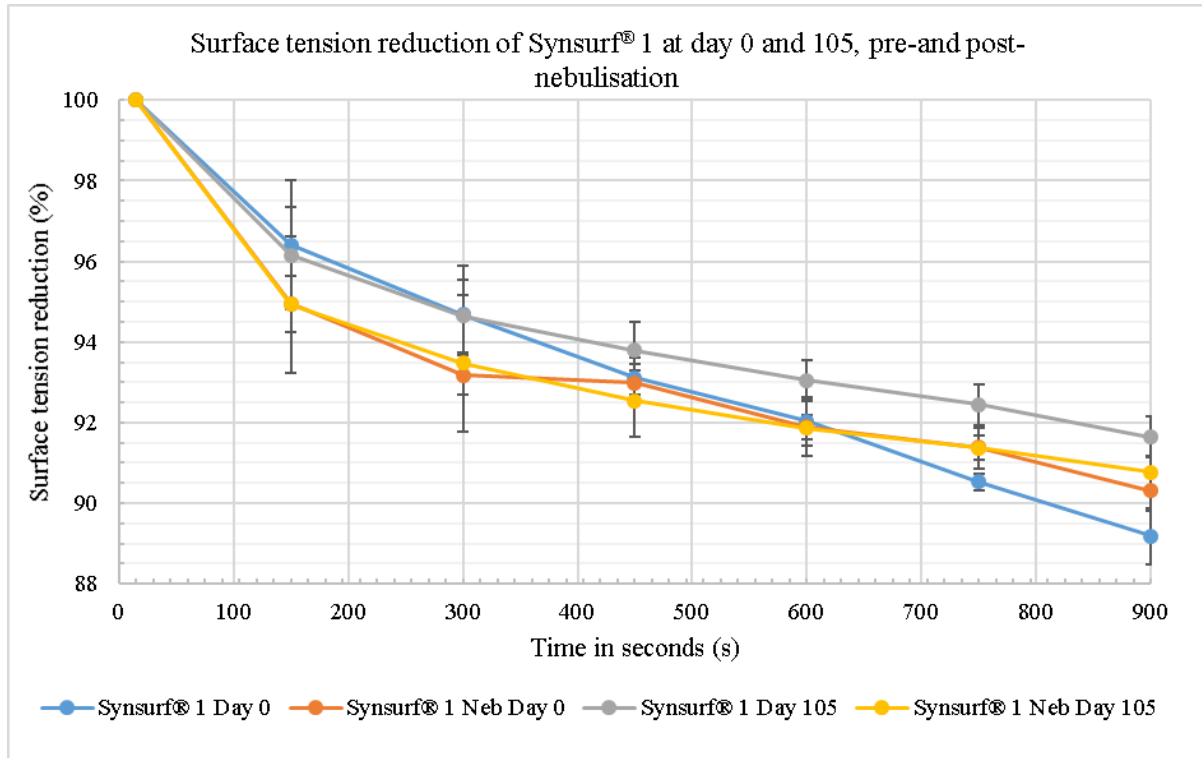


Figure 4.25: Interfacial surface tension reduction (expressed in % and SEM bar indicated) of pre- and post-nebulisation Synsurf® 1 preparation at day 0 and 105, over time. Neb = post- nebulisation.

Synsurf® preparation 2:

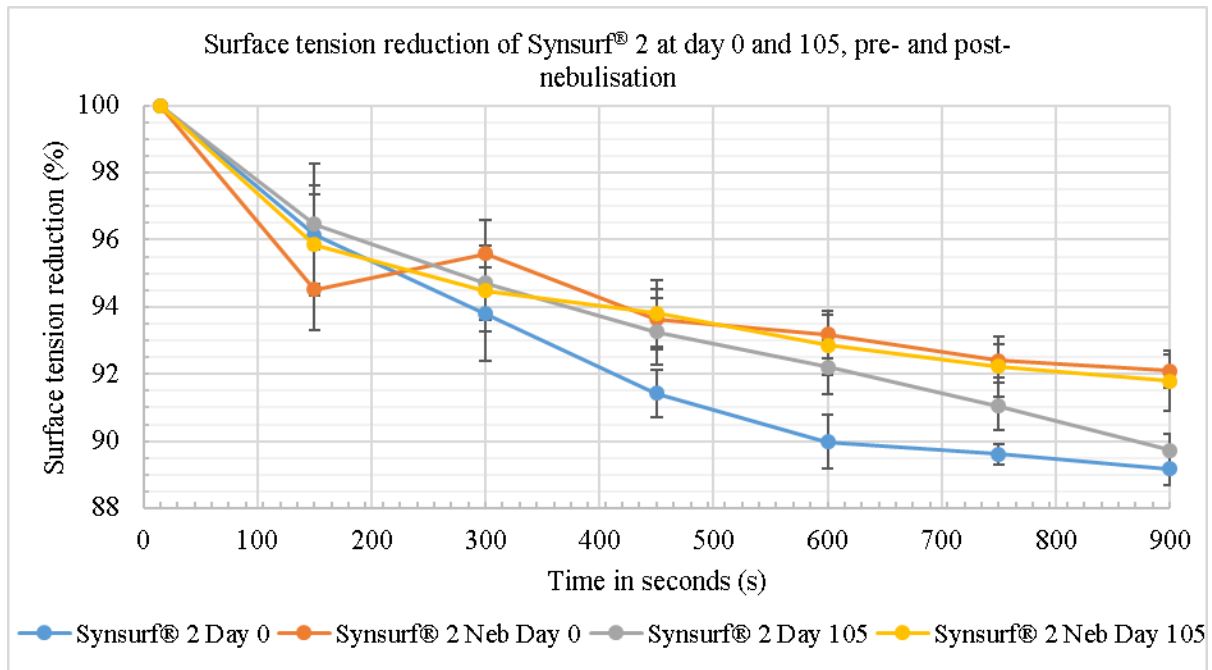


Figure 4.26: Interfacial surface tension reduction (expressed in % and SEM bar indicated) of pre- and post-nebulisation Synsurf® 2 preparation at day 0 and 105, over time. Neb = post- nebulisation.

Synsurf® preparation 3:

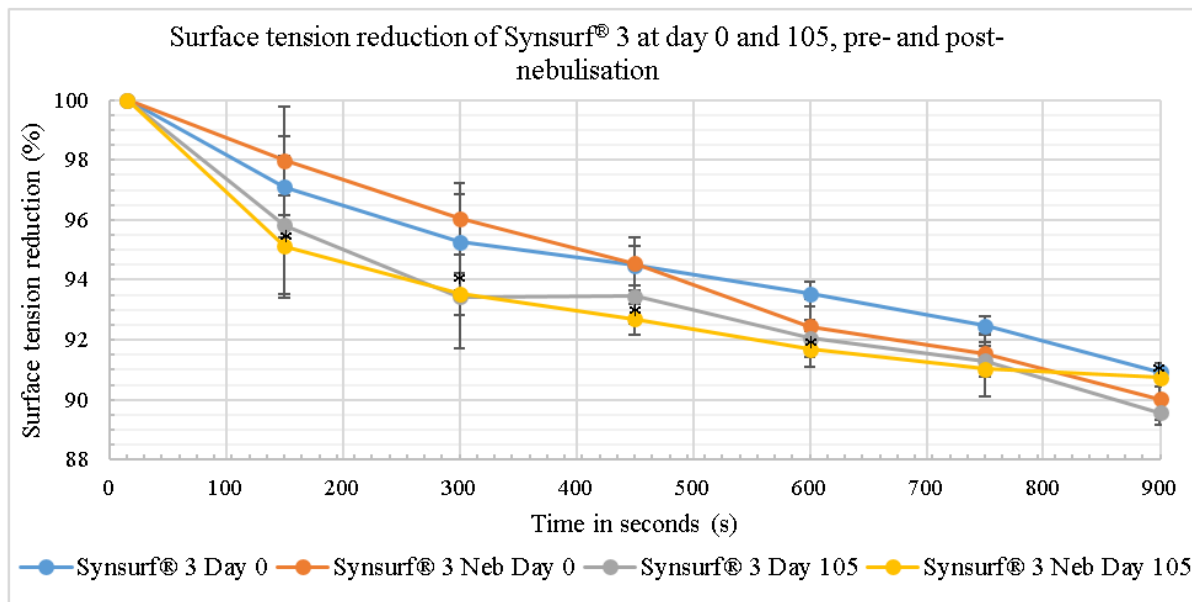


Figure 4.27: Interfacial surface tension reduction (expressed in % and SEM bar indicated) of pre- and post-nebulisation Synsurf® 3 preparation at day 0 and 105, over time. Comparison showed statistical differences between nebulised preparation at day 0 and 105 (shown in orange and yellow) between 600 – 900 seconds. Neb = post- nebulisation. (*: $p < 0.05$ vs Synsurf® 3 post-nebulised day 0)

Synsurf® preparation 4:

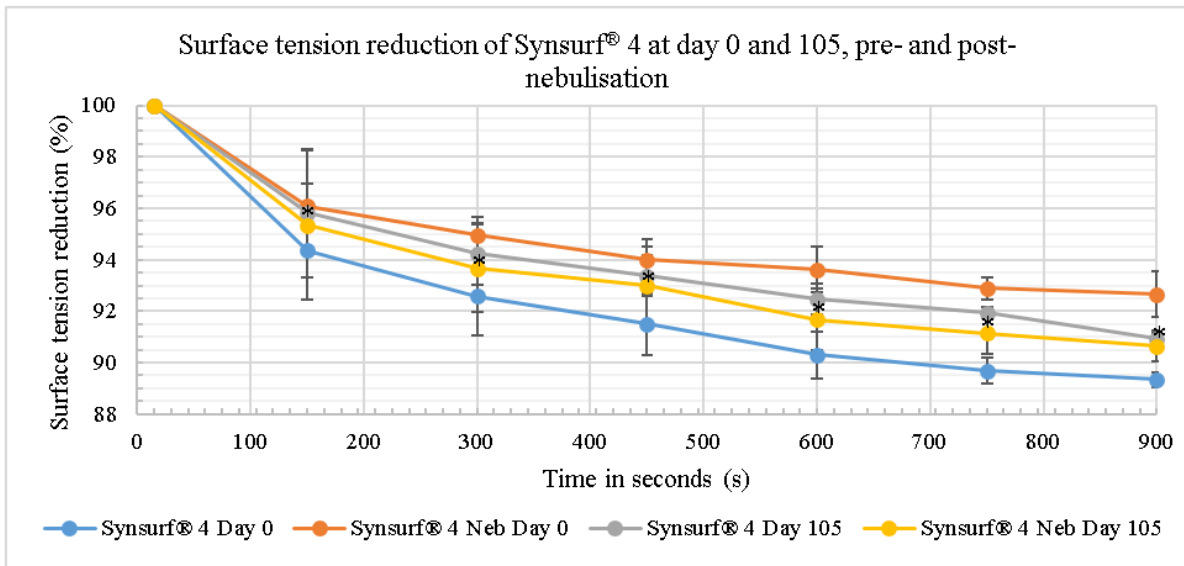


Figure 4.28: Interfacial surface tension reduction (expressed in % and SEM bar indicated) of pre- and post-nebulisation Synsurf® 4 preparation at day 0 and 105, over time. Comparison showed statistical differences ($p < 0.05$) between nebulised preparation at day 0 and 105 (shown in orange and yellow). Neb = post- nebulisation. (*: $p < 0.05$ vs Synsurf® 4 post-nebulised day 0)

Synsurf® preparation 5:

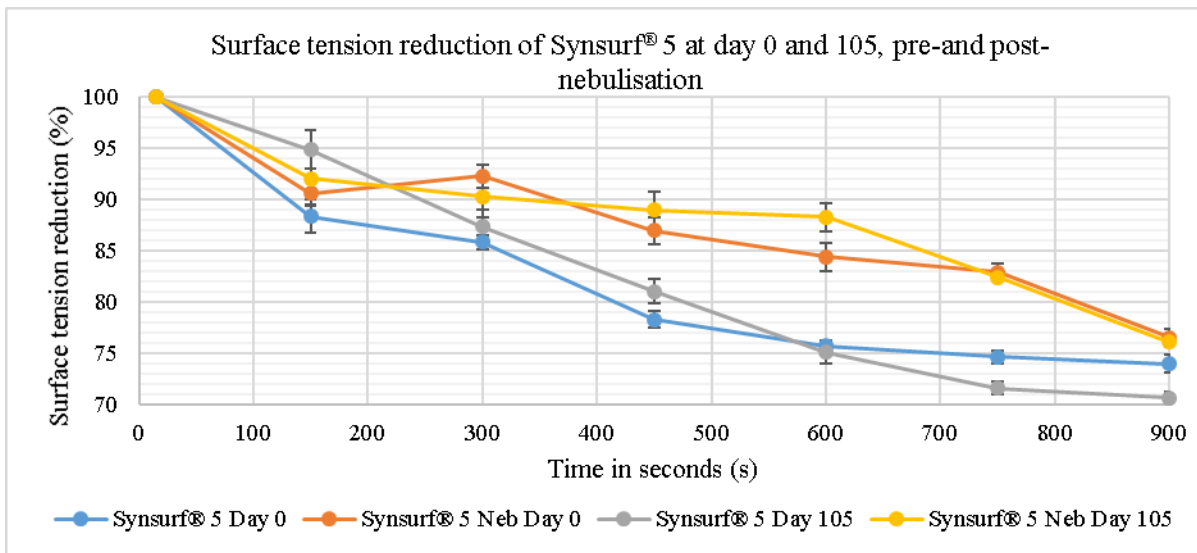


Figure 4.29: Interfacial surface tension reduction (expressed in % and SEM bar indicated) of pre- and post-nebulisation Synsurf® 5 preparation at day 0 and 105, over time. Neb = post- nebulisation.

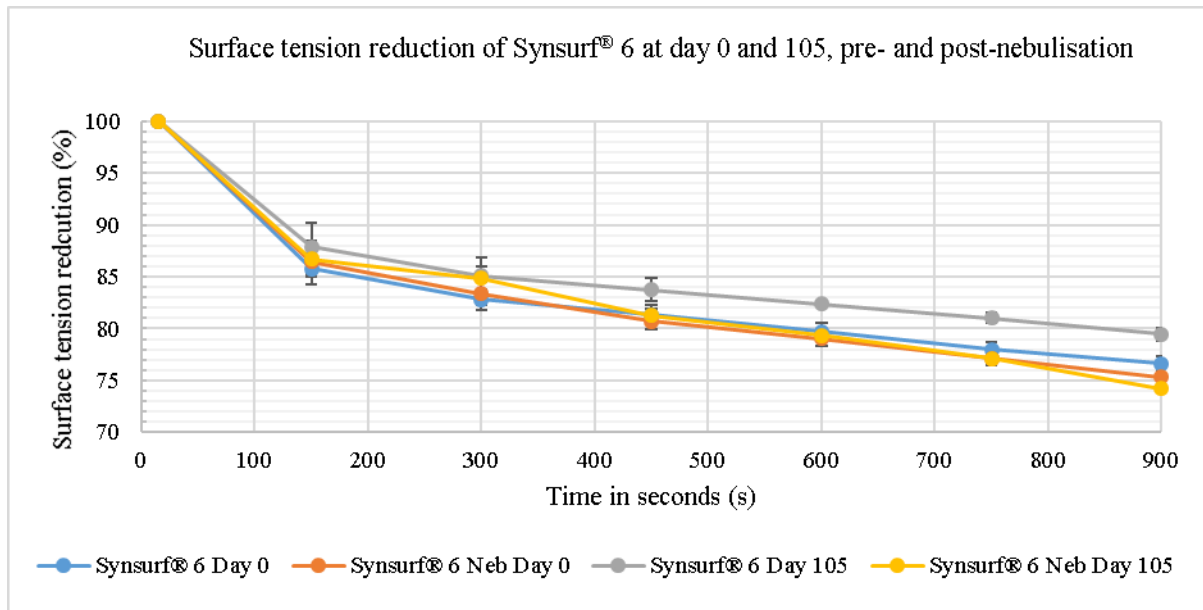
Synsurf preparation 6:

Figure 4.30: Interfacial surface tension reduction (expressed in % and SEM bar indicated) of pre- and post-nebulisation Synsurf® 6 preparation at day 0 and 105, over time. Neb = post- nebulisation.

4.4.5 Interfacial surface tension reduction of Synsurf® samples extruded in synthesis

Comparison of Synsurf® samples prepared with or without an additional extrusion steps, indicated no changes in surface tension reduction for all Synsurf® preparations (1 – 6) pre- and post-nebulisation. Reduction in surface tension of Synsurf® 1 (extruded) pre-nebulisation (Figure 4.31) and post-nebulisation (Figure 4.32) is shown. As extrusion did not significantly change the surface tension reduction ability of Synsurf® preparations (pre- and post-nebulisation), extruded and non-extruded preparations showed similar results.

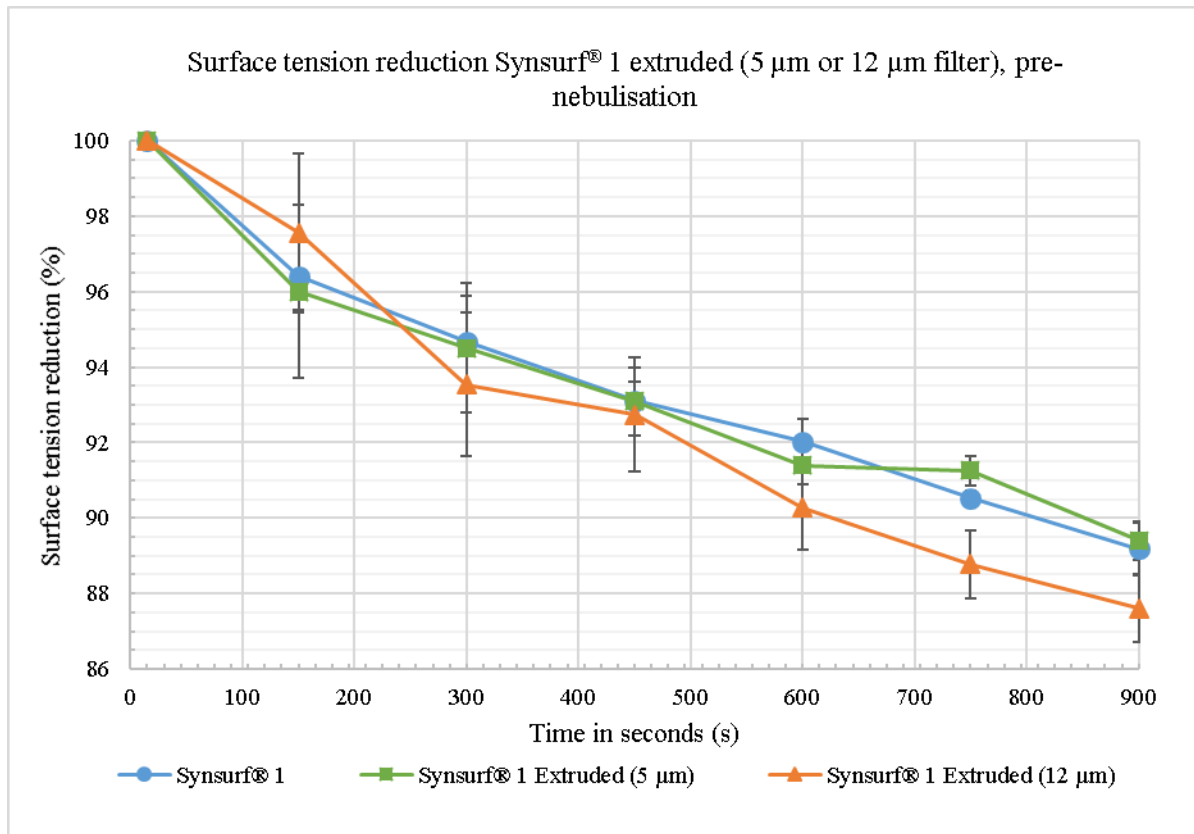
Pre-nebulisation:

Figure 4.31: Interfacial surface tension reduction (expressed in % and SEM bar indicated) of pre-nebulisation Synsurf® 1 (extruded by 5 µm and 12 µm filter), over time.

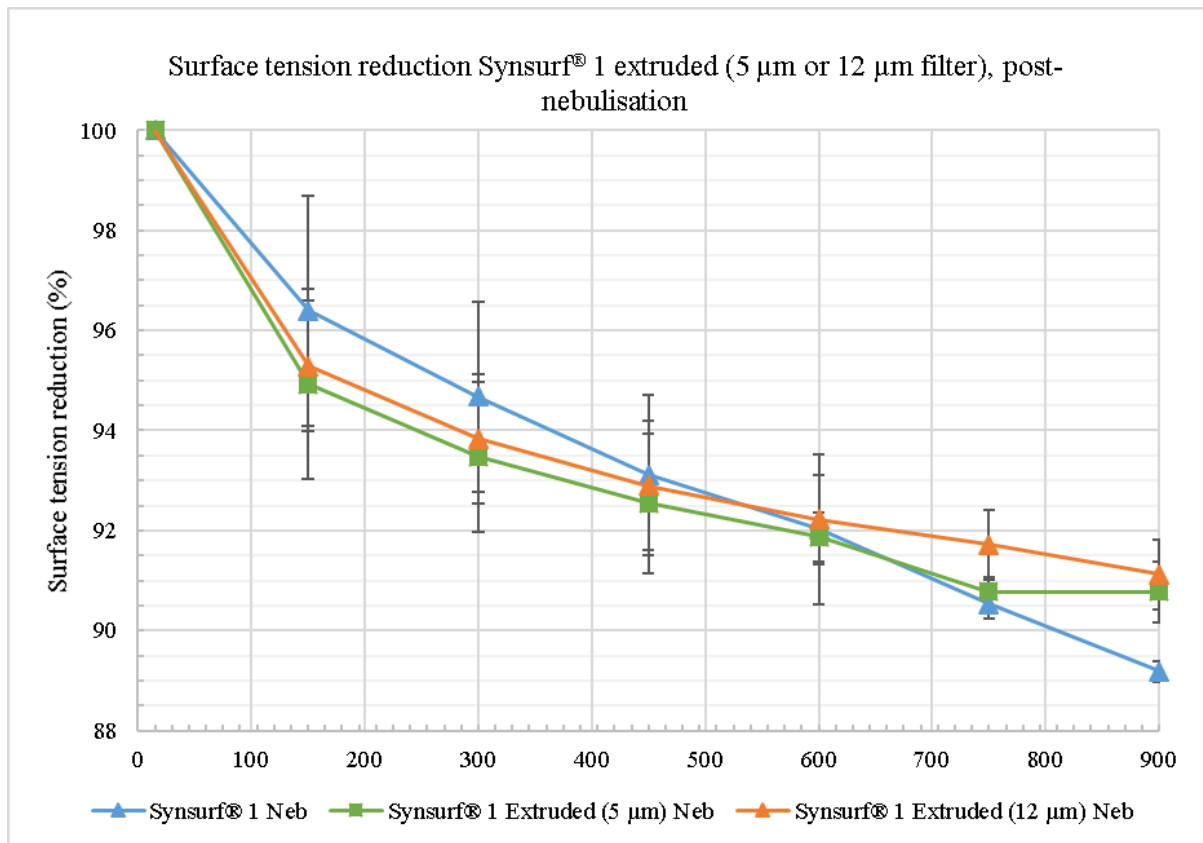
Post-nebulisation:

Figure 4.32: Interfacial surface tension reduction (expressed in % and SEM bar indicated) of post-nebulisation Synsurf® 1, extruded by 5 µm and 12 µm filter, over time. Neb = post-nebulisation.

CHAPTER 5: Discussion

Surfactant replacement therapy (SRT) is an established treatment for infant respiratory distress syndrome (IRDS); however, care of extremely premature infants less than 26 weeks, have encouraged new methods to SRT administration in combination with the clinical focus of reducing and/or avoiding mechanical ventilation.⁸⁵ Older human and animal studies investigating nebulised SRT showed non-beneficial results⁵³ however, recent studies indicated the safety and feasibility of SRT by aerosolisation.^{56,74} Currently, no SRT intended for aerosolisation by nebulisation is available and additionally, previous studies recommended particle profiling in combination with formulation related to viscosity, whilst maintaining surface activity.⁵⁶ Moreover, synthetic surfactant hold advantages that include large reproducibility with no need for harvesting and extraction of surfactant from animal tissue.

Published information regarding particle size profile and surface tension lowering activity of natural and synthetic pulmonary surfactants, pre- and post-nebulisation, is limited. Our aim with this study was to investigate the biophysical properties of respirable particles generated with the use of an Aeroneb[®]Pro vibrating mesh nebuliser. To achieve this, the existing formulation of a novel synthetic pulmonary surfactant Synsurf[®] (in development) was changed by addition of surface active compounds. The analytical approach was based on the main considerations for the early development of inhaled drugs. This consists of properties i.e. particle profile (size), density, viscosity and surface activity which is influenced by composition and aerosol device used. A summary of methods used in this study is shown in Figure 3.3.

It is known that changes in PS composition influence biophysical properties. An example of this is displayed in pneumonia where interactions of bacteria and/or endotoxins (in Type II cells) influence the density and surface tension with a marked decrease in palmitic acid (PA) content within the PS.⁸⁶ Limited information is available with regards to the specific density of PS at varying PL concentrations. However, in comparison to pure DPPC preparations and bronchoalveolar lavage fluid, Synsurf[®] and the other natural surfactants fall within the expected range.^{87,88} Post-nebulisation most preparations showed a decrease in density, which is possibly due to the change lipid orientation. The addition of triacylglycerol and/or free palmitic acid increases the adsorption rate of PS and it is speculated that this is due to small defects induced in the membrane structure.²⁹ In our experiments, only Synsurf[®] with PA or lower concentrations of cholesterol as well Curosurf[®] showed an increase in density post-nebulisation. Although the density analysis used in this study is not ideal for detection of packing properties of lipid membranes, the increase in density of surfactant samples might indicate tighter (ordered) liposome structures generated during nebulisation.

Preparation viscosity is of particular importance when developing an exogenous surfactant for nebulisation as this may influence the device selection, mist/aerosol density and uniform distribution.^{1,3} Additionally, atomisation of liquids with higher viscosities has shown to be less efficacious, which might lead to an increased loss of surfactant preparation. However, increased viscosity is also linked to an increase in aerosol particle size using jet nebulisers.⁸⁹ Our study showed no apparent link between viscosity of surfactants and particle size generated post-nebulisation. This might be attributed to the use of a vibrating mesh nebuliser, which generates less change in temperature during operation in comparison to jet- and ultrasonic-nebuliser.^{11,89} Although additions to Synsurf[®] increase the viscosity of preparations, cholesterol shows a concentration dependent increase in viscosity, which was reinforced with the addition of PA. Due to the complex mixture of lipid and proteins/peptides of synthetic and natural surfactant, variations in viscosity is expected, possibly by aggregation of microstructures dispersed in the aqueous phase.⁹⁰ Previous studies conducted with Survanta[®] (contains additional PA and triPA) and Infracurf[®] (containing 5 % cholesterol), showed a PL concentration and temperature dependent increase in viscosity. These studies suggested that the combination of PA and triPa will

increase the viscosity of surfactant samples by preferential interaction with saturated lipids (DPPC). This contrasts with our viscosity findings of Synsurf[®] with palmitic acid and tripalmitin. However, Survanta[®] and other preparations mentioned were analysed at higher temperatures ($\pm 35^{\circ}\text{C}$ to 37°C) and contained higher fractions of unsaturated lipids.⁹⁰ On the other hand Curosurf[®] and Liposurf[®] showed much lower viscosities in comparison to Synsurf[®] samples. This could possibly be attributed to the calcium chloride buffer solution used in Liposurf[®] preparations⁹¹, as the addition of calcium influence the formation of microstructures by increasing the protein-mediated PL aggregation within this lung surfactant.⁹⁰ This aggregation and/or clustering of lipids previously induced by polymers is linked to a decrease in viscosity.⁹² Furthermore, Curosurf[®] is suspended in a sodium chloride solution and neutral lipids (which includes cholesterol and triacylglycerol) are removed by liquid-gel chromatography during manufacturing.⁴⁹ Moreover, the dilution of PL's from 80 mg/mL to 20 mg/mL, in our experiments might explain the lower viscosity of this surfactant preparation. Although the viscosity analysis method used in this study is designed for sperm samples⁹³, filling times of Leja[®] slides converted to cP, provided substantial differentiation between inter-formulation of preparations that indicate morphological and rheological changes are induced by additional surface-active molecules. Moreover, none of the formulations displayed clogging/blocking of the micro-mesh within the Aeroneb[®]Pro nebuliser, which is a main concern with surfactant formulations intended for nebulisation.¹¹

Nebulised formulations of Synsurf[®] (with the exclusion of Syn 6), Liposurf[®] and Curosurf[®] showed particle generated below the recommend range (1000 d.nm to 3000 d.nm) suggested for optimal peripheral lung deposition.^{11,12,66} This indicates a clear disruption of liposomes within all preparations during aerosolisation. However, it must be noted that Synsurf[®] preparations underwent an ultrasonification step to disrupt large multimellar vesicles, that was not done for Curosurf[®] or Liposurf[®] purchased from the manufactures. Moreover, extrusion of Synsurf[®] preparations, showed a reduction in the change of particle diameters post-nebulisation, most within the recommend range. Previous studies have indicated that extrusion pre-nebulisation through larger filters (i.e. $>1\ \mu\text{m}$ in diameter) may contribute to the stability of vesicles within solution.⁷⁸ Thus extrusion might increase the robustness of

liposomes, and maintain larger liposomes post-nebulisation as shown in Table 4.6. However, the addition of palmitic acid and tripalmitin appeared to aid in the preservation of particle diameter without extrusion, possibly by resisting disruption and penetration of PA into multimellar aggregates. This could affect packing and increase triPA interaction with DPPC.⁹⁰

It is important to note that the recommend range of particle diameters is based on mechanically ventilated infants and insufficient deposition is credited to low tidal volumes and functional residual capacity and high respiratory rates in combination with small airway diameters. This leads to a decrease in particle residence and a diminished deposition pattern of inhaled PS in the lower regions of the infant lungs.⁶⁶ However, previous studies have indicated that nebulised Curosurf[®] administered by nasal CPAP was effective with smaller particles ranging from ± 800 d.nm – 900 d.nm.⁹⁴ Thus deposition could be composition/formulation specific and smaller particles could provide optimal deposition. However, due to a paucity of clinical data in infants, hydrodynamic and aerodynamic particle size analysis can provide information curtailing the development in SRT for IRDS, but additional animal studies should be conducted.

The rate of surface film formation of surfactant preparations was observed over a period of 900 seconds. Most surfactants showed a decline in ability to reduce interfacial surface tension post-nebulisation. However, Synsurf[®] 1 and 6 (PA and triPA) maintained surface-activity pre-nebulisation. Additionally, Synsurf[®] 5 cholesterol (at 1 %) and 6 (PA and triPA) showed an overall greater decrease in surface tension pre- and post-nebulisation. This possibly depicts an increase in overall interfacial adsorption rate which is of more significance to illustrate how effectively lipid molecules adsorb at the air–liquid interface to form the surfactant film. Clinically, fast adsorption is crucial as the surfactant film (monolayer) must be formed rapidly during the initial opening of the lungs.⁹⁵ Extrusion, with either $5 \mu\text{m}$ or $12 \mu\text{m}$ filter, did not change the surface tension reduction properties over the observation period, thus no changes in adsorption properties was detected. Synsurf[®] 2 with only PA was inferior to Synsurf[®] 6 (with the addition of PA and triPA). This observation is supported by previous studies, which concluded that the most effective synthetic surfactant preparation (with regards to surface activity)

consisted of DPPC, PG, PA, triPA and hydrophobic surfactant protein.⁹⁶ The addition of cholesterol to Synsurf[®] enhanced surface adsorption at lower concentration (1 %), but showed a diminished effect when added in higher concentration (2 %). Previous studies using bovine surfactant showed hampering of adsorption at 25°C when cholesterol was removed however, this was not observed at higher temperatures.⁹⁷ This might indicate differences due to the lack of surfactant proteins in Synsurf[®]. However, additional analyses at 37°C will have to be conducted.

In conclusion, this study evaluated the biophysical properties and surface tension reduction ability of Synsurf[®] preparations in comparison to natural surfactants. Through the combination of analytical methods, we showed that extrusion of Synsurf[®] 1 as well as addition of cholesterol (1 %) or tripalmitin and PA, is beneficial to formulate the PS into an aerosol of respirable particles in the size range of 1 µm -3 µm. In addition, PA/triPA inclusion in Synsurf[®] led to an overall better conservation of surface tension and ideal particles sizes with the vibrating mesh nebuliser. Liposurf[®] and Curosurf[®] did illustrate an overall greater decrease in surface tension over the observation period, with lower viscosities (as recommended for nebulisation) however, these natural surfactants did not generate particles within the recommended range when nebulised with a vibrating mesh nebuliser, under the same conditions as Synsurf[®].

Finally, this study has shown that the biophysical properties of Synsurf[®] 1 remains intact pre- and post-nebulisation, a result that merits animal model investigation to establish its efficacy during aerosolisation. In addition to this, aerosol delivery of Synsurf[®] 1 may contribute to its use as a potential carrier of drugs to the air-liquid interface in airways.

REFERENCES

1. El-Gendy N, Kaviratna A, Berkland C, Dhar P. Delivery and performance of surfactant replacement therapies to treat pulmonary disorders. *Therapeutic Delivery*. 2013;4(8):951-980.
2. Polin RA, Carlo WA. Surfactant replacement therapy for preterm and term neonates with respiratory distress. *American Academy of Pediatrics*. 2014;133(1):156-163.
3. Nouraeyan N, Lambrinakos-Raymond A, Leone M, Sant'Anna G. Surfactant administration in neonates: A review of delivery methods. *Canadian Journal of Respiratory Therapy*. 2014;50(3):91-95.
4. Pillow JJ, Minocchieri S. Innovation in surfactant therapy II: Surfactant administration by aerosolization. *Neonatology*. 2012;101(4):337-344.
5. Lopez E, Gascoin G, Flamant C, Merhi M, Tourneux P, Baud O. Exogenous surfactant therapy in 2013: What is next? who, when and how should we treat newborn infants in the future? *BMC Pediatrics*. 2013;13(1):165-175.
6. Fok TF, Al-Essa M, Dolovich M, Rasid F, Kirpalani H. Nebulisation of surfactants in an animal model of neonatal respiratory distress. *Archives of Disease in Childhood Foetal and Neonatal Edition*. 1998;78(1):F3-F9.
7. Fok TF, Monkman S, Dolovich M, et al. Efficiency of aerosol medication delivery from a metered dose inhaler versus jet nebulizer in infants with bronchopulmonary dysplasia. *Pediatric Pulmonology*. 1996;21:301-309.
8. Hou S, Wu J, Li X, Shu H. Practical, regulatory and clinical considerations for development of inhalation drug products. *Asian Journal of Pharmaceutical Sciences*. 2015;10(6):490-500.
9. Dubus JC, Vecellio L, De Monte M, et al. Aerosol deposition in neonatal ventilation. *Pediatric Research*. 2005;58(1):10-14.

10. Patton JS, Fishburn CS, Weers JG. The lungs as a portal of entry for systemic drug delivery. *Proceedings of the American Thoracic Society*. 2004;1(4):338-344.
11. Dhanani J, Fraser JF, Chan H, Rello J, Cohen J, Roberts JA. Fundamentals of aerosol therapy in critical care. *Critical Care*. 2016;20(1):269-285.
12. Ibrahim M, Verma R, Garcia-Contreras L. Inhalation drug delivery devices: Technology update. *Medical Devices: Evidence and Research*. 2015;8:131-139.
13. Davis RP, Mychaliska GB. Neonatal pulmonary physiology. *Seminars in Pediatric Surgery*. 2013;22(4):179-184.
14. Hohlfeld JM. The role of surfactant in asthma. *Respiratory Research*. 2002;3(1):4-12.
15. National Heart Lung and Blood Institute [Public domain], via Wikimedia Commons. Lung structure normal. https://commons.wikimedia.org/wiki/File%3ALung_structure_normal.jpg Updated 16 October 2017. Accessed 03/14, 2017.
16. BéruBé K, Prytherch Z, Job C, Hughes T. Human primary bronchial lung cell constructs: The new respiratory models. *Toxicology*. 2010;278(3):311-318.
17. Nahar K, Gupta N, Gauvin R, et al. In vitro, in vivo and ex vivo models for studying particle deposition and drug absorption of inhaled pharmaceuticals. *European Journal of Pharmaceutical Sciences*. 2013;49(5):805-818.
18. Høiby N. Recent advances in the treatment of pseudomonas aeruginosa infections in cystic fibrosis. *BMC medicine*. 2011;9(1):32-38.
19. Sweet DG, Carnielli V, Greisen G, et al. European consensus guidelines on the management of neonatal respiratory distress syndrome in preterm infants – 2010 update. *Neonatology*. 2010;97(4):402-417.

20. Morton SU, Brodsky D. Foetal physiology and the transition to extrauterine life. *Clinical Perinatology*. 2016;43(3):395-407.
21. Beck S, Wojdyla D, Say L, et al. The worldwide incidence of preterm birth: A systematic review of maternal mortality and morbidity. *Bulletin World Health Organization*. 2010;88(1):31-38.
22. Ware LB, Matthay MA. The acute respiratory distress syndrome. *New England Journal of Medicine*. 2000;342(18):1334-1349.
23. Sweet DG, Carnielli V, Greisen G, et al. European consensus guidelines on the management of neonatal respiratory distress syndrome in preterm infants - 2013 update. *Neonatology*. 2013;103(4):353-368.
24. Enhörning G, Robertson B. Lung expansion in the premature rabbit fetus after tracheal deposition of surfactant. *Pediatrics*. 1972;50(1):58-66.
25. Liggins GC, Howie RN. A controlled trial of antepartum glucocorticoid treatment for prevention of the respiratory distress syndrome in premature infants. *Pediatrics*. 1972;50(4):515-525.
26. Sweet DG, Carnielli V, Greisen G, et al. European consensus guidelines on the management of respiratory distress syndrome - 2016 update. *Neonatology*. 2017;111(2):107-125.
27. Bahadue FL, Soll R. Early versus delayed selective surfactant treatment for neonatal respiratory distress syndrome. *Neonatology*. 2013;104(2):124-126.
28. Rojas-Reyes MX, Morley CJ, Soll R. Prophylactic versus selective use of surfactant in preventing morbidity and mortality in preterm infants. *Cochrane Database of Systematic Reviews*. 2012;1(3):1-69.
29. Veldhuizen EJ, Haagsman HP. Role of pulmonary surfactant components in surface film formation and dynamics. *Biochimica et Biophysica Acta (BBA) - Biomembranes*. 2000;1467(2):255-270.

30. Veldhuizen R, Nag K, Orgeig S, Possmayer F. The role of lipids in pulmonary surfactant. *Biochimica et Biophysica Acta (BBA) - Molecular Basis of Disease*. 1998;1408(2):90-108.
31. de La Serna JB, Perez-Gil J, Simonsen AC, Bagatolli LA. Cholesterol rules: Direct observation of the coexistence of two fluid phases in native pulmonary surfactant membranes at physiological temperatures. *The Journal of Biological Chemistry*. 2004;279(39):40715-40722.
32. Parra E, Pérez-Gil J. Composition, structure and mechanical properties define performance of pulmonary surfactant membranes and films. *Chemistry and Physics of Lipids*. 2015;185:153-175.
33. Foot NJ, Orgeig S, Daniels CB. The evolution of a physiological system: The pulmonary surfactant system in diving mammals. *Respiratory Physiology & Neurobiology*. 2006;154(1):118-138.
34. Wauthoz N, Amighi K. Phospholipids in pulmonary drug delivery. *European Journal of Lipid Science and Technology*. 2014;116(9):1114-1128.
35. King RJ, Macbeth MC. Physicochemical properties of dipalmitoyl phosphatidylcholine after interaction with an apolipoprotein of pulmonary surfactant. *Biochimica et Biophysica Acta (BBA) - Biomembranes*. 1979;557(1):86-101.
36. Kishore U, Greenhough TJ, Waters P, et al. Surfactant proteins SP-A and SP-D: Structure, function and receptors. *Molecular Immunology*. 2006;43(9):1293-1315.
37. Pastva AM, Wright JR, Williams KL. Immunomodulatory roles of surfactant proteins A and D: Implications in lung disease. *Proceedings of the American Thoracic Society*. 2007;4(3):252-257.
38. Stevens TP, Sinkin RA. Surfactant replacement therapy. *Chest*. 2007;131(5):1577-1582.
39. Blanco O, Pérez-Gil J. Biochemical and pharmacological differences between preparations of exogenous natural surfactant used to treat respiratory distress syndrome: Role of the different components in an efficient pulmonary surfactant. *European Journal of Pharmacology*. 2007;568(1):1-15.

40. Goerke J. Pulmonary surfactant: Functions and molecular composition. *Biochimica et Biophysica Acta (BBA)-Molecular Basis of Disease*. 1998;1408(2):79-89.
41. Davis P, Fleming B, Coolbear K, Keough K. Gel to liquid-crystalline transition temperatures of water dispersions of two pairs of positional isomers of unsaturated mixed-acid phosphatidylcholines. *Biochemistry*. 1981;20(12):3633-3636.
42. Parra E, Alcaraz A, Cruz A, Aguilera V, Pérez-Gil J. Hydrophobic pulmonary surfactant proteins SP-B and SP-C induce pore formation in planar lipid membranes: Evidence for proteolipid pores. *Biophysical Journal*. 2013;104(1):146-155.
43. Oosterlaken-Dijksterhuis MA, Haagsman HP, Van Golde LM, Demel RA. Characterization of lipid insertion into monomolecular layers mediated by lung surfactant proteins SP-B and SP-C. *Biochemistry*. 1991;30(45):10965-10971.
44. Taneva S, Keough KM. Cholesterol modifies the properties of surface films of dipalmitoylphosphatidylcholine plus pulmonary surfactant-associated protein B or C spread or adsorbed at the air–water interface. *Biochemistry*. 1997;36(4):912-922.
45. Schürch S. Surface tension at low lung volumes: Dependence on time and alveolar size. *Respiration Physiology*. 1982;48(3):339-355.
46. Moya F, Maturana A. Animal-derived surfactants versus past and current synthetic surfactants: Current status. *Clinics in Perinatology*. 2007;34(1):145-177.
47. Halliday HL. Surfactants: Past, present and future. *Journal of Perinatology*. 2008;28:47-56.
48. Seehase M, Collins JJ, Kuypers E, et al. New surfactant with SP-B and C analogs gives survival benefit after inactivation in preterm lambs. *PLoS ONE*. 2012;7(10):1-13.

49. Chiesi Farmaceutici SpA. Curosurf® (poractant alfa) package insert. https://resources.chiesiusa.com/Curosurf/CUROSURF_PI.pdf Updated 2014. Accessed October 15, 2017.
50. Bloom BT, Clark RH. Comparison of infasurf (calfactant) and survanta (beractant) in the prevention and treatment of respiratory distress syndrome. *Pediatrics*. 2005;116(2):392-399.
51. Najafian B, Karimi-Sari H, Khosravi MH, Nikjoo N, Amin S, Shohrati M. Comparison of efficacy and safety of two available natural surfactants in iran, curosurf and survanta in treatment of neonatal respiratory distress syndrome: A randomized clinical trial. *Contemporary Clinical Trials Communications*. 2016;3:55-59.
52. Ramanathan R, Rasmussen MR, Gerstmann DR, Finer N, Sekar K, North American Study Group. A randomized, multicenter masked comparison trial of poractant alfa (Curosurf) versus beractant (Survanta) in the treatment of respiratory distress syndrome in preterm infants. *American Journal of Perinatology*. 2004;21(3):109-119.
53. Berggren E, Liljedahl M, Winbladh B, et al. Pilot study of nebulized surfactant therapy for neonatal respiratory distress syndrome. *Acta Paediatrica*. 2000;89(4):460-464.
54. Sweet DG, Turner MA, Stranak Z, et al. A first-in-human clinical study of a new SP-B and SP-C enriched synthetic surfactant (CHF5633) in preterm babies with respiratory distress syndrome. *Archives of Disease in Childhood Foetal and Neonatal Edition*. 2017;102(6):F497-F503.
55. Hidalgo A, Salomone F, Fresno N, Orellana G, Cruz A, Perez-Gil J. Efficient interfacially driven vehiculization of corticosteroids by pulmonary surfactant. *Langmuir*. 2017;33:7929-7939.
56. Finer NN, Merritt TA, Bernstein G, Job L, Mazela J, Segal R. An open label, pilot study of Aerosurf® combined with nCPAP to prevent RDS in preterm neonates. *Journal of Aerosol Medicine and Pulmonary Drug Delivery*. 2010;23(5):303-309.

57. Smith L. Discovery laboratories: An update on the surfaxin launch and the phase 2 clinical trial program for aerosurf®. <https://smithonstocks.com/discovery-laboratories-an-update-on-the-surfaxin-launch-and-the-phase-2-clinical-trial-program-for-aerosurf-dsco-buy-1-72-paid-subscribers-only/>

Updated 2014. Accessed 03/11, 2017.

58. Lampland AL, Wolfson MR, Mazela J, et al. Aerosolized KL₄ surfactant improves gas exchange and survival in spontaneously breathing piglets with HCL-induced acute lung injury. *Pediatric Pulmonology*. 2014;49:482-489.

59. Van Zyl JM, Smith J. Surfactant treatment before first breath for respiratory distress syndrome in preterm lambs: Comparison of a peptide-containing synthetic lung surfactant with porcine-derived surfactant. *Drug Design, Development and Therapy*. 2013;7:905-916.

60. Van Zyl JM, Smith J, Hawtrey A. The effect of a peptide-containing synthetic lung surfactant on gas exchange and lung mechanics in a rabbit model of surfactant depletion. *Drug Design, Development and Therapy*. 2013;7:139-148.

61. Engle WA and American Academy of Pediatrics Committee on Fetus and Newborn. Surfactant-replacement therapy for respiratory distress in the preterm and term neonate. *Pediatrics*. 2008;121(2):419-432.

62. Miyoshi MH. Surfactant replacement therapy. *Jornal de Pediatria*. 2001;77(1):S3-S16.

63. Pfister RH, Soll R, Wiswell TE. Protein containing synthetic surfactant versus animal derived surfactant extract for the prevention and treatment of respiratory distress syndrome. *Evidence-Based Child Health: A Cochrane Review Journal*. 2010;5(1):17-51.

64. Heyder J. Definition of an aerosol. *Journal of Aerosol Medicine*. 1991;4(3):217.

65. Ruppert C, Kuchenbuch T, Boensch M, et al. Dry powder aerosolization of a recombinant surfactant protein-C-based surfactant for inhalative treatment of the acutely inflamed lung. *Critical Care Medicine*. 2010;38(7):1584-1591.
66. Mazela J, Polin RA. Aerosol delivery to ventilated newborn infants: Historical challenges and new directions. *European Journal of Pediatrics*. 2011;170(4):433-444.
67. Tena AF, Clarà PC. Deposition of inhaled particles in the lungs. *Archivos de Bronconeumología (English Edition)*. 2012;48(7):240-246.
68. O'Doherty MJ, Thomas SHL, Page CJ, Treacher DF, Nunan TO. Delivery of a nebulized aerosol to a lung model during mechanical ventilation. *The American Review of Respiratory Disease*. 1992;146(2):383-388.
69. Yang W, Peters JI, Williams RO. Inhaled nanoparticles—a current review. *International Journal of Pharmaceutics*. 2008;356(1):239-247.
70. Radhakrishnan H, Kassinos S. "CFD modeling of turbulent flow and particle deposition in human lungs" in proceedings of 31st Annual International Conference of the IEEE, Minneapolis, Minnesota, USA. *Engineering in Medicine and Biology Society*. 2009:2867-2870.
71. Schlesinger RB. Comparative deposition of inhaled aerosols in experimental animals and humans: A review. *Journal of Toxicology and Environmental Health*. 1985;15(2):197-214.
72. Minocchieri S, Burren JM, Bachmann MA, et al. Development of the premature infant nose throat-model (PrINT-model)—an upper airway replica of a premature neonate for the study of aerosol delivery. *Pediatric Research*. 2008;64(2):141-146.
73. Willson DF. Aerosolized surfactants, anti-inflammatory drugs, and analgesics. *Respiratory Care*. 2015;60(6):774-793.

74. Walther FJ, Hernández-Juviel JM, Waring AJ. Aerosol delivery of synthetic lung surfactant. *PeerJ*. 2014;2:e403; DOI 10.7717/peerj.403
75. Ghazanfari T, Elhissi AMA, Ding Z, Taylor KMG. The influence of fluid physicochemical properties on vibrating-mesh nebulization. *International Journal of Pharmaceutics*. 2007;339(1):103-111.
76. Robillard E, Alarie Y, Dagenais-Perusse P, Baril E, Guilbeault A. Microaerosol administration of synthetic beta-gamma-dipalmitoyl-L-alpha-lecithin in the respiratory distress syndrome: A preliminary report. *Canadian Medical Association Journal*. 1964;90:55-57.
77. Lewis JF, Tabor B, Ikegami M, Jobe AH, Joseph M, Absolom D. Lung function and surfactant distribution in saline-lavaged sheep given instilled vs. nebulized surfactant. *Journal of Applied Physiology*. 1993;74(3):1256-1264.
78. Elhissi AMA, Faizi M, Naji WF, Gill HS, Taylor KMG. Physical stability and aerosol properties of liposomes delivered using an air-jet nebulizer and a novel micropump device with large mesh apertures. *International Journal of Pharmaceutics*. 2007;334(1):62-70.
79. Hoorfar M, Neumann A. Recent progress in axisymmetric drop shape analysis (ADSA). *Advances in Colloid and Interface Science*. 2006;121(1):25-49.
80. Douglas-Hamilton DH, Smith NG, Kuster CE, Vermeiden JP, Althouse GC. Capillary-Loaded particle fluid dynamics: Effect on estimation of sperm concentration. *Journal of Andrology*. 2005;26(1):115-122.
81. Leja[®] Products. Manual for the assessment of sperm count. https://leja.nl/data/FCK/File/H01_manual_20m.pdf Accessed 03/11, 2017.

82. Farnoud AM, Fiegel J. Low concentrations of negatively charged sub-micron particles alter the microstructure of DPPC at the air–water interface. *Colloids and Surfaces A: Physicochemical and Engineering Aspects*. 2012;415:320-327.
83. Malvern Instruments Youtube Channel. Simple, versatile dynamic light scattering system - zetasizer nano. <https://www.youtube.com/watch?v=6Y4gsIP6bsg> Updated 2014. Accessed 07/23, 2016.
84. Prokop RM, Jyoti A, Cox P, Frndova H, Policova Z, Neumann AW. Surface tension as a sensitive measure to distinguish between pulmonary surfactant from different lavages. *Colloids and Surfaces B: Biointerfaces*. 1999;13(3):117-126.
85. Niemarkt HJ, Hutten MC, Kramer BW. Surfactant for respiratory distress syndrome: New ideas on a familiar drug with innovative applications. *Neonatology*. 2017;111(4):408-414.
86. Schmidt R, Meier U, Yabut-Perez M, et al. Alteration of fatty acid profiles in different pulmonary surfactant phospholipids in acute respiratory distress syndrome and severe pneumonia. *American Journal of Respiratory and Critical Care Medicine*. 2001;163(1):95-100.
87. Woodka AC, Butler PD, Porcar L, Farago B, Nagao M. Lipid bilayers and membrane dynamics: Insight into thickness fluctuations. *Physical Review Letters*. 2012;109(5):1-5.
88. Mukherjee D, Porter A, Ryan M, et al. Modeling in vivo interactions of engineered nanoparticles in the pulmonary alveolar lining fluid. *Nanomaterials*. 2015;5(3):1223-1249.
89. Taylor KM, McCallion ON. Ultrasonic nebulisers for pulmonary drug delivery. *International Journal of Pharmaceutics*. 1997;153(1):93-104.
90. King DM, Wang Z, Palmer HJ, Holm BA, Notter RH. Bulk shear viscosities of endogenous and exogenous lung surfactants. *American Journal of Physiology-Lung Cellular and Molecular Physiology*. 2002;282(2):L277-L284.

91. Cipla Medpro (EDMS) BPK 2011. Liposurf® (bovine lipid extract surfactant suspension) package insert. https://www.cipla.co.za/wp-content/uploads/2014/05/Liposurf_PI.pdf Updated 2011. Accessed September 11, 2017.
92. Lu KW, Pérez-Gil J, Taeusch HW. Kinematic viscosity of therapeutic pulmonary surfactants with added polymers. *Biochimica et Biophysica Acta (BBA)-Biomembranes*. 2009;1788(3):632-637.
93. Rijnders S, Bolscher JG, McDonnell J, Vermeiden JP. Filling time of a lamellar capillary-filling semen analysis chamber is a rapid, precise, and accurate method to assess viscosity of seminal plasma. *Journal of Andrology*. 2007;28(4):461-465.
94. Smedsaas-Löfvenberg A, Nilsson K, Moa G, Axelsson I. Nebulization of drugs in a nasal CPAP system. *Acta Paediatrica*. 1999;88(1):89-92.
95. Yu LMY, Lu JJ, Chiu IWY, et al. Poly(ethylene glycol) enhances the surface activity of a pulmonary surfactant. *Colloids and Surfaces B: Biointerfaces*. 2004;36(3):167-176.
96. Tanaka Y, Takei T, Aiba T, Masuda K, Kiuchi A, Fujiwara T. Development of synthetic lung surfactants. *Journal of Lipid Research*. 1986;27(5):475-485.
97. Yu SH, Possmayer F. Interaction of pulmonary surfactant protein A with dipalmitoylphosphatidylcholine and cholesterol at the air/water interface. *Journal of Lipid Research*. 1998;39(3):555-568.

APPENDICES/ADDENDUM A

This study presented in part and in its entirety at a Stellenbosch University based academic year day and national conferences.

- 1. 59th Academic Year day, Medicine and Health Sciences, Stellenbosch University: Held at Tygerberg Campus, Western Cape hosted by Stellenbosch University on the 13th of August 2015.**
Abstract Title: Poster
Development of experimental compositions for aerosolisation of a synthetic pulmonary surfactant Synsurf[®]: Biophysical properties and effect of cholesterol on phospholipid-protein mixtures.
C Agenbag¹, JM Van Zyl¹, J Smith²
- 2. SASBCP and TOXSA Congress held at The Wits Club, Johannesburg on the 31st August until 2nd September 2015.**
Abstract Title: Oral Presentation
Development of experimental compositions for aerosolisation of a synthetic pulmonary surfactant Synsurf[®]: Biophysical properties and effect of cholesterol on phospholipid-protein mixtures.
C Agenbag¹, JM Van Zyl¹, J Smith²
- 3. All African Congress on Pharmacology and Pharmacy held at Misty Hills Hotel, Gauteng on the 5th to 8th of October 2016.**
Abstract Title: Poster
Biophysical Properties of Experimental Compositions of a Synthetic Pulmonary Surfactant Synsurf[®] For Aerosolisation.
C Agenbag¹, JM Van Zyl¹, J Smith²
- 4. 61st Academic Year day, Medicine and Health Sciences, Stellenbosch University: Held at Tygerberg Campus, Western Cape hosted by Stellenbosch University on the 30th of August 2017.**
Abstract Title: Poster
Biophysical Properties of Experimental Compositions of a Synthetic Pulmonary Surfactant Synsurf[®] For Aerosolisation.
C Agenbag¹, JM Van Zyl¹, J Smith²

¹Division of Clinical Pharmacology, Department of Medicine, Faculty of Medicine and Health Sciences, Stellenbosch University, Western Cape, South Africa.

²Department of Paediatrics & Child Health, Tygerberg Children's Hospital, Faculty of Medicine and Health Sciences, Stellenbosch University, Western Cape, South Africa.